Design and Development of Cellulose Saccharification Process Based on Ionic Liquid Aqueous Two-Phase System

Kazuhiko Tanimura

January 2020

Design and Development of Cellulose Saccharification Process Based on Ionic Liquid Aqueous Two-Phase System

A dissertation submitted to

THE GRADUATE SCHOOL OF ENGINEERING SCIENCE

OSAKA UNIVERSITY

in partial fulfillment of the requirements for the degree of

DOCTOR OF PHILOSOPHY IN ENGINEERING

BY

Kazuhiko Tanimura

January 2020

PREFACE

This dissertation work was conducted under the supervision of Professor Hiroshi Umakoshi at Division of Chemical Engineering, Graduate School of Engineering Science, Osaka University from 2016 to 2020.

The objective of this thesis is to qualitatively and quantitatively characterize a new cellulose saccharification process using an ionic liquid aqueous phase system and apply it to process design. The design aspects of the liquid aqueous two-phase system were studied, and the enzymatic hydrolysis of cellulose using IL-ATPS was evaluated with a focus on actual industrial processes.

The author hopes that this research would contribute to a technology for bioethanol production based on cellulose saccharification with low environmental impact by combining ionic liquid and water-soluble enzyme. The insights gained in this study are expected to contribute to the adsorption and desorption near the interface between cellulose and its hydrolase, and to the sustained and improved enzyme activity in ionic liquid systems.

Kazuhiko Tanimura

Division of Chemical Engineering
Graduate School of Engineering Science
Osaka University
Toyonaka, Osaka, 560-8531, Japan

Abstract

Since the strong crystal structure of cellulose cannot be maintained in IL, ionic liquid (IL) is recognized as a new cellulose solvent. Cellulose extracted with an anti-solvent such as water is called regenerated cellulose, and its crystallinity is significantly lower than before treatment. In addition, effective use of IL is expected to reduce environmental impact because it does not use acids or organic solvents. In terms of reducing environmental impact, a method of enzymatic hydrolysis of cellulose is known be commonly used. It is only necessary to dissolve insoluble cellulose and efficiently hydrolyze it with a water-soluble enzyme, but IL also interacts with the enzyme to reduce its activity. In other words, cellulose amorphization and maintenance of enzyme activity proceed in a very delicate environment. In this paper, it was evaluated the amorphization of cellulose by IL and the optimization of enzyme reaction, as well as basic research leading to the application to industrial processes.

In Chapter 1, focusing on the current status of biomass and green chemicals as the background of the research, the previous researches were summarized in relation to cellulose pretreatment, physical properties of ionic liquid, cellulose interaction, and cellulase, which are the main points of this research, together with the survey on the trends in the aqueous two-phase systems and ionic liquid aqueous two-phase systems, in order to find the tips for process design.

In Chapter 2, in the enzymatic hydrolysis of crystalline cellulose, dissolution and non-crystallization of cellulose is one of the rate-limiting steps. In order to analyze the kinetic parameters, both Langmuir adsorption model and Michaelis-Menten model were adopted to evaluate enzymatic hydrolysis of cellulose in the low IL concentration range. The effect of IL species on cellulose dissolution was quantitatively evaluated based on kinetic parameter analysis. It was suggested that the control of IL concentration may greatly affect the efficiency of enzymatic saccharification in batch reactions.

In Chapter 3, to investigate the phase separation behavior of the IL-ATPSs, binodal curves were drawn at different temperatures, and the length and slope of the tie lines were analyzed. Furthermore, the phase separation behavior was evaluated by changing the combination of salt and ionic liquid. Using the IL-ATPS, the distribution coefficients K_{aa} of amino acids were determined and used to characterize the hydrophobicity index (*HF*) between the top and bottom phases, which is a good indicator to understand the molecular partitioning behaviors in conventional ATPSs. The *HF* value of IL-ATPS was found to be almost the same as that reported for ATPS composed of polyethylene glycol and salt.

In Chapter 4, regenerated cellulose can be prepared by treatment with an ionic liquid (IL) and an anti-solvent such as water, which significantly enhances the physiological hydrolysis in comparison to crystalline cellulose. The IL-aqueous two-phase system (IL-ATPS) is consisted of IL-condensed upper phase and salt-condensed bottom phase, which could be suitable to produce regenerated cellulose with smaller amount of IL. Several IL-ATPS were prepared by combining different types of ionic liquids and salts to determine the enzymatic saccharification efficiency of crystalline cellulose. In addition, the effects of salt on pH were evaluated, and logic leading to process design was developed.

In Chapter 5, as a general conclusion of this study, in the IL-ATPS with a combination of IL and salt, UCST-type phase separation in which most IL is separated in the upper phase occurs in a self-organized manner. It was also shown that processes incorporating these into the enzymatic hydrolysis of cellulose could lead to future bioethanol production technologies.

Contents

Chapter 1
General Introduction

The energy problem is a serious social problem associated with industrial development and population growth. In recent years, renewable energy has attracted attention as an alternative to fossil fuels. In particular, the use of biomass is supported by its effectiveness in combination with the reduction of CO_2 emissions, and bioethanol is expected to be an effective alternative to fossil fuels. This is an area that will continue to attract interest in related technology development. This study focuses on the amorphization and enzymatic hydrolysis of cellulose in wastes, such as woody, vegetation biomass and paper waste, and presents a new approach to these problems.

In this chapter, some previous research relating to the general concepts of the use of cellulosic biomass by using ionic liquid and aqueous two-phase system, together with their combination (ionic liquid aqueous two-phase system; IL-ATPS) were introduced to shed the light on the key concepts in this study.

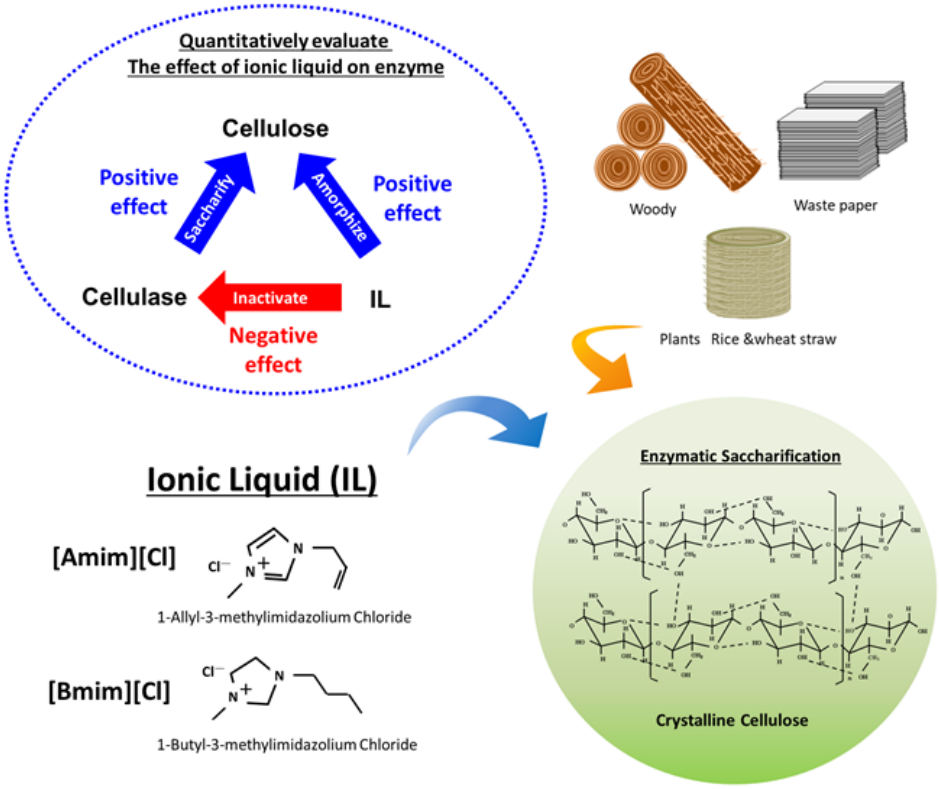

Figure 1-1 Key concepts in this study

1. Global circumstances of biomass demand and domestic unused biomass

Biomass includes waste biomass, unused biomass, and resource crops which are plants grown for the purpose of producing energy and products.

There are data compiled by the IEA about the potential for biomass energy in the world (**Figure 1-2**). According to this data, the utilization rate of renewable energy corresponds to 13% of the total energy, which is about twice the nuclear energy. Among them, biomass accounts for 77%. That is, 10% of the whole is energy by biomass. Technical biomass potential (capacity) will be 50 to 1,500 EJ / year (1EJ = 1018 J) in 2050, and biomass potential (available capacity) is 200 to 500 on the premise of sustainable resource use. It becomes EJ / year. The world's biomass demand is estimated to be 50 to 250 EJ / year in 2050, and if the total energy demand in the world is 600 to 1,000 EJ / year, it will occupy up to about 40%.

In addition, the Intergovernmental Panel Climate Change (IPCC) on Climate Change has summarized the potential of technological biomass energy by region (**Figure 1-3**). According to this data, there are over 60% of the reserves in Africa and Latin America, and the world total is 171 EJ / year. Although this is on the lower limit side, it is included in the range of technical biomass potential estimates (50 to 1,500 EJ) by the IEA (**Figure 1-2**). Among the unutilized biomass in Japan, the largest amount of plant biomass (rice straw, rice husk, straw) is 14 million tons annually, with 70% available. The amount of woody biomass (forest remnants, lumber mill residuals, construction-generated lumber) is 8 million tons annually, and the usable amount is 98% (**Table 1-1**).

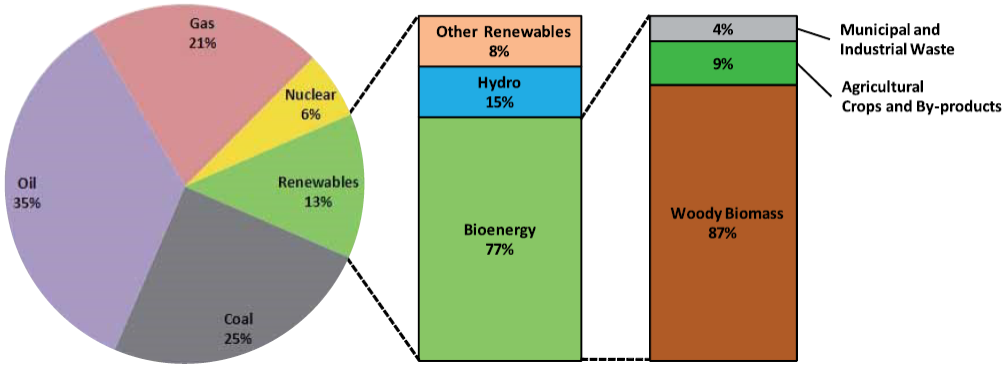

Figure 1-2 Share of bioenergy in the world primary energy mix. Sours: Extracted from Bioenergy – a Sustainable and Reliable Energy Source.it is based on IEA,2006IPCC,2007

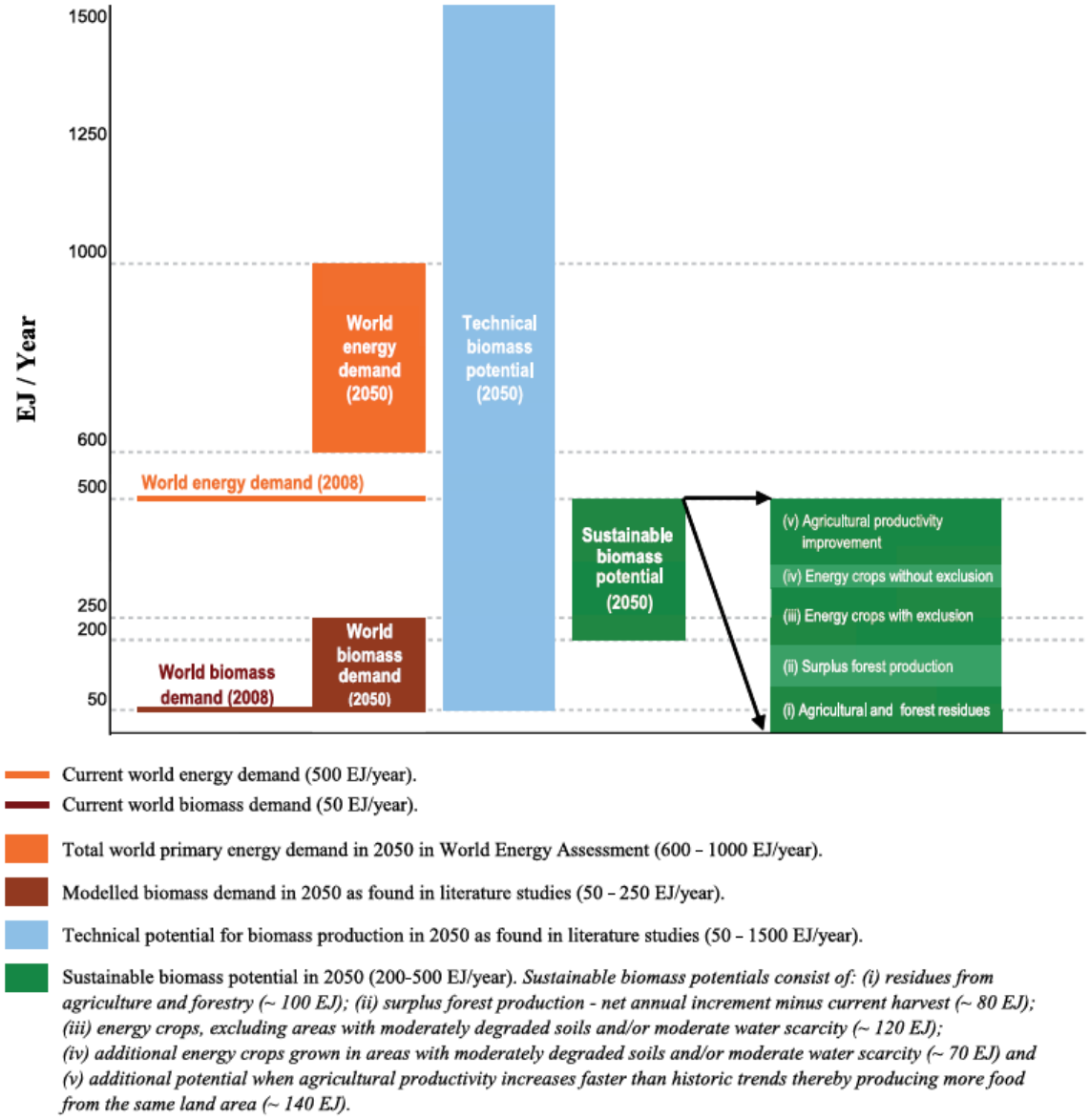

Figure 1-3 Technical biomass supply potentials, sustainable biomass potential, expected demand for biomass (primary energy) based on global energy models and expected total world primary energy demand in 2050. Current world biomass use and primary energy demand are shown for comparative purposes. Adapted from Dornburg et al,(2008) based on several review studies. Sours: Extracted from Bioenergy – a Sustainable and Reliable Energy Source.

Table 1-1 Potential of domestic biomass (annual generation and reusability rate)

Waste derived cellulose		Production volume (10^4t / year)	Concentrativity place of occurrence	Availability	Available quantity (10^4t / year)
Plants	Rice straw wheat straw	1,400	Farmland	70%	980
Woody	Forestland remainde	340	Forestland	98%	330
	Sawmill remainde	430	Factory	98%	330
	Building waste	470	Factory	30%	140
Paper	Waste paper	3,063	Urban area	9%	279

Survey by Hitachi Zosen Corporation: “Biomass Nippon Integrated Strategy Promotion Conference material (February, 2007)”, “Biomass, Energy, and Environment” (January, 2007)

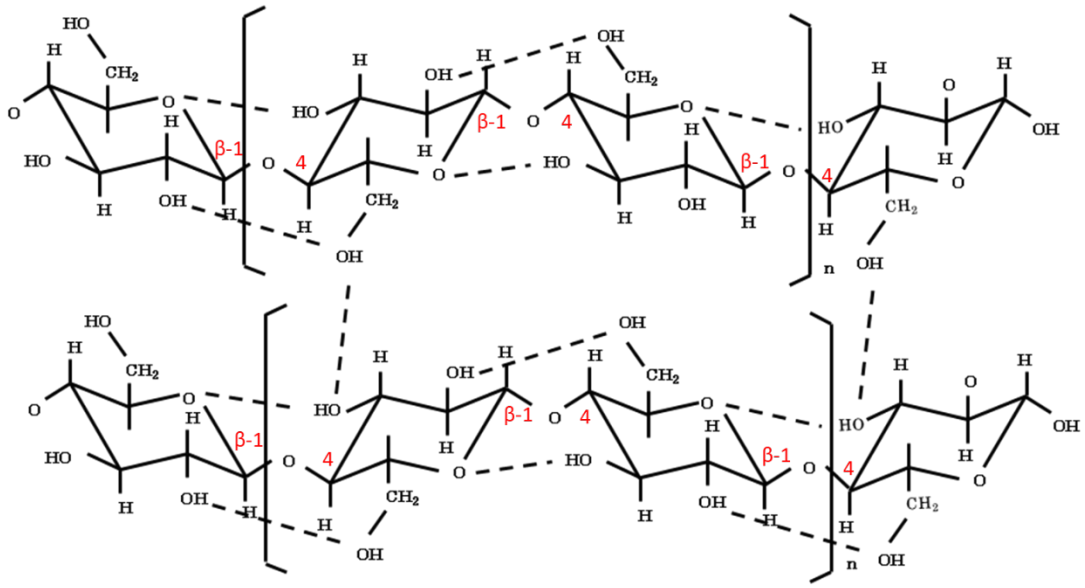

Figure 1-4 Molecular structure of cellulose. The structural unit is cellobiose, which is a structure in which glucose is linked by β-1,4 glycosides. In the cellulose molecule, the O-6 and O-2 positions, and the O-3 and O-1 positions of glucose residues are hydrogen. Bonded together, the molecules are harder to twist and stronger, and adjacent molecules also hydrogen bond.

2. Properties of cellulosic biomass

Cellulose is the main component of plant cell walls and plant fibers, and is the most abundant carbohydrate on earth. Cellulose is composed of cellobiose, a glucose precursor (a disaccharide in which two glucose molecules are connected by a β1-4 bond) (**Figure 1-4**). It is also known to have very attractive properties such as biocompatibility, biodegradability, thermal and chemical stability [Tsioptsias et al., 2008]. In addition, hydrogen bonds between adjacent sugar chains result in a highly crystalline, sparingly soluble polymer solid. Because of this monotonic molecular structure, research has been carried out as an extremely effective biomass resource that can produce glucose only by hydrolysis. In addition, humans do not have the digestive enzymes necessary to use cellulose as a nutrient source, so it does not develop into a competition between food and energy. Cellulosic biomass contains not only cellulose but also hemicellulose, lignin, etc. as the main constituents, which have a complex intertwined structure.

3. Cellulosic biomass pretreatment method

As a method for producing glucose from cellulose, acid hydrolysis method, hydrothermal treatment method, enzyme hydrolysis method is generally known. Both methods have been studied for the purpose of producing glucose efficiently and in large quantities.

(1) Acid treatment method

The acid hydrolysis method is divided into a dilute acid method and a concentrated acid method depending on the acid concentration [Grethlein, 1991, Knappert, 1980]. This pretreatment method makes it possible to break the rigid structure of lignin-hemicellulose in agricultural residues and woody biomass and is used in hemicellulose degradation. However, this mainstream process has some disadvantages [Teramoto et al., 2008]. First, recovery of sulfuric acid used for production and waste liquid treatment are expensive and have a high environmental impact. Secondly, the formation of aldehydes such as furfural when monosaccharides are produced reduces the conversion yield of polysaccharides to monosaccharides, thereby inhibiting the EtOH fermentation

process. Furthermore, it is also problematic that sulfuric acid corrodes the reaction vessel and that operations such as pH preparation before the EtOH fermentation process are complicated.

In the dilute acid method, both temperature and pressure are high, and there are problems with equipment corrosion due to the acid added and how to remove the acid from the product. In order to avoid this problem, if the acid concentration is suppressed, the production rate of glucose is lowered. In the concentrated acid method, since the temperature and pressure are lower than in the diluted acid method, an inexpensive reactor material (for example, glass fiber FRP) can be used, and the yield of glucose is also high. On the other hand, there are disadvantages that the reaction time is long and there is no economically effective acid recovery method.

(2) Hydrothermal treatment (supercritical and subcritical water treatment methods)

This is a method of hydrolyzing cellulose using subcritical or supercritical water. In recent years, methods for producing oligosaccharide or monosaccharide glucose have been proposed [Chung et al., 2007]. This technology makes use of the characteristics of supercritical water and can completely decompose cellulose into oligosaccharides and monosaccharides in a short processing time. On the other hand, oligosaccharides and monosaccharides produced by hydrolysis are subjected to high temperature reaction conditions. The yield of glucose is around 20% because it is converted into a secondary product by pyrolysis reaction. In addition, this method can be an economic disadvantage because it requires an acid treatment method and high-temperature and high-pressure conditions [Yoshida et al., 2005, Yüksel et al., 2016, Yousefifara et al., 2017].

(3) Enzymatic saccharification method

Enzymatic hydrolysis method has no merit and has the advantage that it can be reacted under mild conditions compared to the above two methods. For example, cellulase known as a general cellulose hydrolase has an optimum reaction condition of 45 °C under pH-4.8 conditions. On the other hand, the

reaction rate is relatively low, and it is necessary to devise measures to improve factors such as enzyme adsorption and product inhibition. As a result, research for practical use is still being conducted.

Even in the enzymatic saccharification method, the slow reaction rate, the high price of the enzyme, and the need for pretreatment are cited as problems. In recent years, enzymatic saccharification methods are often used, because there are advantages such as low environmental burden to eliminate the disadvantages of using mineral acids such as sulfuric acid and high recovery of monosaccharides. However, lignocellulose is a state in which cellulose, hemicellulose, lignin and the like are mainly intertwined. For this reason, the enzyme alone cannot easily access the substrate and is difficult to hydrolyze. Therefore, it is important to increase the accessibility of the enzyme to cellulose by pretreatment.

4. Enzymatic hydrolysis of cellulosic biomass.

Cellulase is a general term for enzymes that hydrolyze the β-1,4-glycosidic bonds of cellulose chains.

(1) Cellobiohydrolase (CBH; EC 3.2.1.91, EC 3.2.1.176)

An enzyme that hydrolyzes cellobiose units from the end of the cellulose chain, regardless of the crystalline or amorphous region, and acts on the non-reducing end (EC 3.2.1.91) and CBH (EC 3.2.1.176) acting on the reducing end.

(2) Endoglucanase (EG; EC 3.2.1.4)

An enzyme that randomly cleaves within the amorphous region of the cellulose chain and produces cellooligosaccharides, cellobiose, glucose, and so on. Little effect on the crystalline region.

(3) β-Glucosidase (BGL; EC 3.2.1.21)

An enzyme that cleaves the β-glycosidic bond at the non-reducing end and hydrolyzes cellooligosaccharides and cellobiose produced by the above two enzymes to produce glucose.

It is speculated that these three substances act synergistically during the decomposition of crystalline cellulose and the decomposition proceeds. In other words, EG cleaves the amorphous region partially present in crystalline cellulose, resulting in a new sugar chain end. CBH acts on this end, scraping the surface of crystalline cellulose fiber, and the amorphous region inside the cellulose fiber is exposed on the surface and EG acts. In this way, CBH and EG create a region where they can interact with each other, and it is thought that a synergistic effect occurs (endo-exo synergy model)

Some cellulases have carbohydrate adsorption modules in addition to the catalytic domain responsible for catalytic activity. It is considered that the carbohydrate adsorption module interacts with cellulose as a substrate, so that the catalytic domain approaches the cellulose surface and contributes to the efficiency of cellulose degradation.

Hemicellulase is a general term for enzymes that degrade hemicellulose. Since hemicellulose is a heteropolysaccharide and its structure varies depending on the plant species, many types of enzymes are involved in hemicellulose degradation. Various endo- and exo-type enzymes are required for complete degradation of hemicellulose, and the degradation process is very complicated. This is due to the fact that hemicellulose has a branched structure and the substrate recognition of enzymes involved in degradation. Cellulase and hemicellulase information is shown in **Table 1-2**.

Table 1-2 An enzyme that selectively hydrolyzes cellulose, hemicellulose, etc. and a binding site involved in degradation.

Znzyme	Mode of hydrolysis of cellulose and hemicellulose	CAZy Familles	EC number
Cellotiohydrolase	Hydrolyze each end of the cellulose chain. Mainly produces cellobiose.	GH5,6,7,9,12,48	EC3,2.1.91 EC 3.2.1.176
β-1,4-endoglucanase	Random hydrolysis of the amorphous cellulose chain. Produces glucose, cellobiose and cellooligosaccharides.	GH5,6,7,8,9, 12,44,45,48, 51,74,124	EC3.2.1.4
β-1,4-glucosidase	Hydrolysis of the non-reducing end of cellobiose and cellooligoid produces glucose	GH1,3,30,116	EC3.2.1.21
endo-8-1,4-ylanase	Randomly hydrolyze the inside of the xylan main chain. Mainly produces quinrobiose and xylo-oligosaccharides	GH5,8,10, 11, 43	EC3.2.1.8
β-1,4 endomannannase	Hydrolyzes the bond between mannose inside the main chain to produce galactoglucomannan, etc.	GH 5,26, 113	EC3.2.1.78
xyloglucan 8-1.4-endoglucanase	Hydrolyzes glycosidic bonds inside the xyloglucan backbone.	GH5.12.16.44.74	EC3.2.1.151
β-1,4-xylosidaso	Hydrolyzes xylobiose, xylooligosaccharides, etc. Releases non-reducing end xylose.	GH 3.30.39.43.52.54.120	EC3.2.1.37
α.L-arabinofuranosidase	Hydrolyze side chains such as glucuronoarabinoxylan. Release α-L-arabinofuranose from the non-reducing terminal.	GH3.43.51.54.62	EC 3.2.1.55
β-mannosidase	Hydrolyzes oligosaccharides such as galactoglucomannan. Releases β-mannose from the non-reducing terminal.	GH 1.2.5	EC 3.2.1.25
xylan α-1,2-glucuronidase	Hydrolyze side chains such as glucuronoxylan. Release glucuronic acid from the non-reducing terminal..	GH 57.115	EC 3.2.1.131
α-galactosidase	Hydrolyze side chains such as galactoglucomannan. Releases galactose from the non-reducing terminal.	GH 4.27.36.57.97.110	EC 3.2.1.22
β-galactosidase	Hydrolyze side chains such as xyloglucan. Releases galactose from the non-reducing terminal..	GH 1.2.35.42	EC 3.2.1.23
α-fucosidase	Hydrolyze xyloglucan side chain to release terminal L-fucose.	GH 29.95	EC 3.2.1.51
α-xylosidase	Hydrolyzes xyloglucan side chain, isoprimivelose. Release α-D-xylose from the non-reducing terminal.	GH 31	EC 3.2.1.177
Acetylesterase	Hydrolyzes acetyl groups in various carbohydrates	CE 16	EC 3.1.1.6
acetykylan esterase	Hydrolysis of acetyl group on xylan side chain.	CE 1.2.3.4.5.6.7.12	EC 3.1.1.72
feruloyl cstcrase	Hydrolyzes ester bonds between feruloyl groups and carbohydrates.	carbohydrate	EC 3.1.1.73

5. Properties and application fields of ionic liquids

(1) Types and configurations of ionic liquids

The ionic liquid is a compound composed of a strong electrostatic interaction force acting between a cation and an anion, and is a molten salt that becomes a liquid near 100 °C [Rogers et al., 2003, Seddon et al., 1997]. Furthermore, various ionic liquids can be prepared depending on the combination [Matsumoto et al., 2000, Forsyth et al., 2004]. An ionic substance is an insulating solid with no vapor pressure.

However, when melted, it becomes solvent-free and ion-conductive liquid. This was originally the name for the liquid state of ionic substances called ionic liquids or molten salts. Since the 1980s, many low-melting salts using cations such as alkylammonium have been developed. In particular, many room temperature molten salts that exhibit a liquid state even near room temperature have been synthesized. Since the 1990s, stable salts that hardly absorb moisture in the air and do not hydrolyze have appeared [Wilkes et al., 1992, Bonhote et al., 1996]. From this time on, the name ionic liquid has been used as a generic term for a group of ionic compounds exhibiting such a low melting point, not in the state of ionic substances.

Typical cations and anions have been reported [Ngo et al., 2000, Carmichael et al., 2000, Earle et al., 2000, Noda et al., 2000]. (**Figure 1-5**).

Representative cations

Derived from aromatic amines: dialkylimidazolium and alkylpyridinium.

Aliphatic amines: tetraalkylammonium, cyclic pyrrolidinium, phosphonium Compounds

Representative anions

Halogen anion: Cl^-, Br^-, I^-, etc

Many fluorine-containing anions: BF^-, PF^-, CF^-, etc.

RTILs consist of organic anions: $[CF_3SO_3]^-$, $[(CF_3SO_2)_2N]^-$, $[CF_3CO_2]^-$

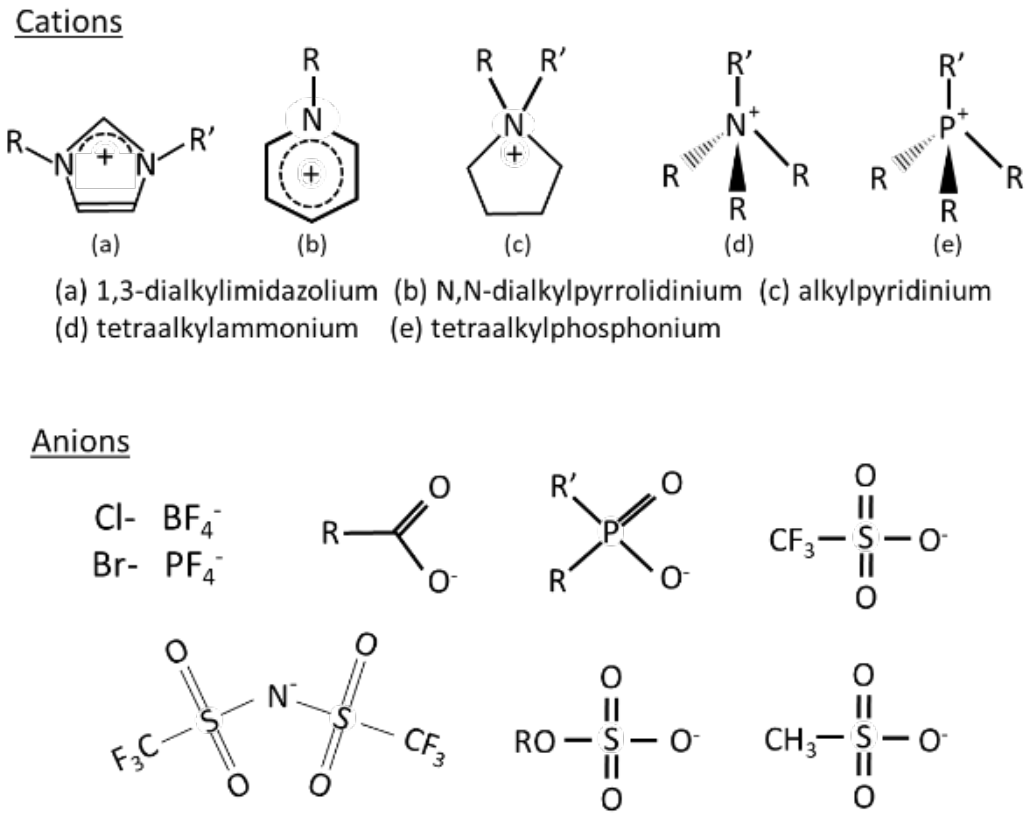

Figure 1-5 Typical cations and anions in ionic liquids.

The nature of the ionic liquid changes depending on various factors such as the molecular size of the constituent ions, molecular structure, charge distribution (delocalization) within the molecule, and electrostatic interaction between the molecules (between cation and anion) Although it is difficult to predict, the structure and physical properties of ionic liquids basically depend on their chemical structure. For example, viscosity and conductivity increase as the alkyl chain length of the cation increases (molecular weight increases), and the viscosity increases and the melting point and conductivity decrease [Takahashi et al., 1991].

In addition, with regard to reduction resistance, reduction resistance improves when the proton at the 2-position of the imidazolium cation is substituted with an alkyl group [Gifford et al., 1987]. Because ionic liquids have

non-volatile, non-flammable, and conductive properties, they are widely applied to catalysts, extraction, electrochemistry, synthetic chemistry, etc. [Gifford et al., 1987]. Because ionic liquids have characteristics such as non-volatility, nonflammability, conductivity, and a wide liquid range, they are used in a wide variety of applications such as catalysis, extraction, electrochemistry, and synthetic chemistry [Hagiwara et al., 2004, Bosmann et al., 2001, Galinski et al., 2006, Adams et al., 1998, Fischer et al., 1999, Snedden et al., 2003]. For this reason, a large number of ionic liquids have been synthesized by combinations of cations and anions and the selection of functional groups on cations depending on the application. Since ionic liquids consist only of ions, there are no neutral molecules in the liquid that have no charge. Phenomenon released from the atmosphere, that is, does not evaporate (volatilize). Such properties of ionic liquids are maintained until the liquid reaches the pyrolysis temperature at high temperatures. For this reason, the gas evaporated from the liquid surface is not supplied for combustion like ordinary organic compound liquids, and it exhibits incombustibility or flame retardancy. Naturally, ions have fluidity. Therefore, unlike ordinary organic solvents, ion migration occurs when an electric field is applied, that is, conductivity is a major feature

(2) IL as a cellulose solvent

The research on green chemistry introduced in this paper is a field that has received much attention in recent years. The research on green chemistry introduced in this paper is a field that has received much attention in recent years. Until 2002, Rogers et al. Revealed that the ionic liquid 1-butyl-3-methylimidazolium chloride ([C4mim] Cl) dissolves cellulose, the chemical conversion of cellulose in clothing fibers and papers Difficult [Pinkert et al., 2009, Sen et al., 2013, De Maria et al., 2014]. In addition, it was reported that regenerated cellulose precipitated from this solution significantly accelerates hydrolysis to glucose by cellulase [Swatloski et al., 2002]. Enzymes that exhibit a catalytic function using only ionic liquid as a solvent are limited to lipase, while many examples of enzyme activity appear in mixed solvents of water and

ionic liquid [Itoh et al., 2017]. Cellulose, a biopolymer, does not dissolve in water or many molecular liquids.

The mechanism by which polymers such as cellulose dissolve in ionic liquids is an interesting research theme from the standpoint of polymer chemistry. For this reason, the development of ionic liquids that dissolve biopolymers such as cellulose, chitin, and lignin began to compete. The mechanism by which polymers such as cellulose dissolve in ionic liquids is also an interesting research theme from the standpoint of polymer chemistry.

Therefore, the development of ionic liquids that dissolve biopolymers such as cellulose, chitin, and lignin began to compete. Ohno et al. Suggest that the key to cellulose solubility is the hydrogen bond acceptability of ionic liquids [Ohno et al., 2009, Fukuya et al., 2008, Abe et al., 2010]. As a result, research has progressed rapidly, and the number of papers is increasing.

6. Aqueous two-phase system (ATPS)and research trends

When two polymers with different chemical structures are dissolved in water, it may separate into two phases. This system is called an aqueous polymer two-phase system. In addition, various materials can be separated using these two-phase distributions. Similarly, aqueous two-phase systems can be prepared by adding specific salts to the polymer. ATPS has been applied as a liquid-liquid extraction method, and is a technology applied to the separation and extraction of amino acids, proteins, nucleic acids, viruses, etc. The aqueous two-phase systems reported so far are classified as follows:

(1) Polymer - polymer system formed from two different types of polymers

The polymer-polymer system is characterized by low ionic strength. That is, it is used to separate, recover and purify solutes that are sensitive to the ionic environment. Generally, these are formed with polyethylene glycol (PEG) and dextran. Especially in the field of biochemistry, two-phase systems using polyethylene glycol and dextran have been used [Albertsson et al., 1990]. In this case, the upper phase is an aqueous solution containing PEG, and the lower

phase is an aqueous solution containing dextran. An aqueous two-phase system can also be prepared using an aqueous PEG solution and a highly concentrated aqueous inorganic salt solution, where the PEG separates into the upper phase and the salt is concentrated into the lower phase. There have been several reports on the phase separation of aqueous polymer solutions. The cause of phase separation is considered by the theory of Flory-Huggins [Gustafsson et al., 1986, Sioberg et al., 1989]. Compared to the case where different polymers coexist and the case where monomer units exist independently, the mixing entropy is smaller. This is because high-molecular polymers are connected in a chain, and phase separation occurs even if the repulsion between different monomer units is weak. The PEG / dextran system is widely used in the biochemical field, and separation of biopolymers, membranes, cells, etc. has been performed.

In a report on the hydrolysis of cellulose by an enzyme, a semi-continuous reaction using an aqueous two-phase system [Tierneld et al., 1985, Tierneld et al., 1985], cellulose particles and enzyme are distributed in the lower phase, and the product moves to the upper phase. Here, the most important factor is the affinity between the enzyme and cellulose [Tierneld et al., 1985], and it has been clarified that the molecular weight of the lower phase polymer is reduced, and that the smaller the upper phase polymer, the smaller the enzyme partition coefficient.

(2) Systems formed from polymers and salts

In the industrial field, PEG / salt systems that are economically superior in enzyme extraction are widely used [Kula et al., 1982, Hustedt et al., 1985, Hustedt et al., 1985, Veide et al., 1984, Kroner et al., 1984]. Mainly used is a system formed by polymer and phosphate, sulfate, citrate, etc. It is characterized by low viscosity and high density between phases compared to polymer / polymer system. In this field, phosphate has been used for a long time, and in recent years, wastewater treatment is an important issue in industrial processes, and the case of using citric acid has been studied. Furthermore, depending on the combination of alcohol and salt, a two-phase separation system is formed.

In the polymer-polymer system, water is the main component in both phases, and so much research has been done on the separation of biopolymers. On the other hand, the usual salting out operation may cause unnecessary chemical reaction, and the polymer as the phase separation agent is expensive and difficult to recover. Therefore, a two-phase separation system using the salting out effect has attracted attention. This method uses a water-miscible organic solvent such as ethanol and a salt as a phase separation agent. The water-miscible organic solvent undergoes phase separation due to the interaction of high-concentration salt and water molecules.

Extraction separation of lipase [Merchuk et al., 1998] and 2,3-butanediol [Ooi et al., 2009] has been reported in this field. These systems are also characterized by low viscosity, simple component recovery, and reduced settling time, but the main disadvantage of using this type of ATPS is that many proteins are not compatible with alcohol-rich phases [Louwrier et al., 1998, Jiang et al., 2009].

A few micelle / reverse micelle systems using non-ionic / ionic surfactants have been reported [Gutowski et al., 2003].

(3) System formed from ionic liquid and salt

The ionic liquid aqueous two-phase system (IL-ATPS) handled in this study is the two-phase system that has received the most attention in recent years. Bis (trifluoromethanesulfonyl) imide ([Tf2N]-) and hexafluorophosphate (PF6) are used as constituent ions. Hydrophobic ionic liquids that phase separate from water can be obtained using anions containing fluorine atoms such as-) [Bonhote et al., 1996, Huddleston et al., 2001].

On the other hand, even if it is a hydrophilic ionic liquid that is miscible with water in any proportion, it is separated into a hydrated ionic liquid phase and an aqueous inorganic salt phase by appropriately mixing an inorganic salt with a high salting-out effect [Gutowski et al., 2003]

These ionic liquid-salt aqueous two-phase systems are stable and are always easy to handle because they maintain a phase-separated state, and are being

developed in various fields from interface state analysis to compound solubility control.

7. Overview of this study

The final purpose of this study is to analyze the kinetics of cyclic hydrolysis of regenerated cellulose prepared by IL, and to develop the separation and recovery of IL by IL-ATPS and the design of saccharification process. In particular, the design of IL-ATPS was compiled from the viewpoint of quantitative evaluation of two-phase separation using phase diagrams and the effect of low-concentration ionic liquids on saccharification. In addition, the basic concepts of process design with a focus on industrial processes were presented.

In Chapter 1, Focusing on the current status of biomass and green chemicals as the background of the research, and it was summarized the research on cellulose pretreatment, physical properties of ionic liquid, cellulose interaction, and cellulase, which are the main points of this research, and also surveyed trends in the types of aqueous two-phase systems and ionic liquid aqueous two-phase systems, and found process design tips.

In Chapter 2, In the enzymatic hydrolysis of crystalline cellulose, dissolution and non-crystallization of cellulose is one of the rate-limiting steps. In order to analyze the kinetic parameters, Langmuir adsorption model and Michaelis menten model were adopted to evaluate enzymatic hydrolysis of cellulose in the low IL concentration range. The effect of IL species on cellulose dissolution was quantitatively evaluated based on kinetic parameter analysis. It was suggested that the control of IL concentration may greatly affect the efficiency of enzymatic saccharification in batch reactions.

In Chapter 3, To investigate the phase separation behavior of the IL-ATPSs, binodal curves were drawn at different temperatures, and the length and slope of the tie lines were analyzed. Furthermore, the phase separation behavior was evaluated by changing the combination of salt and ionic liquid. Using the IL-ATPS, the distribution coefficients Kaa of amino acids were determined and used to characterize the hydrophobicity index (HF) between the top and bottom phases, which is a good indicator to understand the molecular partitioning behaviors in conventional ATPSs. The HF value of IL-ATPS was

found to be almost the same as that reported for ATPS composed of polyethylene glycol and salt.

In Chapter 4, Regenerated cellulose can be prepared by treatment with an ionic liquid (IL) and an anti-solvent such as water, which significantly enhances the physiological hydrolysis in comparison to crystalline cellulose. The IL-aqueous two-phase system (IL-ATPS) is consisted of IL-condensed upper phase and salt-condensed bottom phase, which could be suitable to produce regenerated cellulose with smaller amount of IL. Several IL-ATPS were prepared by combining different types of ionic liquids and salts to determine the enzymatic saccharification efficiency of crystalline cellulose. In addition, it was evaluated the effect of salt on pH and developed the logic that led to process design.

In Chapter 5, As a general conclusion of this study, in the IL-ATPS with a combination of IL and salt, UCST-type phase separation in which most IL is separated in the upper phase occurs in a self-organized manner. It was also shown that processes incorporating these into the enzymatic hydrolysis of cellulose could lead to future bioethanol production technologies.

The framework and flowchart for this study are shown in **Figure 1-6** and **Figure 1-7**, respectively

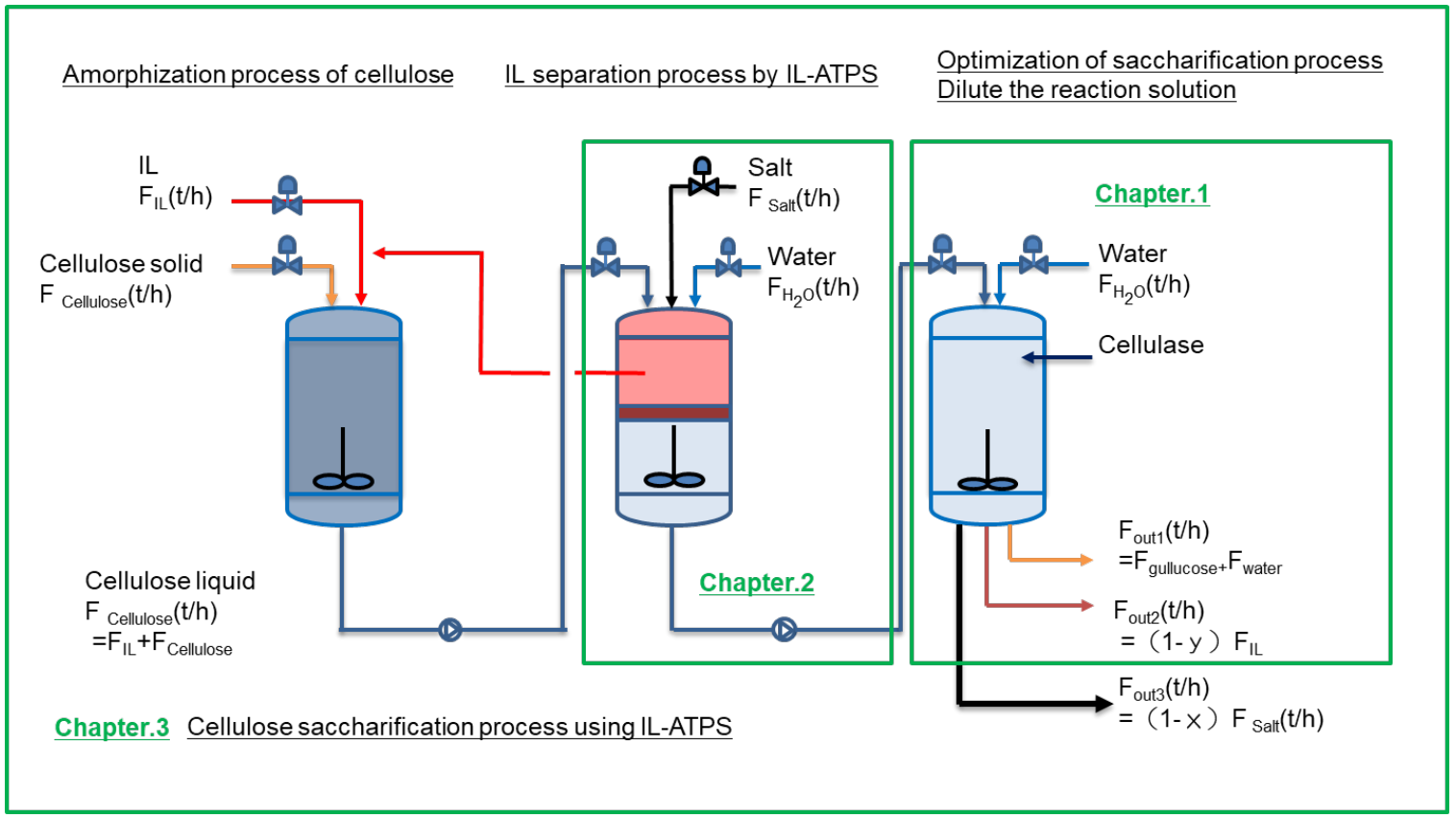

Figure 1-6 Concept map of this study

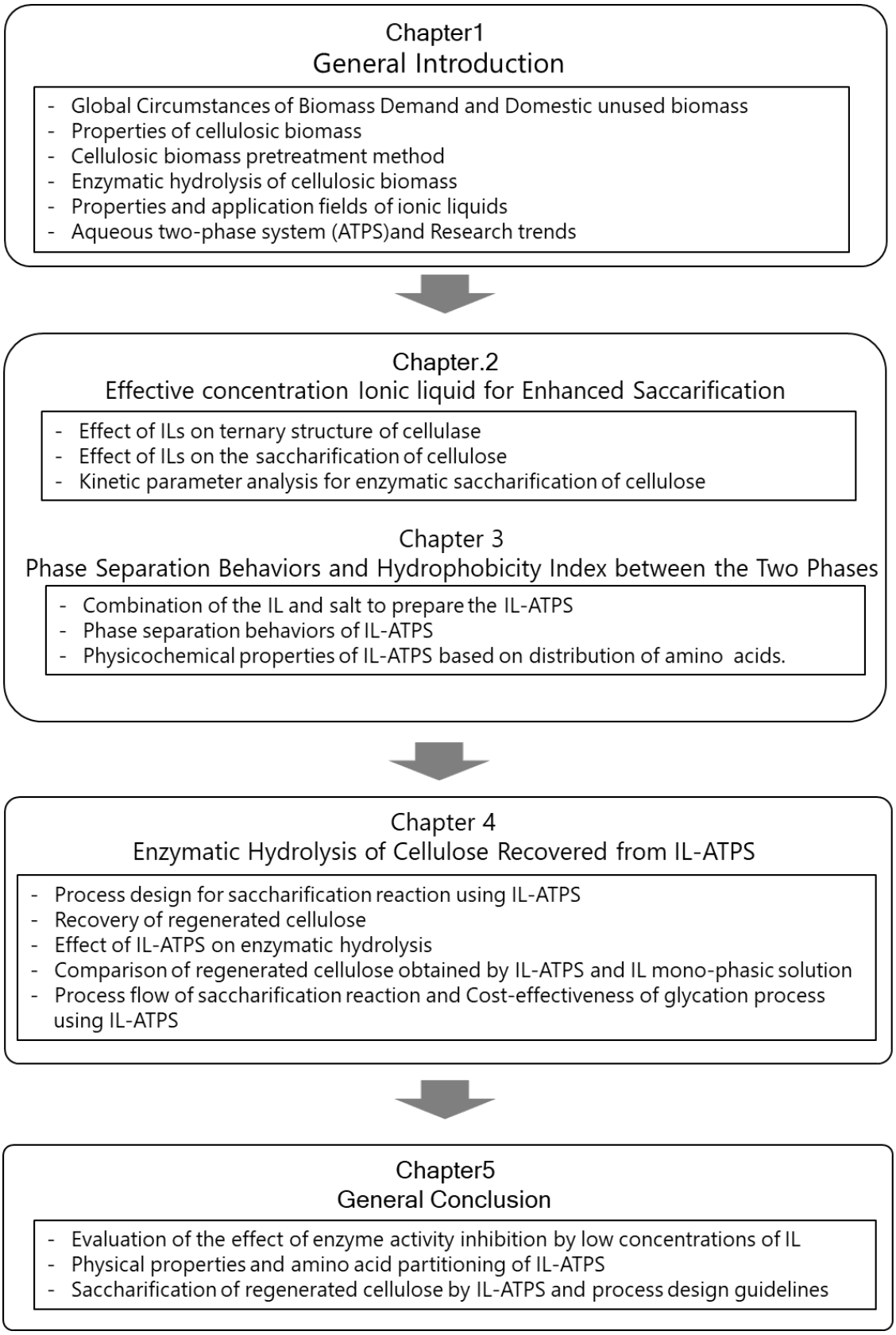

Figure 1-7 Framework of this study

Chapter 2

Effective Concentration of Ionic Liquids for Enhanced Saccharification of Cellulose

1. Introduction

Cellulose is a woody biomass which is attracting attention as renewable energy. Cellulose has high crystallinity and is insoluble both in water and in organic solvents. The enzymatic saccharification is environmental-friendly energy generating process, while, the irreversible adsorption of the enzyme on the crystalline cellulose surface causes deactivation and reduction of contact efficiency. This prevents continuous glucose production in aqueous phase [Mansfield et al., 1999, Beldman et al., 1987]. To overcome such insolubility of crystalline cellulose, the dissolution methods have been developed, by utilizing acids (sulfuric acid or hydrochloric acid), alkali (NaOH, KOH, $Ca(OH)_2$, or ammonia), organic solvents (ethylene glycol, glycerol, tetrahydrofurfuryl alcohol), amphiphilic polymers, and ionic liquids (ILs) [Ghasemi et al., 2017, Agbor et al., 2011, Karimi et al., 2016].

ILs are organic salts comprised of anion forming an ion pair for organic cation and it. In order to develop a cellulose saccharification process with high efficiency, it is necessary to achieve (i) dissolution of crystalline cellulose and (ii) hydrolysis of regenerated cellulose in aqueous phase [Dadi et al., 2006, Mora-Pale et al., 2011, Moniruzzaman et al., 2013, Vancouver et al., 2012, Zhao et al., 2009, Zhao et al., 2010], at the same time. On the other hand, enzymes tend to interact with IL and then their activities can be decreased due to denaturation. It has been reported that the ternary structure of cellulase, which is monitored by intrinsic tryptophan (Trp) fluorescence (ex: 295 nm, em: 330-350nm), can be denatured by the presence of tris-(2-hydroxyethyl)-methylammonium methylsulfate and 1-butyl-3-methylimidazolium chloride ([Bmim][Cl]) [Turner et al., 2003, Bose et al., 2012]. Thus, the competitive effects are derived by the use of IL in enzymatic saccharification processes: i.e., a promoting effect due to enhanced dissolution of cellulose, on the other hand, an inhibiting effect due to the denaturation of enzymes.

The enzymatic saccharification processs of biomass source have been studied, especially focusing on the pretreatment methods: physical, chemical, physico-chemical,

biological and combined pretreatments [Kumari et al., 2018]. Alkaline treatment is popular and easier in large scale reaction, while most of cellulase is optimized in acidic condition [Zhang et al., 2012]. Ultrasonic irradiation can be applied to various kinds of cellulose source [Li et al., 2004]. A huge number of studies have been carried out for the treatment of cellulose with IL [Wahlström et al., 2015]. Via overviewing on the reported works, it is obvious that the positive effect of IL, i.e. dissolution of crystalline cellulose and the negative effect of IL, i.e. inactivation due to denaturation, is competitive (trade-off relationship), however, an systematic studies to investigate the optimized IL conditions are not well studied.

The aim of this study is to investigate the effect of ILs on the enzymatic saccharification of cellulose using cellulase from *Trichoderma viride*, based on kinetic analysis. The saccharification of dissolved cellulose was estimated by monitoring the production of glucose, in the presence of ILs with various concentrations. It is also necessary to discuss the conformational stabilize of cellulase, and its enzymatic activity. Based on the kinetic parameters obtained, different effects of [Bmim][Cl] and 1-allyl-3-methylimidazolium chloride ([Amim][Cl]) were discussed.

2. Materials and Methods

2.1. Materials

1-Butyl-3-methylimidazolium chloride ([Bmim][Cl]) and 1-allyl-3-methylimidazolium chloride ([Amim][Cl]) were purchased from Kanto Kagaku (Tokyo, Japan) and Sigma-Aldrich (St. Louis, MO), respectively. Crystalline cellulose powder was purchased from Nacalai Tesque (Kyoto, Japan). Cellulase from *Trichoderma viride* (≥5,000 units/g solid) was purchased from Yakult Pharmaceutical Industry (Tokyo, Japan). Other chemicals were obtained from Wako Pure Chemical Corporation (Osaka, Japan), and used without further purification.

2.2. Evaluation of IL concentration dependence of cellulose saccharification activity

Based on the reference, the reaction mixtures were prepared [Yoshimoto, M. et al., 2013]. Briefly, an aliquot amount of IL ([Amim][Cl] or [Bmim][Cl]) and cellulose was heated at 100 °C for 5 minutes to dissolve cellulose, with stirring at 750 rpm. After cooling down to room temperature, an aliquot amount of acetate buffer (25 mM, pH 4.8)

including cellulase was added to adjust the reaction volume to 20 mL. The final cellulose concentration was 2 g/L, and the final cellulase concentration was 9.1 mg/L. The final concentration of IL was varied from 0 to 15 wt%., and then the sample was incubated at 45°C, with a stroke speed of 60 rpm. Glucose concentration was measured using Glucose CII Test Wako kit® [Miwa et al., 1972].

2.3. Measurement of intrinsic Trp fluorescence

IL solution was prepared by adding 25 mM acetate buffer (pH 4.8) while heating and stirring with [Amim][Cl] or [Bmim][Cl] for 5 minutes at 100 °C. After cooling down to room temperature, then cellulase solution was added to the prepared IL solution. The total cellulase concentration was 9.1 mg/L. The final concentration of IL was varied from 0 to 7.5 wt%. The prepared sample was incubated at 45 °C for 5 min. After that, the fluorescence spectrum of intrinsic tryptophan (Trp) was measured at 45 °C. An excitation wavelength was 295 nm, and the spectrum was recorded at every 0.1 nm, using a Spectrofluorometer (FP-8500, JASCO, Tokyo, Japan).

3. Results and Discussion

3.1. Effect of ILs on ternary structure of cellulase

Intrinsic Trp fluorescence derived from protein or enzyme can be a good indicator for its ternary conformation, because the emission peak of Trp can be shifted by the surrounding dielectric environment: when Trp is exposed to a hydrophobic environment, the emission peak has responded to shift to a lower wavelength [Zahid et al., 2013]. Conformational changes of cellulase in the presence of ILs were determined by monitoring the emission peaks of intrinsic Trp (**Figure 2-1**). In both cases of [Amim][Cl] and [Bmim][Cl] at 45 °C, the emission peaks were slightly to higher frequency (red-shift), just after mixing of cellulose and IL. No significant peak shifts were observed in [Amim][Cl] under IL concentration of <5wt%, while [Bmim][Cl] gradually induced red-shift, in proportion to IL concentration. The fluorescent intensities of Trp drastically decreased by ILs (data not shown). Turner *et al*. reported that the denaturation of cellulase from *Trichoderma reesei* can be induced by the presence of sodiumdodecylsalfate, urea, and [Bmim][Cl] [Turner et al., 2003]. It has been also reported that the intrinsic Trp fluorescence of hexsokinase can be depending on the type of the additives, where the

wave length was shifted with 2-4 nm [Umakoshi et al., 2012]. In the presence of 7.5wt% IL, the red-shifts were significantly observed (~ 10 nm) in both cases of [Amim][Cl] and [Bmim]][Cl], suggesting that the presence of IL with the concentration more than 7.5wt% lead the cellulase denaturation at 45 ℃. IL itself could be hydrophobic as compared to water. Thus, the red-shift of Trp peak in the presence of 7.5wt% IL suggests that the intrinsic Trp in cellulase could be exposed to bulk water by the denaturation effect of IL. Although the Trp fluorescence could be influenced by the viscosity of solution, the increase of IL concentrations hardly observed even in the IL concentration of 15 wt% (**Figure 2-2**). Therefore, the peak shift of intrinsic Trp could be derived by the denaturation of cellulase by IL.

The viscous environment, coursed by the presence of IL and dissolved cellulose, might inhibit the diffusion of substrate and enzyme. The viscosity of the reaction mixture (in the absence of enzyme) was analyzed as a function of IL concentration (**Figure 2-2**). With a treatment of [Amim][Cl], the viscosity slightly increased in proportion to IL concentration. In contrast, the [Bmim][Cl] samples showed almost similar viscosities in the absence or presence of cellulose. In both cases, the increase of the viscosity was only slightly, suggesting that the influence of solution viscosity on saccharification reaction could be negligible.

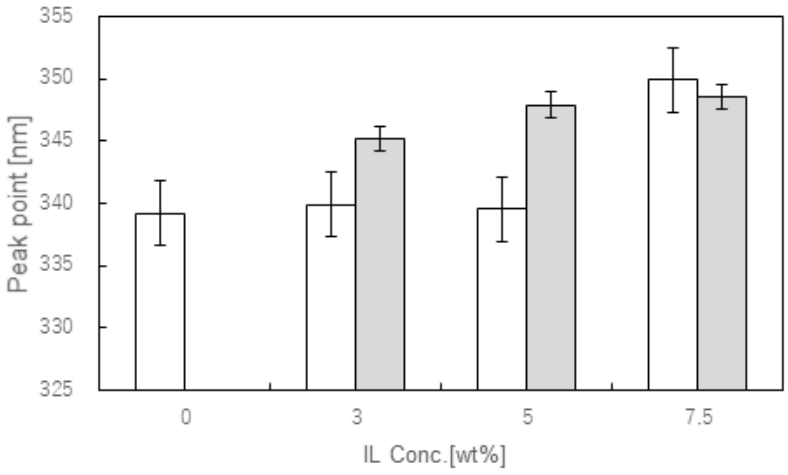

Figure 2-1 Intrinsic Trp fluorescence emission peaks of cellulase in the presence of [Amim][Cl] (*open bar*) and [Bmim][Cl] (*closed bar*). The measurements were conducted at 45 ℃.

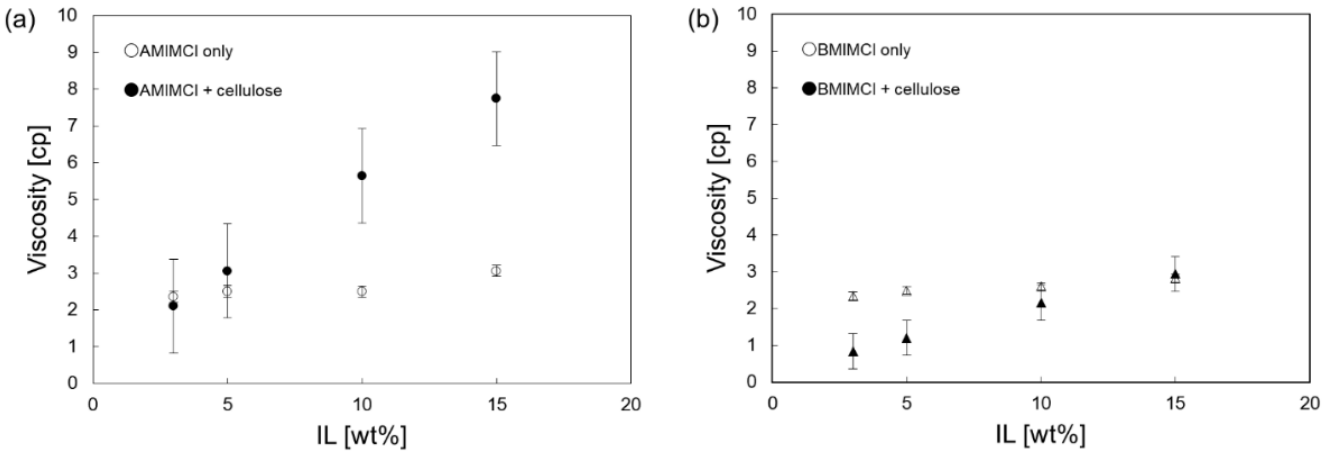

Figure 2-2 Viscosities of solutions including (a) [Amim][Cl] and (b) [Bmim][Cl], in the presence of cellulose.

3.2. Effect of ILs on the saccharification of cellulose

The dissolution of cellulose is a bottleneck step in enzymatic saccharification process, in which IL can promote the dissolution of crystalline cellulose [Lopes et al., 2017]. In the absence of ILs, the saccharification reaction could be carried out at the solid-liquid reaction between crystalline cellulose and cellulase, resulted in less productivity of glucose. In this case, the reaction of cellobiohydrolase could be dominant because it binds to the terminal of non-reducing crystalline cellulose, however the hydrolysis reaction at the amorphous part could be weaken. Totally, the glucose production could not be promoted without ILs [Dadi et al., 2006]. By pretreatment of cellulose with ILs, most parts of crystalline cellulose turned to be amorphous state, thus the hydrolysis of soluble cellulose can be drastically improved [Bose et al., 2012]. Herein, the cellulose hydrolysis reaction was carried out with different concentrations of IL: 0 to 15 wt% in 25 mM acetate buffer (pH 4.8) (**Figure 2-3**). The glucose production was most increased with 5wt%-ILs, in both cases of [Amim][Cl] and [Bmim][Cl]. Since the regenerated cellulose was accumulated in the reaction mixture as amorphous state, the activity of endoglucanase could be enhanced. Although the presence of ILs can promote the dissolution of cellulose, the glucose productions were inhibited with higher concentrations of ILs ([IL] >10wt%) (**Figure 2-3(c)**). The inactivation effect was more

significant with [Bmim][Cl]. This could be related to the denaturation effect of IL: the peak shift of intrinsic Trp fluorescence by [Bmim][Cl] was greater than that by [Amim][Cl] (**Figure 2-1**). It is concluded that the enzymatic saccharification of cellulose was optimized with 5wt%-ILs.

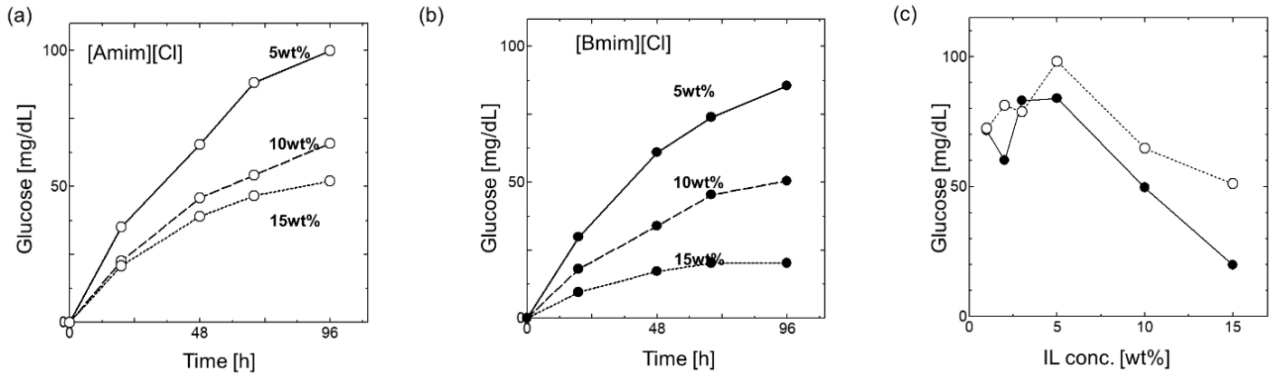

Figure 2-3 Glucose production in the presence of (a) [Amim][Cl] and of (b) [Bmim][Cl]. (c) Dependence of IL concentration on the glucose production, with [Amim][Cl] (*open circle*) or with [Bmim][Cl] (*closed circle*). All experiments were conducted at 45 ^{o}C with 96 h incubation, 20 mg of cellulose, 9.1 μg/mL of cellulase. The sample volume was 20 mL.

3.3. Kinetic parameter analysis for enzymatic saccharification of cellulose

In this reaction system, the initial concentration of glucose precursor was 1.23×10^{-2} M (2 g/L of ($C_6H_{10}O_5$)), while the obtained glucose concentration was ~ 6.17×10^{-3} M (~100 mg/dL of ($C_6H_{12}O_6$)). Such saturations in conversion values were due to adsorption of cellulose onto amorphous cellulose. Herein, the Langmuir type adsorption model and a first-order reaction kinetics were applied to analyze obtained data. Experimental data were fitted using following equation:

$$C = C_{ini} \times Q_{max} (1 - \text{Conv}\%) \qquad \text{(Eq.2-1)}$$

wherin C, Q_{max}, and Conv% represent the actual concentration of glucose precursor available for reaction, the maximal adsorption value, and obtained conversion value,

respectively. C_{ini} was 2 g/L, thus 1.23×10^{-2} M. The Langmuir adsorption isotherm is described as followings:

$$C/C_{enz} = Q_{max}\, K\, C_{ini}\times\mathrm{Conv}\% / (1 + K\, C_{ini}\times\mathrm{Conv}\%)$$
$$= Q_{max}\, K\, Y / (1 + K\, Y) \qquad \text{(Eq.2-2)}$$

wherein C_{enz}, Q_{max}, and K represent the concentration of enzyme, maximal adsorption value, and affinity between enzyme and substrate (i.e., glucose precursor), respectively. The constants Q_{max} and K were decided by try-and-error method, which satisfied the R^2 value >0.99. Here, KY is defined as conversion capacity. This value indicates the degree of inactivation of the enzyme to IL. Fitting results are shown in **Figure 2-4** and **Table 2-1**. In the case of [Bmim][Cl], the Q_{max} values were decreased in proportion to IL concentration, suggesting that the amount of substrate (i.e., dissolved cellulose) decreased. This indicate that a high concentration of [Bmim][Cl] can inhibit the binding of enzyme such as endoglucanase. Then, the analyzed reaction rate constants, k_c, are summarized in **Figure 2-5** Furthermore, the sensitivity of Q_{max} and KY to IL concentration was evaluated as a relative value based on IL5 wt% (Table 2-1). Ionic liquids amorphize cellulose, which may increase the adsorption between enzyme and substrate, but the decrease in Q_{max} with increasing IL concentration inhibits enzyme and substrate adsorption by IL Suggest that. Also, the KY reduction rate tends to be stronger than that of Q_{max}.

That is, it was quantitatively determined that the enzyme in IL was affected by both adsorption and deactivation. The k_c values increased in proportion to IL concentration (region α), while they decreased with higher IL concentration (region β). It is suggested that the decrease of saccharification efficiency could be due to the denaturation of enzymes, as a result, the enzyme could lose the binding affinity toward substrate.

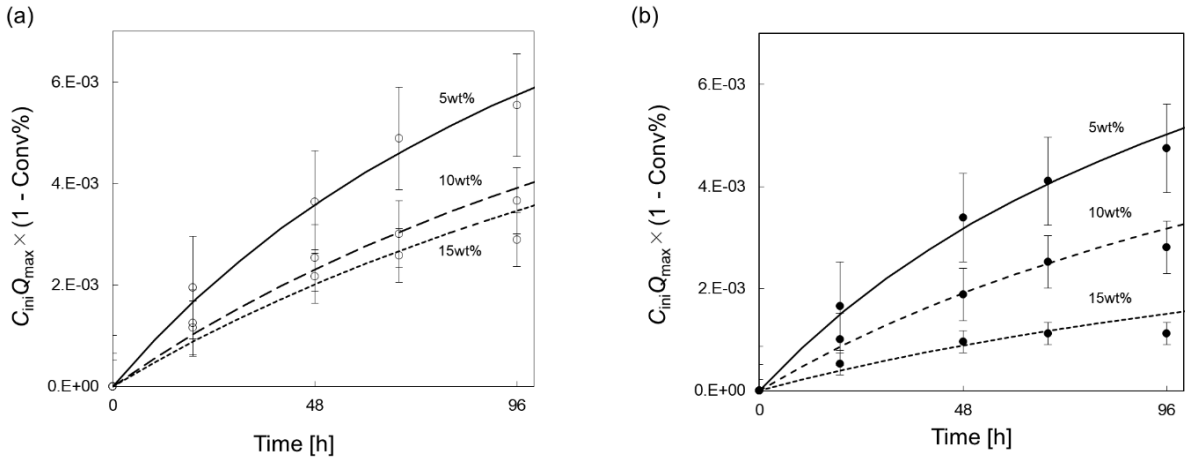

Fig.2-4 Time vs. *C* plot for [Amim][Cl] (a) and for [Bmim][Cl] (b).

Fitting parameters in Langmuir adsorption isotherms are shown in **Table 2-1**. *C* values were calculated based results shown in **Figure 2-3**, and were fitted based on (Eq.2-1) and (Eq.2-2).

Table 2-1 Fitting parameters, Q_{max} and K in Langmuir isotherm plot.

IL	**IL conc.**	Q_{max}	K	KY	**Relative value**	
					Q_{max}	KY
	[wt%]	**[g/g]**	**[-]**	**[-]**	**[%]**	**[%]**
[Amim][Cl]	5	1.45×10^{-2}	6.85×10^{-3}	5.82×10^{-2}	100	100
[Amim][Cl]	10	1.30×10^{-2}	4.50×10^{-3}	2.30×10^{-2}	89.7	43.6
[Amim][Cl]	15	1.25×10^{-2}	4.00×10^{-3}	8.00×10^{-3}	86.2	15.2
[Bmim][Cl]	5	1.20×10^{-2}	7.50×10^{-3}	7.50×10^{-2}	100	100
[Bmim][Cl]	10	9.50×10^{-3}	5.25×10^{-3}	3.46×10^{-2}	79.2	46.1
[Bmim][Cl]	15	5.00×10^{-3}	4.50×10^{-3}	2.34×10^{-2}	41.7	31.2

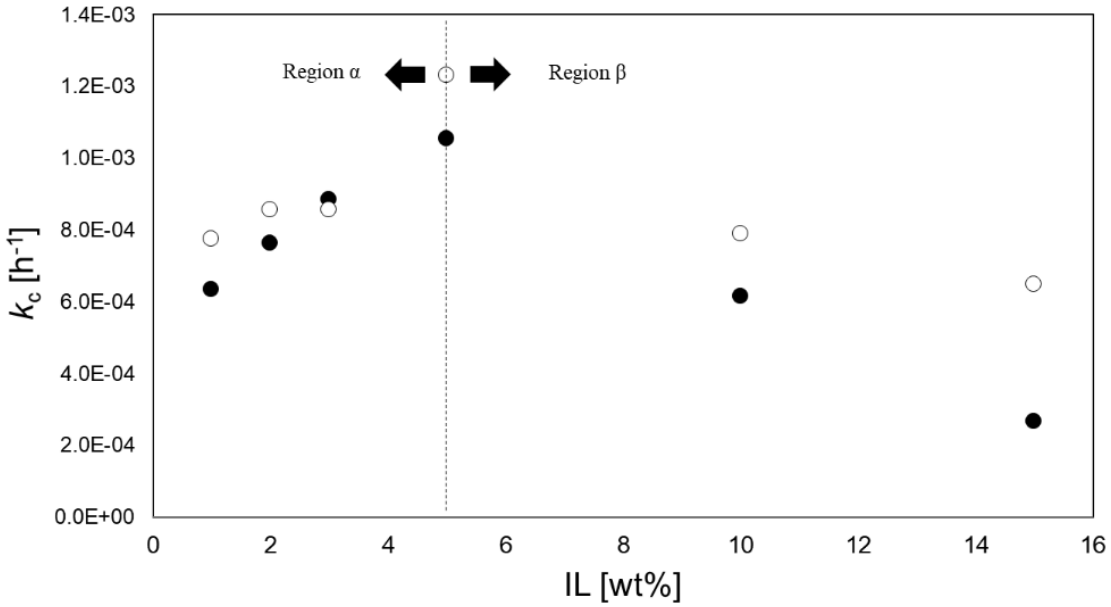

Figure 2-5 Correlation between reaction rate constant and IL concentration. [Amim][Cl] (*open circle*), [Bmim][Cl] (*closed circle*).

3.4. Effect of IL species and concentration for kinetic analysis

In the region α in **Figure 2-5**, the substrate concentration available for saccharification reaction could be proper to the IL concentration. The reaction rate constants, k_c were analyzed using a first-order reaction equation, wherein C_0 (from eq. Eq.2-1) was employed as initial substrate concentration:

$$-dC/dt = k_c C \qquad \text{(Eq.2-3)}$$

wherein C, t, and k_c represent the concentration of glucose precursor, time, and first-order reaction rate constant, respectively. The hydrolysis by cellulase might be relevant to the dissolution of cellulose. Herein, the kinetic parameters for the enzymatic reaction was also analyzed based on Michaelis-Menten model: the substrate concentration [S] could be proportional to IL concentration ([IL]):

$$V = \frac{V_{max}[S]}{K_m + [S]} \qquad \text{(Eq.2-4)}$$

$$[S] \propto [IL] \qquad \text{(Eq.2-5)}$$

wherein V_{max} and K_m represent maximum reaction rate and substrate affinity, respectively. Based on Eq. 2-4, Lineweaber-Burke plot was described (see supporting information **Figure 2-6** and **Figure 2-7**):

$$\frac{1}{V} = \frac{K_m+[S]}{V_{max}[S]} = \frac{K_m}{V_{max}} \times \frac{1}{[S]} + \frac{1}{V_{max}} \qquad \text{(Eq.2-6)}$$

V_{max} and K_m obtained from [Amim][Cl] and [Bmim][Cl] in the α region were compared in **Table 2-2**. Michaelis-Menten constant K_m corresponds to the substrate concentration at the time of giving a rate of 1/2 of the maximum reaction rate. The V_{max} values of [Amim][Cl] and [Bmim][Cl] were almost same, indicating that no inhibitory effect of IL occurred at region α. The K_m value was 5.27×10^{-1} for [Amim][Cl] and 8.70×10^{-1} for [Bmim][Cl]. This suggests that [Amim][Cl] produced a better substrate for saccharification. It is reported that [Amim][Cl] exhibits excellent ability to destroy the crystal structure in cellulose, as compared to [Bmim][Cl] [Yoshimoto et al., 2013]. Concentration of the results so far suggests that the rate-limiting step in region α is the adsorption of enzyme to dissolved substrate.

In this study, the apparent kinetic rate constants (k_c) were obtained with the values of 10^{-3}~10^{-4} (**Figure 2-6**). These values are smaller as compared to alkaline treated cellulose saccharification (k ~10^{-2}) [Zhang et al., 2012]. It is also notable that the β-glucosidase activity of cellulase, determined by the hydrolysis by using cellobiose as substrate, could not be inhibited by 15wt% [Bmim][Cl] [Yoshimoto et al., 2013]. Therefore, the rate-limiting step in the enzymatic hydrolysis could be the reactions of endoglucanase or cellobiohydrolase.

Table 2-2 V_{max} and K_m values obtained from Lineweaver-Burke plot.

IL	$\boldsymbol{V_{max}}$	$\boldsymbol{K_m}$	$\boldsymbol{V_{max}/K_m}$
[Amim][Cl]	5.70×10^{-3}	5.27×10^{-1}	1.08×10^{-2}
[Bmim][Cl]	5.80×10^{-3}	8.70×10^{-1}	0.67×10^{-2}

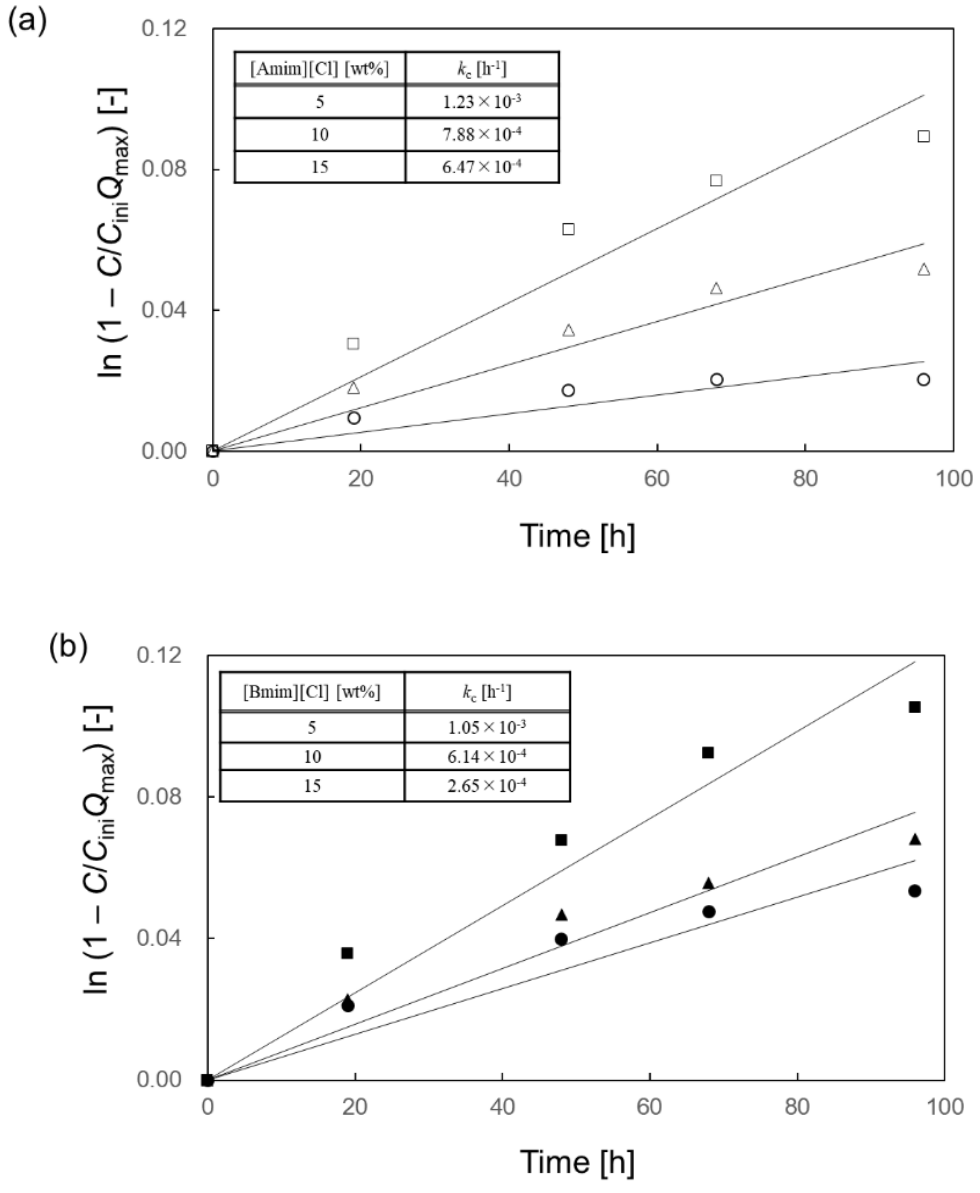

Figure 2-6 Correlation between IL concentration and reaction rate constant.

(a) [Amim][Cl]; 5wt% (*open square*); 10wt% (*open triangle*); and 15wt% (*open circle*).

(b) [Bmim][Cl]; 5wt% (*closed square*); 10wt% (*closed triangle*); 15wt% (*closed square*).

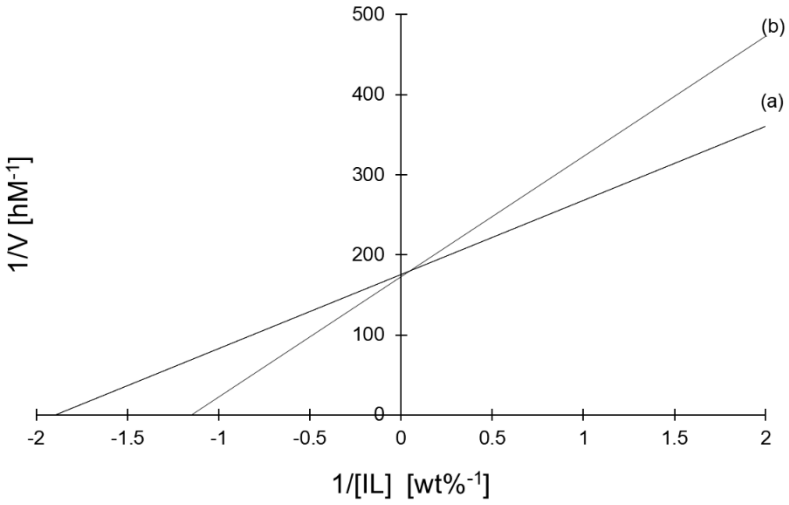

Figure 2-7 Lineweaver-Burke plot in region α which IL concentration from 1 to 5wt%.

(a) [Amim][Cl], V_{max} =5.70×10^{-3} [M/h], K_m =5.27×10^{-1} [wt%].

(b) [Bmim][Cl], V_{max} =5.80×10^{-3} [M/h], K_m =8.70×10^{-1} [wt%].

4. Summary

Cellulose hydrolysis was promoted and inhibited by ILs ([Amim][Cl], [Bmim][Cl]). Depending on the IL concentration. In the presence of IL with higher concentration ([IL] >5wt%), a denature of cellulase was significant, which reduced the substrate affinity. Furthermore, it was quantitatively evaluated that the sensitivity of the maximum adsorption amount Q_{max} and the conversion ability KY to IL concentration decreased with increasing IL concentration using Langmuir adsorption and first-order kinetics. That is, it was proposed that kinetic analysis by trial and error be applied to the experimental results in various ionic liquids. When IL concentration lower than 5wt%, the Langmuir adsorption model can be applied to understand the actual concentration of substrate (dissolved cellulose) available for hydrolysis reaction. Based on the kinetic parameter analysis, the effect of [Amim][Cl] for cellulose dissolution was more effective as compared to [Bmim][Cl]. It is important to maintain lower IL concentration for enzymatic activity, while higher IL concentration are considered to be superior to generate dissolved substrate. Thus, the control of IL concentration could be dominantly affected on the efficiency in enzymatic saccharification, in batch reactor process.

Chapter 3

Characterization of Ionic Liquid Aqueous Two-Phase Systems: Phase Separation Behaviors and Hydrophobicity Index between the Two Phases

1. Introduction

Ionic liquids (ILs) are a type of molten salts that are liquid at standard condition [Wilkes et al., 2002, Rogers et al., 2003]. ILs have low volatility, low viscosity, and high ionic conductivity [Welton et al., 1999, Wasserscheid et al., 2000]. Due to these unique properties, ILs are expected to find applications in various research fields. In recent years, many researchers have focused their attention on the utilization of ILs as green chemicals because they can solubilize crystalline cellulose [Mora-Pole et al., 2011, Moniruzzaman et al., 2013, Vancouver et al., 2011]. ILs have also attracted attention as functional electrolytes in secondary batteries for electrochemical applications [Ohno et al., 2011]. Water soluble ILs, such as 1-allyl-3-methylimidazolium chloride ([Amim][Cl]) and 1-butyl-3-methylimidazolium chloride ([Bmim][Cl]), are good candidates for environmentally friendly processes (e.g., enzymatic hydrolysis of cellulose).

Recent reports have also focused on the use of ILs in bioseparation. Similar to polymer-polymer aqueous two-phase systems (ATPSs), ATPSs can be formed by mixing an IL and a specific salt in aqueous solution. In addition, novel extraction and reaction systems have been developed using ionic liquid aqueous two-phase systems (IL-ATPSs) [Pratiwi et al., 2015, Matsumoto et al., 2014, Liu et al., 1998]. Gutowski and Broker first reported the formation of an IL–water biphasic system based on [Bmim][Cl], water, and K_3PO_4 [Gutowski et al., 2003]. The application of IL-ATPSs in bioconversion using the cellulose enzyme has also been reported [Bridges et al., 2007, Deng et al., 2009, Deng et al., 2007, Pei et al., 2007]. In these IL-ATPSs, the top phases are enriched in the IL whereas the bottom phases are enriched in salt (lower IL content). These systems seem to be suitable for the enzymatic saccharification (hydrolysis) of cellulose, because a high concentration of IL is required for the dissolution of cellulose [Tanimura et al., 2018]. However, the IL itself presents the risk of inactivating the enzymes [Turner et al., 2003, Yoshimoto et al., 2013]. In general, most water-soluble proteins (or enzymes) are

localized in the bottom phase of ATPSs due to their hydrophilic surface properties [Kuboi et al., 2006]. To apply an IL-ATPS to a bioprocess, its phase behaviors should be characterized, along with other properties of the ATPS, for example, the hydrophobicity index between the two phases.

Since the initial research into ATPSs was reported by Albertsson and his co-workers [Albertsson et al., 1970], many researchers have investigated the basic properties of ATPSs, along with their possible applications in bioseparation processes. ATPSs that comprise an aqueous polymer and an aqueous polymer or salt phase are compatible with biological molecules, and have been utilized for the reaction and separation of biomolecules [Tjerneld et al., 2000]. Several reports on the separation behavior of proteins in ATPSs have been published [Abbott et al., 1993]. Kuboi and co-workers previously reported a method to characterize the properties of an ATPS. They focused mainly on the hydrophobicity between the two phases; they determined the hydrophobicity factor (*HF*), which is an index of the hydrophobicity at the interface, based on the partitioning of standard molecules (amino acids) and their hydrophobicity indices (Nozaki-Tanford index) [Yano et al., 1994, Nozaki et al., 1970]. The *HF* value can be obtained from the experimentally determined distribution coefficient *K* of amino acids in the ATPS. The obtained *HF* value of an ATPS can determine the molecular partitioning behaviors of bio(macro)molecules based on the surface properties of the target molecules. The ATPS can then be used to characterize their surface net hydrophobicity (*HFS*). Kuboi et al. also reported the design of a protein separation method based on the *HF* (a characteristic of the ATPS) and the *HFS* (a property of the target molecules) by employing several case studies [Kuboi et al., 2006, Yano et al., 1994, Umakoshi et al., 1996, Kuboi et al., 1993]. Thus, to rationally design a bioconversion process (i.e., the hydrolysis of cellulose), the hydrophobic character of IL-ATPSs should be studied by employing the previous method based on the partitioning behaviors of standard amino acids, together with their Nozaki-Tanford values.

In this work, we characterized IL-ATPSs prepared from an IL and a specific salt, focusing on their phase separation behavior and hydrophobicity. The IL-ATPSs were prepared by combining an imidazolium IL ([Amim][Cl] or [Bmim][Cl]) and a salt (K_2CO_3, K_2HPO_4, $(NH_4)_2CO_3$, K_2SO_4, Na_2CO_3, $ZnCO_3$, or $MgCO_3$). After the investigation of the phase separation behaviors of the IL-ATPSs using their binodal

curves at different temperatures, the tie-line length and slope of the tie-line were analyzed. To compare the characteristics of the IL-ATPSs with those of conventional ATPSs, the hydrophobicity index between the two phases (*HF*) [Kuboi *et al*., 2006.] was determined by monitoring the partitioning coefficients of amino acids.

2. Materials and Methods

2.1. Materials.

1-Butyl-3-methylimidazolium chloride ([Bmim][Cl]) and 1-allyl-3-methylimidazoli -um chloride ([Amim][Cl]) were purchased from Sigma Aldrich Japan (Tokyo, Japan). Crystalline cellulose powder was purchased from Nacalai Tesque (Kyoto, Japan). Potassium carbonate (K_2CO_3) and dipotassium hydrogenphosphate (K_2HPO_4) were purchased from Kanto Kagaku (Tokyo, Japan). Other chemicals were obtained from Wako Pure Chemical Corporation (Osaka, Japan), and used without further purification. Tryptophan, phenylalanine, glycine were purchased from Peptide institute (Osaka, Japan).

2.2 Salt effect of IL-saline biphasic system.

[Bmim][Cl] or [Amim][Cl] powder was weighed into a screw tube and heated at 100℃ for 5 minutes using a hot stirrer to melt it. Further, an aqueous solution in which various kinds of salts were dissolved was added to the screw tube. After stirring the sample thoroughly, it was allowed to stand for 5 minutes to observe whether or not a two-phase system was formed. For the sample in which the two-phase system was formed, the phase separation behavior was observed by changing the weight fraction of salt, IL and water.

2.3 Temperature dependence of IL-ATPS.

A phase diagram was created to quantitatively evaluate the separation behavior under each temperature condition. K_2HPO_4 and K_2CO_3 were selected as salts forming [Bmim][Cl] or [Amim][Cl] with IL-ATPS and changes in phase separation behavior were observed at 45°C, 30°C, 15°C and 5°C. The sample was allowed to stand in a constant temperature bath for 20 minutes, and it was confirmed that it was separated into two phases. The density of the prepared sample was measured as follows. The top

phase or the bottom phase of each of the two phases separated samples was transferred into a 2 ml volumetric flask using a micropipette and the weight was determined. The sample having the same composition ratio as that of the density measurement was prepared and transferred to a 4 ml graduated cylinder. These were allowed to stand in a constant temperature bath in the same manner as the density measurement condition and the volumes of the bottom phase and the top phase at each temperature were measured.

2.4 Evaluate the distribution of amino acids to IL-ATPS.

IL-ATPS (composition: IL = 30wt%, salt = 15wt%, water = 55wt%) was prepared. Tryptophan or valine, glycine was dissolved in pure water to prepare an amino acid solution having a concentration of 1.0 mM, which was mixed in the IL-ATPS solution using a micropipette. The amino acid concentration relative to the whole was 0.5 mM. The bottom phase was sampled and the Trp concentration was determined by UV absorption (280 nm) and Val and Gly concentrations were determined by fluorescamine fluorescence measurement [Stein et al., 1973]. Distribution coefficient (*K*) was calculated from material balance and the hydrophobicity factor (*HF*) and the relative hydrophobicity (*RH*) between the two phases were evaluated [Kuboi *et al* 2006.]

2.5 Supplementary method for Hydrophobicity Factor (*HF*) of Aqueous Two-Phase Systems (ATPS)

A systematic approach to the characterization and quantitative determination of surface properties of biomolecules has previously been reported by using an aqueous two-phase system (ATPS) [Yano et al., 1994]. Previous researchers mainly focused on the use of functional polymers in the ATPS, such as charged ligands (tetra-methyl-acetate-PEG or PEG-sulfonate) [Miorner et al., 1982, Johansson et al., 1976], hydrophobic ligands (palmitate- PEG [Johansson et al., 1970, Miorner et al., 1983], and biospecific ligands (antibodies-PEG) [Karr et al., 1988]. If such ligands are not attached to the polymer, the partition coefficient of biomolecules in an ATPS has been found empirically to depend upon several factors, which act independently. The partitioning coefficients of biomolecules, such as amino acids, peptides, proteins (enzymes), liposomes and cells, may therefore be expressed as follows [Tjerneld et al., 2000, Baskir et al., 1989]:

$$\ln K = \ln K_{\text{electorostatic}} + \ln K_{\text{hydrophobic}} + \ln K_{\text{salt}} + \ln K_{\text{lignd}} + \ldots \quad (1)$$

where $K_{\text{electorostatic}}$, $K_{\text{hydrophobic}}$, K_{salt}, and K_{lignd} represent the contribution to the partitioning of the biomolecules by electrostatic, hydrophobic, salt and ligand effects, respectively. From consideration of these effects, the surface of biomolecules can be systematically characterized. It is then considered that the ATPS method can also be applied to the characterization of the surface properties of bacterial cells, which are highly organized biomolecular assemblies.

Tjerneld has found that the pH dependence of the partition coefficient of cells in an ATPS containing some types of salt showed a common cross point at pI (cross partition method) [Tjerneld et al., 2000]. At the pI and low ionic strength, the values of ln $K_{\text{electorostatic}}$ and lnK_{salt} can be ignored, and the following relationship can then be obtained,

$$\ln K = \ln K_{\text{hydrophobic}} \quad (2)$$

Nozaki and Tanford evaluated the hydrophobicities of several amino acids in water/ethanol and water/dioxane systems [Nazaki et al., 1970]. In our previous study, a relationship between the Nozaki-Tanford values and the partition coefficients of amino acids was elaborated [Yano et al., 1994], and the following equation on the definition of hydrophobicity factor (*HF*) values can then be obtained:

$$\ln K = HF \times (RH + B) \quad (3)$$

where *RH* is the relative hydrophobicity based on the Nozaki-Tanford value and *B* is the normalization constant defined as the ratio of the partition coefficient and the hydrophobicity of glycine, ln $K_{\text{Gly}}/\Delta G_{\text{Gly}}$. The hydrophobicity differences between the two phases in an ATPS can be described as *HF*, as for example shown in **Figure.3-1** and the surface net hydrophobicity of protein (*HFS*) from the slope of Eq. (4) using ATPS.

$$\ln K = HFS \times HF \quad (4)$$

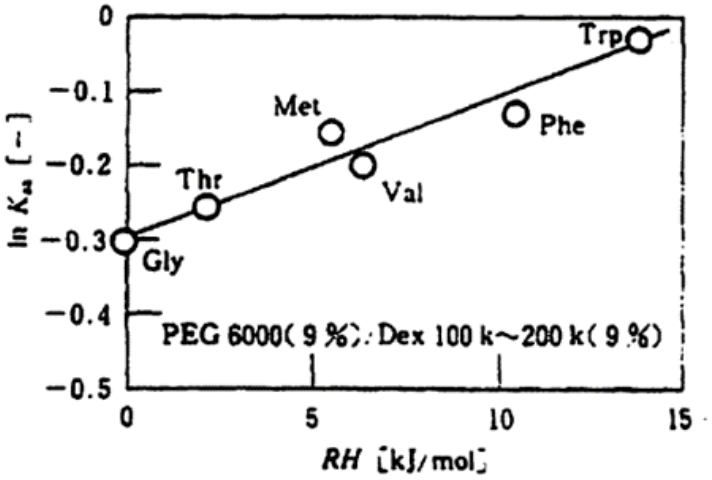

Figure 3-1 Relationship between the partition coefficients of amino acids and their hydrophobicities determined by Nozaki and Tanford [Nozaki et al., 1970].

The above equation can provide quantitative data based on the surface properties of a variety of biomolecules such as amino acids, peptides, proteins (enzymes), liposomes and bacterial cells. As an analogy, the hydrophobicity of other types of aqueous two-phase systems such as reverse micellar systems (RVMS) [Yamada et al., 1995] and liposome membrane systems (LMS) [Kuboi et al., 1997] can also be evaluated based on the partition behavior of amino acids between two phases. **Figure 3-2** shows the *HF* values of some aqueous systems such as RVMS and LMS, which are evaluated based on the relationship between the partitioning behaviors of amino acids and their hydrophobicity (**Figure 3-2(a))** [Kuboi et al., 2006]. As shown in **Figure 3-2(b)**, the ATPS was in general found to provide the wide spectra of *HF* values from 0.005-0.35mol/kJ, depending on the type and concentration of phase forming components such as poly (ethylene glycol), dextran, phosphate salts and the random copolymer of PO and EO (BREOX) [Yoshimoto et al., 2003]. The *HF* values for the RVMS were higher than that usually found for ATPSs and they varied with the water contents and types of detergents. The LMS indicated lower *HF* value and, especially in the cease of the POPC liposome, the *HF* value was nearly equal to that of PEC6 (9%) /dextran (9%) two phase system, which can be classified as an ATPS with a higher *HF*

value in PEG/dextran aqueous polymer two phase system. It was this found that the *HF* values for various types of aqueous two phase systems could be characterized on the same scale based on the Nozaki-Tanford value and the partitioning behaviors of large target biomolecules in the systems could be controlled by the *HF* values.

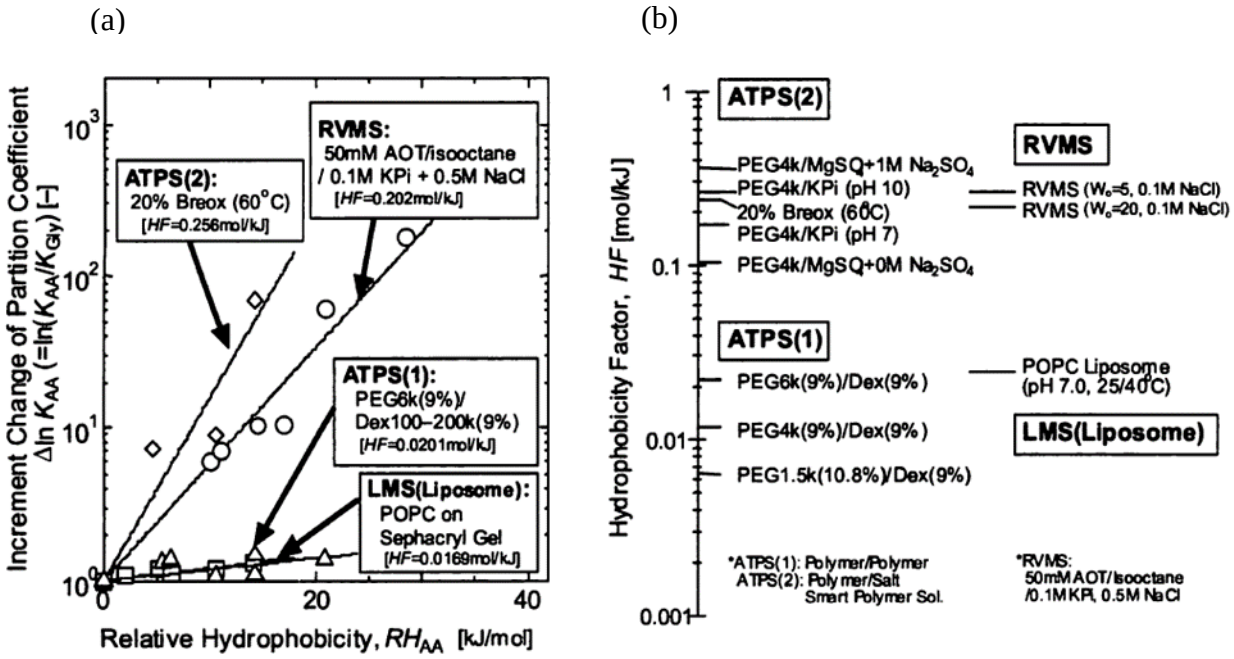

Figure 3-2. *HF* value of various aqueous two-phase systems [Kuboi et al., 2006].

(a) Relationship between the partition coefficients of amino acid and their hydrophobicities determined by Nozaki and Tanford in various aqueous two-phase systems such as ATPS, RVMS, and LMS. (b) *HF* ladder for these systems.

3. Results and Discussion

3.1. Combination of the IL and salt to prepare the IL-ATPS.

As reported previously [Gutowski et al., 2003], the IL-ATPSs were formed by combining [Bmim][Cl] and K_2CO_3 in various compositions (**Table 3-1**). At the composition of IL=30 wt% and salt=15 wt%, some of the [Bmim][Cl]-salt combinations did not form IL-ATPSs (**Table 3-2**). This was attributed to the low solubility of the salts (K_2SO_4, $ZnCO_3$, and $MgCO_3$); they seem to have precipitated before phase separation. In the case of Na_2CO_3, although the formation of a two-phase system was confirmed, salt precipitation occurred in the bottom phase. According to the Hofmeister series

[Zhang, Y. et al., 2006], salts with a high precipitation ability do not form two-phase systems. No precipitation was observed in the [Bmim][Cl]-$(NH_4)_2CO_3$ system, but the ATPS was not formed because of the chaotropic effect of NH_4^+. Considering the liquid–liquid two-phase equilibrium, an IL-ATPS without precipitates is desired. In the following procedures, K_2HPO_4 and K_2CO_3 were chosen as the salts to form IL-ATPSs with [Bmim][Cl] or [Amim][Cl].

Table 3-1 IL-ATPS composed of [Bmim][Cl] and K_2CO_3 at room temperature.

IL [wt%]	salt [wt%]	water [wt%]
30	10	60
30	15	55
20	20	60
10	30	60
10	40	50
10	40	60
10	50	50

Table 3-2 Effect of salt species on the formation of [Bmim][Cl] (30wt%)-salt (15wt%) ATPS.

	K_2CO_3	K_2HPO_4	$(NH_4)_2CO_3$	K_2SO_4	Na_2CO3	$ZnCO_3$	$MgCO_3$
Formability	○	○	×	×	△	×	×
pH	11	8.7~9.3	alkaline	5~8	11~12	alkaline	alkaline

Formability indicates as follows: ○, two-phase without precipitates; Δ, two-phase system with precipitates in bottom phase; ×, single-phase with precipitates. After equilibrium, the bottom phase was carefully corrected and then pH was measured. “Alkaline” indicates pH >12.

3.2. Phase separation behaviors of IL-ATPS.

To understand the phase separation behaviors of the IL-ATPSs, a phase diagram was prepared for each sample. For an aqueous two-phase system in a polymer system, different phase diagrams are drawn depending on the conditions of pH and temperature [Bridges et al., 2007, Hatti-Kaul et al., 2000]. The phase diagrams of an IL-ATPS

formed by the combination of a chaotropic salt and kosmotropic salt have been reported [Bridges et al., 2007]. The concentrations of the components of the top and bottom phase forming the two-phase system can be determined by preparing the phase diagram, and the ratio of the volumes of each phase can be recorded.

3.2.1. Basis for phase diagram.

The conceptual phase diagram of an IL-ATPS is shown in **Figure 3-3** The top and bottom regions of the binodal curve, indicated by the T-B curve, comprise two phases and a single-phase system, respectively. The straight line connecting the points T-X-B is a tie line. Samples existing on this straight line have the same top phase composition and bottom phase equilibrium composition, although the volume ratios of the top and bottom phases are different. Point C on the binodal curve is a critical point, since the volume ratio of both phases is theoretically equal; the tie line length (TLL) becomes 0 at this point. The TLL has units of mass% [w/w], similar to the component concentration. Therefore, the IL and salt at the uppermost intersection T, where the binodal curve intersects the tie line, have the coordinates (W_1^t,W_2^t). The IL and salt at the lowermost intersection B, where the binodal curve intersects the tie line, have the coordinates (W_1^b,W_2^b). Any sample existing at point X on the tie line has the coordinates (W_1^x,W_2^x). The TLL and slope of the tie line (STL) are related to the mass according to the following equations:

$$\mathrm{TLL} = [(W_1^t - W_1^b)^2 + (W_2^t - W_2^b)^2]^{0.5} \ldots \text{(Eq.3-1)}$$

$$\mathrm{STL} = (W_2^t - W_2^b)/(W_1^t - W_1^b) \ldots \text{(Eq.3-2)}$$

The sample at point X is prepared by mixing the IL and salt at an arbitrary ratio. This point is the center of gravity of the tie line. The length XT above the center of gravity is the mass of the bottom phase, W^b. The length XB below the center of gravity is the mass of the top phase, W^t. The lengths up to the intersection points, XT and XB, of the tie line are related to the mass according to the following equations:

$$\mathrm{XT} = [(W_1^t - W_1^x)^2 + (W_2^t - W_2^x)^2]^{0.5} \quad \text{(Eq.3-3)}$$

$$\mathrm{XB} = [(W_1^x - W_1^b)^2 + (W_2^x - W_2^b)^2]^{0.5} \quad \text{(Eq.3-4)}$$

These are related to the volume and density of each phase according to the following equation:

$$V_t\rho_t / V_b\rho_b = W_t / W_b = XB/XT \quad \text{(Eq.3-5)}$$

The binodal curve of each sample was determined using the cloud point method. By applying the data least squares approximation obtained, the most probable value was determined by trial and error. Since the composition of the prepared samples was 30 wt% IL and 15 wt% salt, the coordinates of the center of gravity point X were (15, 30). The tie line was determined using the volume and density data, W^t and W^b, of the top and bottom phases (**Table 3-3**).

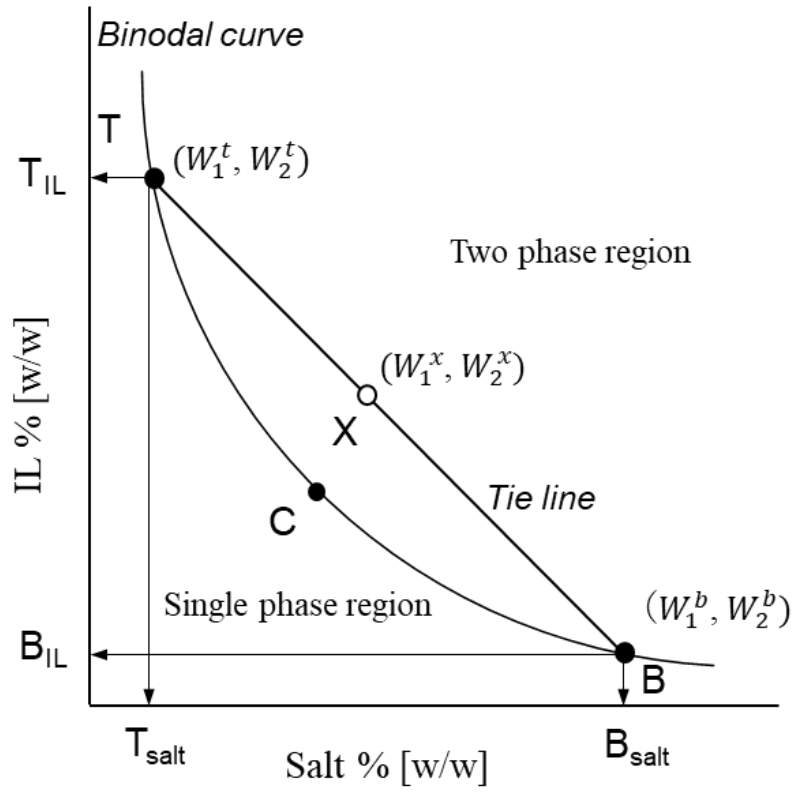

Figure 3-3 Conceptual diagram of IL-ATPS formed by IL and salt. For an ATPS prepared at the composition X, T and B indicate the compositions of the top and bottom phases, respectively. C indicates the critical point. The upper side of the binodal curve is a two-phase system, and the lower side is a single phase system.

Table 3-3 Density, volume, and weight fraction of each phase at different temperatures.

	T[°C]	ρ[g/ml]		V [ml]		W [mg]	
		ρ_t	ρ_b	V_t	V_b	W_t	W_b
[Bmim][Cl] K_2HPO_4	45	1.067	1.622	2.430	0.870	2.592	1.411
	25	1.070	1.624	2.420	0.870	2.589	1.413
	15	1.074	1.675	2.400	0.850	2.579	1.424
	5	1.077	1.669	2.400	0.850	2.584	1.418
[Bmim][Cl] K_2CO_3	45	1.069	1.559	2.310	0.990	2.470	1.544
	25	1.079	1.482	2.360	0.990	2.546	1.468
	15	1.077	1.429	2.400	1.000	2.584	1.429
	5	1.069	1.447	2.400	1.000	2.566	1.447
[Amim][Cl] K_2HPO_4	45	1.100	1.518	2.410	0.890	2.652	1.351
	25	1.094	1.559	2.390	0.890	2.615	1.388
	15	1.093	1.557	2.380	0.900	2.602	1.401
	5	1.095	1.636	2.310	0.900	2.530	1.473
[Amim][Cl] K_2CO_3	45	1.124	1.399	2.430	0.910	2.732	1.273
	25	1.119	1.532	2.210	1.000	2.473	1.532
	15	1.115	1.552	2.200	1.000	2.453	1.552
	5	1.113	1.568	2.190	1.000	2.437	1.568

ρ_t ,V_t and W^t for top phase, ρ_b ,V_b and W^b for bottom phase. The mass W^t and W^b are calculated based on Eq. 3-5.

3.2.2. Temperature effects.

Some biphasic systems show reversible phase separation behavior (single liquid phase ⇄ two-liquid phases) depending on the temperature [Trindade et al., 2007, Kohno et al., 2012, Kohno et al., 2015, Annat et al., 2012, Fukuya et al., 2007, Fukumoto et al., 2007, Kohno et al., 2011, Kohno et al., 2012, Satia et al., 2014, Visak et al., 2007, Il'in, et al., 2013]. They become single-phase systems at high temperatures and separate into two phases as the temperature decreases. The critical temperature for such a phase separation is known as the upper critical solution temperature, and its phase diagram is called UCST-type [David et al., 2015]. Some IL and salt combinations may show the opposite behavior, and are called LCST-type. For all the samples prepared in this study, a temperature drop increased the concentration of the two-phase region (**Figure 3-2**, **Table 3-4**). Therefore, the IL-ATPSs optimized in this study were considered UCST-type.

Since an exothermic reaction occurs in an IL-ATPS exhibiting two-phase separation behavior of the UCST-type, the equilibrium is inclined toward the two-phase separation as the temperature decreases. The hydration entropy is thought to be the driving force for biphasic separation, and it is speculated that the salt precipitation ability will increase as the hydration entropy increases; the tendency of biphasic separation follows the Hofmeister series. For kosmotropic ions, the ΔG_{hyd} has a large negative value [Shahla et al., 2012]. As the temperature decreases, the solubility decreases and the interaction between the IL and the salt becomes strong, that is, the phase formation ability is improved upon lowering the salt concentration for phase formation.

The TLL increases with the temperature (**Figure 3-5, Table 3-4**). The increase in TLL implies that the water molecules move from the top phase to the bottom phase and the IL concentration increases in the top phase. In addition, the salt concentration decreases in the bottom phase. This is considered the reason for the equilibrium composition changes due to temperature variation. The longer the TLL, the greater the composition ratio of both phases. In other words, the top phase is enriched in chaotropic salts and the bottom phase is richer in kosmotropic salts [Cínthiadas et al., 2017]. These

factors can be used to predict the distribution of amino acids. The hydrophobicity of the IL and the amino acid alkyl chain affect amino acid partitioning.

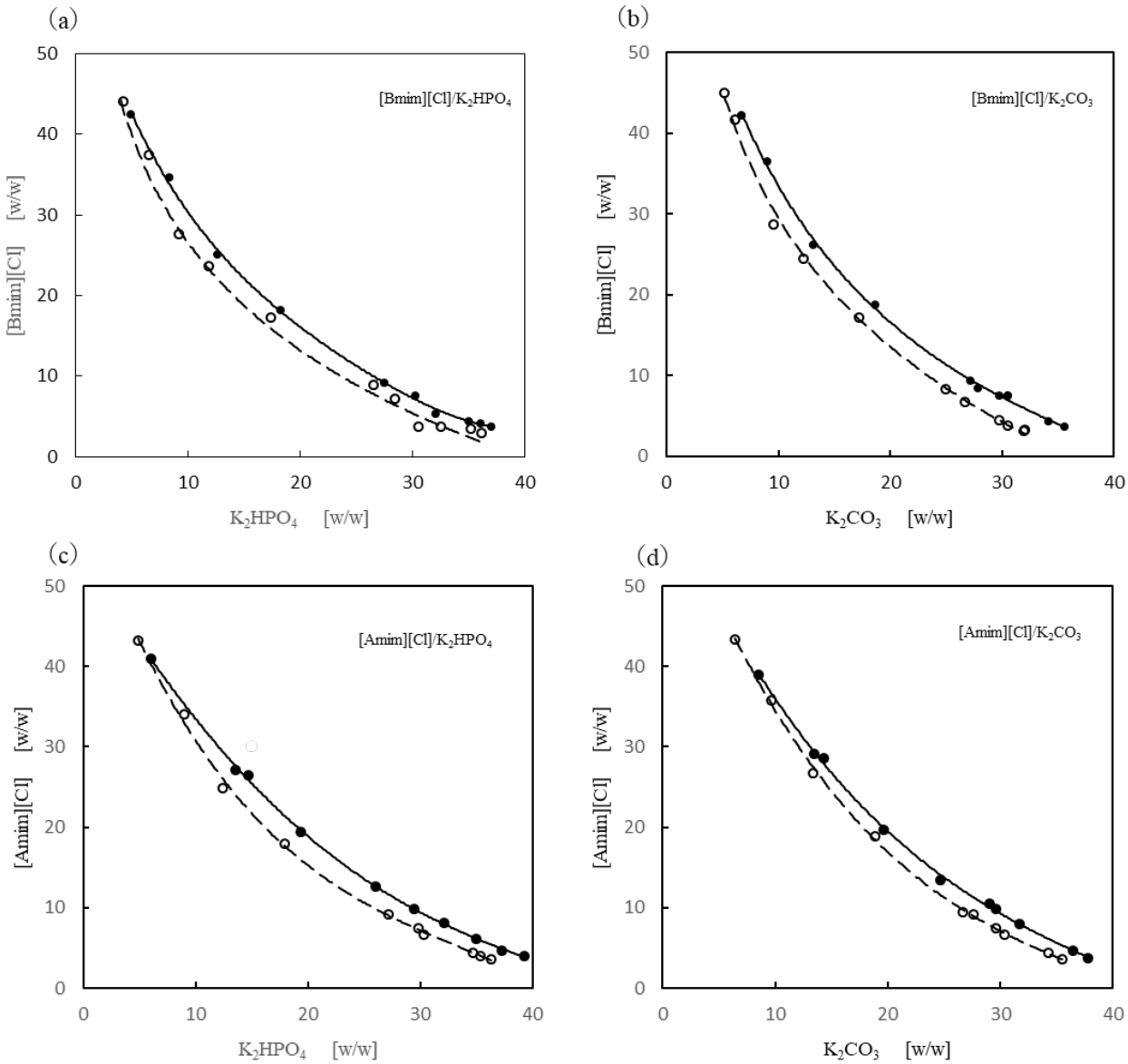

Figure 3-4 Effect of temperature on the phase separation behaviors of ATPS.

(a) [Bmim][Cl]/K_2HPO_4, (b) [Bmim][Cl]/K_2CO_3, (c) [Amim][Cl]/K_2HPO_4, (d) [Amim][Cl]/K_2CO_3. (●)45℃, (○)5℃.

Table 3-4 Weight fraction of component and TLL at different temperatures.

	T[°C]	IL [wt%]		Sal [wt%]		TLL		
		W_1^t	W_1^b	W_2^t	W_2^b	XT	XB	Total
[Bmim][Cl] K_2HPO_4	45	42.5	4.2	4.9	36.0	16.1	33.3	49.3
	25	43.8	3.0	4.4	36.3	17.4	34.4	51.8
	15	44.1	3.0	4.2	36.1	17.8	34.3	52.0
	5	44.6	2.5	4.0	36.2	18.3	34.7	53.0
[Bmim][Cl] K_2CO_3	45	42.3	7.5	6.7	30.5	14.8	27.3	42.2
	25	43.5	4.5	6.1	31.5	16.2	30.4	46.5
	15	44.5	3.5	5.5	32.0	17.3	31.5	48.8
	5	45.0	3.3	5.2	32.0	17.9	31.7	49.6
[Amim][Cl] K_2HPO_4	45	41.0	6.2	6.0	35.0	14.2	31.1	45.3
	25	41.5	6.0	5.5	34.5	14.9	30.9	45.8
	15	42.5	4.5	5.0	35.5	16.0	32.7	48.7
	5	43.2	4.0	4.9	35.4	16.6	33.0	49.7
[Amim][Cl] K_2CO_3	45	39.0	10.5	8.5	29.0	11.1	24.0	35.1
	25	41.5	9.5	7.5	29.0	13.7	24.8	38.6
	15	42.3	8.0	7.0	29.7	14.7	26.5	41.1
	5	43.4	6.6	6.4	30.4	15.9	28.0	43.9

W_1^t and W_2^t for top phase, W_1^b and W_2^b for bottom phase. Each value was calculated using Eq. 3-1- Eq. 3-4.

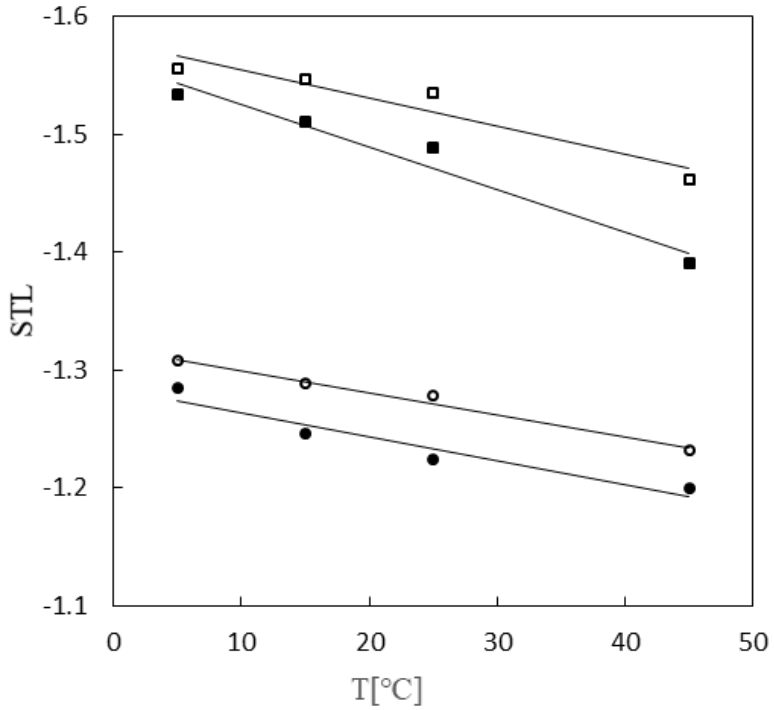

Figure 3-5 Temperature dependence of STL. (□) [Bmim][Cl]/K_2CO_3, (■)[Amim][Cl]/K_2CO_3, (○) [Bmim][Cl]/K_2HPO_4, (●)[Amim][Cl]/K_2HPO_4.

IL-ATPSs were prepared with 30 wt% of IL and 15 wt% of salt.

3.2.3. Effects of salt type and IL type.

To evaluate the phase separation behavior due to the difference in IL species, the binodal curves at 5 °C, at which remarkable temperature dependence was observed, were compared. The IL-ATPS composed of [Bmim][Cl] and K_2CO_3 had a binodal curve below that of the IL-ATPS composed of [Amim][Cl] and K_2CO_3, i.e., the two-phase range was enlarged (**Figure 3-6(a)**). Similarly, for the system using K_2HPO_4, the phase separation range was wider than that of the system using K_2CO_3 (**Figure 3-6(b)**). The extent of the phase separation range represents the ease of separation. Therefore, the order of ease of phase separation was [Bmim][Cl]/K_2HPO_4 > [Bmim][Cl]/K_2CO_3 > [Amim][Cl]/K_2HPO_4 > [Amim][Cl]/K_2CO_3. In other words, most of the IL in the system would be distributed to the top phase. Given the application to the enzymatic saccharification reaction process, this is useful for IL recovery and glycation reaction using the bottom phase. The imidazolium ILs with more hydrophobic cations are likely to be separated into two phases, and the salts are easier to separate than those with higher salt precipitation capacity. The order of the ease of separation is known to follow the Hofmeister series. The results obtained in this study were similar to previous findings [Bridges et al., 2007, Pei et al., 2007, Nockemann et al., 2008, Zafarani-Moattar et al., 2007, Pei et al., 2009].

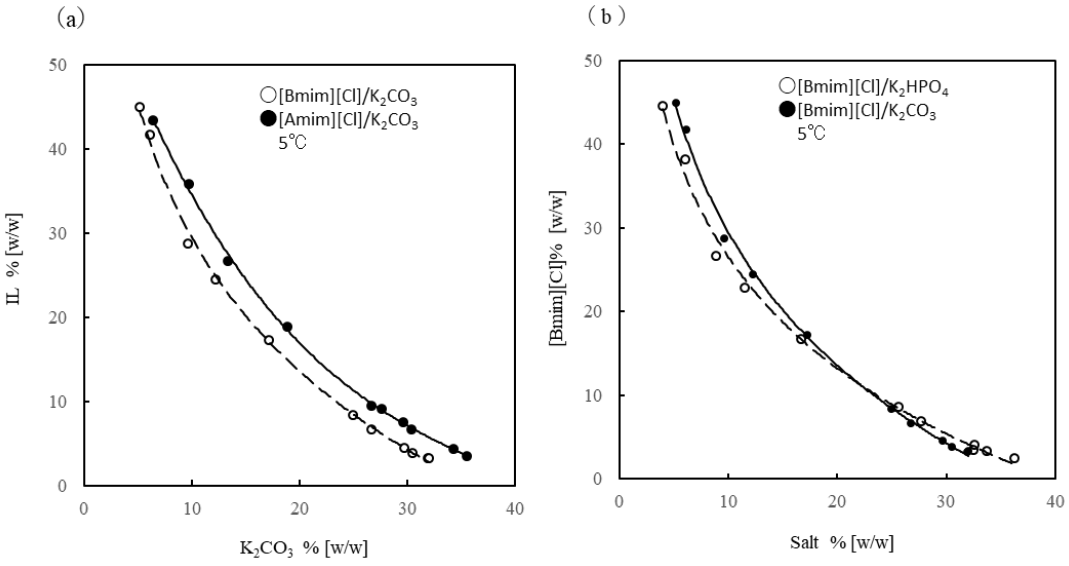

Figure 3-6 Comparison of binordal curves in phase diagram. (a) Effect of IL species at 5 ℃. (○) [Bmim][Cl]/K_2CO_3, (●) [Amim][Cl]/K_2CO_3. (b) Effect of salt species at 5 ℃. (○) [Bmim][Cl] /K_2HPO_4, (●) [Bmim][Cl]/K_2CO_3.

3.2.4. Quantitative evaluation of separation and recovery of ILs.

The design of an IL-ATPS for cellulose hydrolysis using enzymes has two objectives. One is to design a system with a low IL concentration that causes inhibition of enzyme activity by biphasic separation. The other is the recovery of the IL for the purpose of reuse. A reaction system using an IL as the solvent has a demerit in that the material cost is high. Repeated separation and recovery of the IL is proposed as an effective method to solve such problems. Using the phase diagram obtained in this study, the masses of the IL and salt distributed in the top and bottom phases were calculated. The masses of the IL and salt in each phase were defined using the following equations:

IL mass in top phase: $W^{t}{}_{\text{-IL}}$: $W_1^t \times W^t /100$ … (Eq.3-6)

IL mass in bottom phase: $W^{b}{}_{\text{-IL}}$: $W_1^b \times W^b /100$ … (Eq.3-7)

Total IL mass in system: $W_{\text{IL-total}}$: (Eq.3-6)+(Eq.3-7)

Mass of salt in top phase: $W^{t}{}_{\text{-Salt}}$: $W_2^t \times W^t /100$ … (Eq.3-8)

Mass of salt in bottom phase : $W^{b}{}_{\text{-Salt}}$: $W_2^b \times W^b /100$ … (Eq.3-9)

Total salt mass in system: $W_{\text{Salt-total}}$: (Eq.3-8)+(Eq.3-9)

The amounts of the components separated into each phase were calculated with respect to the total amount of IL or salt in the sample, and the ratio was determined. As shown by the temperature dependence of the binodal curve, the IL concentration in the top phase increases as the temperature decreases. In the system formed from [Bmim][Cl] and K_2HPO_4, which promoted the highest separation, about 97% of the total IL was separated into the top phase (**Table 3-5**). These results suggest that the IL can be reused at a high rate in the recycling process. On the other hand, the top phase contained about 17% of the salt of the whole system. This can be recovered to some extent by precipitation from the recovered top phase [Zafarani-Moattar et al., 2007].

Table 3-5 Mass and fraction of component distributing in top and bottom phases.

	T[°C]	IL Mass			Salt Mass		
		$W_{t\text{-}IL}$	$W_{b\text{-}IL}$	$W_{IL\text{-}tota}$	$W_{t\text{-}Salt}$	$W_{b\text{-}Sal}$	$W_{Salt\text{-}total}$
[Bmim][Cl] K_2HPO_4	45	1.10 (94.9)	0.06 (5.11)	1.2 -	0.13 (20.0)	0.51 (80.0)	0.6 -
	25	1.13 (96.4)	0.04 (3.60)	1.2 -	0.11 (18.2)	0.51 (81.8)	0.6 -
	15	1.14 (96.4)	0.04 (3.62)	1.2 -	0.11 (17.4)	0.51 (82.6)	0.6 -
	5	1.15 (97.0)	0.04 (2.98)	1.2 -	0.10 (16.8)	0.51 (83.2)	0.6 -
[Bmim][Cl] K_2CO_3	45	1.04 (90.0)	0.12 (9.98)	1.2 -	0.17 (26.0)	0.47 (74.0)	0.6 -
	25	1.11 (94.4)	0.07 (5.63)	1.2 -	0.16 (25.1)	0.46 (74.9)	0.6 -
	15	1.15 (95.8)	0.05 (4.17)	1.2 -	0.14 (23.7)	0.46 (76.3)	0.6 -
	5	1.15 (96.0)	0.05 (3.97)	1.2 -	0.13 (22.4)	0.46 (77.6)	0.6 -
[Amim][Cl] K_2HPO_4	45	1.09 (92.8)	0.08 (7.15)	1.2 -	0.16 (25.2)	0.47 (74.8)	0.6 -
	25	1.09 (92.9)	0.08 (7.13)	1.2 -	0.14 (23.1)	0.48 (76.9)	0.6 -
	15	1.11 (94.6)	0.06 (5.39)	1.2 -	0.13 (20.7)	0.50 (79.3)	0.6 -
	5	1.09 (94.9)	0.06 (5.11)	1.2 -	0.12 (19.2)	0.52 (80.8)	0.6 -
[Amim][Cl] K_2CO_3	45	1.07 (88.9)	0.13 (11.1)	1.2 -	0.23 (38.6)	0.37 (61.4)	0.6 -
	25	1.03 (87.6)	0.15 (12.4)	1.2 -	0.19 (29.5)	0.44 (70.5)	0.6 -
	15	1.04 (89.3)	0.12 (10.7)	1.2 -	0.17 (27.1)	0.46 (72.9)	0.6 -
	5	1.06 (91.1)	0.10 (8.91)	1.2 -	0.16 (24.7)	0.48 (75.3)	0.6 -

Weight fraction of each component is shown in parenthesis. The values are calculated using Eq. 3-6- Eq. 3-9

3.3. Physicochemical properties of IL-ATPS based on distribution of amino acids.

According to previous reports [Kuboi et al., 2006, Baskir et al., 1989], in an ATPS that is composed of two polymers or a polymer and salt, the partitioning behaviors of target molecules (i.e., amino acids, proteins, nucleic acids, cells, etc.) are derived from the hydrophobic, electrostatic, and biological interactions between the ATPS itself and the target molecules to be partitioned in the ATPS. These relationships are expressed by the following equation (10):

$$\ln K = \ln K_{\text{electrostatic}} + \ln K_{\text{hydrophobic}} + \ln K_{\text{salt}} + \ldots \quad \text{(Eq.3-10)}$$

The partitioning coefficient in the ATPS ignores the effect of salting out under low-salt conditions, as reported in previous studies [Albertsson et al., 1970]. The first term on the right side represents the contribution from the electrostatic effect, which depends on the surface charge of the target molecule and the electrostatic potential difference between the two phases. At the isoelectric point or at the same pH for the same target molecule, the first of these terms can be ignored, and K can be approximated using only the contribution of the second term, the hydrophobic effect. According to a previous report describing the characterization of the ATPS itself in relation to the hydrophobicity, the partition coefficient K can be described using the hydrophobicity factor (HF [mol/kJ]) of the ATPS itself and the surface net hydrophobicity (HFS [kJ/mol]) under the abovementioned conditions as described in the following equation:

$$\ln K = \ln K_{\text{hydrophobic}} = HF \times HFS \quad \text{(Eq.3-11)}$$

Herein, the HF value can be determined from the partitioning behaviors of amino acids based on the followings [Kuboi et al., 1990, Umakoshi et al., 1996]:

$$K_{aa} = [\text{amino acid}]_{\text{top}} / [\text{amino acid}]_{\text{bottom}} \quad \text{(Eq.3-12)}$$

$$\ln K_{aa} = HF \times (RH + \ln K_{gly}) \quad \text{(Eq.3-13)}$$

$$\Delta \ln K_{aa} = \ln (K_{aa}/K_{gly}) \quad \text{(Eq.3-14)}$$

where the amino acids are standard molecules whose hydrophobicity (relative hydrophobicity, *RH* [kJ/mol]) has been determined from their solubility in a water/1,4-dioxane system by Tanford [Tanford et al., 1962]. The hydrophobicity index (*HF*) can be uniquely and easily calculated by analyzing the partitioning behaviors of the standard amino acids in a given ATPS based on the previously defined *RH* values. The partitioning coefficients (K_{aa}) of the amino acids in various IL-ATPSs were determined (**Table 3-8**).

Hydrophobic amino acids were easily partitioned into the IL phase, and a correlation was found between the K_{aa} and *RH*. The *HF* value of the IL-ATPS was similar to that of the PEG-salt ATPS (**Figure 3-7**), and the K_{aa} increased for the [Bmim][Cl]/K_2CO_3 and [Amim][Cl]/K_2CO_3 systems. The largest *HF* was that of the [BMIM][Cl]/K_2HPO_4 system. This result is in agreement with the fact that [BMIM][Cl]/K_2HPO_4 promotes phase separation most conspicuously. The *HF* values of the IL-ATPSs were 0.13-0.41 mol/kJ, which were almost the same as the *HF* values reported for the ATPS composed of polyethyleneglycol and a salt [Kuboi et al., 2006]. The relatively high *HF* values indicate a large gap between the hydrophobicity of the IL phase and that of the aqueous salt phase, probably due to the hydrophobic nature of the IL molecules themselves. This implies that target molecules with large surface hydrophobicity (*HFS*) magnitudes could undergo extreme partitioning (top phase partitioning for a positive HFS value and vice versa) in the given IL-ATPS according to Eq.3-10.

Finally, we discuss the possible applications of the IL-ATPSs based on their measured characteristics. Many case studies describing the design of polymer-polymer ATPSs for various applications based on the *HF* and *HFS* values, including the bioseparation of α-lactalbumin and β-lactoglobulin, the recovery of molecular chaperones (GroEL and GroES), and the characterization of bovine carbonic anhydrase with different conformations, among others [Kuboi et al., 1995,1997]. When both the *HF* of the ATPS and the *HFS* of the target molecule can be determined, the partitioning behavior of the target can be calculated, allowing pre-optimization of the bioseparation process. The use of an IL-salt ATPS could be beneficial in the enzymatic saccharification of cellulose via cellulase, because of the cellulose-solubilizing and phase-separation properties of the IL. As an example, the *HFS* value of cellulase was determined based on its partitioning behaviors in a polyethylene glycol/dextran

(PEG/Dex) system (**Figure 3-8**). The *HFS* value was found to be −222.1 kJ/mol; unlike other proteins, cellulase has a hydrophilic surface. The characteristics of the IL-ATPSs discussed above and those of the possible target molecule (i.e., cellulase) imply that an IL-ATPS with a higher *HF* value could be applied to the cellulose saccharification process; hydrophilic cellulase would partition to the low-IL concentration bottom phase. In addition, it might be possible to recover ILs by taking advantage of the phase separation behaviors of the IL-ATPS. It is thus possible that the fundamental characteristics of the IL-ATPSs that were obtained in this study could be utilized to design possible applications for IL-ATPSs.

Table 3-6 Amino acid partitioning coefficient in ATPS composed of [Bmim][Cl]/K_2CO_3 or [Bmim][Cl]/K_2HPO_4.

		Trp	Val	Gly
RH [kJ/mol]		14.2	6.3	0.0
K [-]	K_2CO_3	113.1	18.5	14.6
	K_2HPO_4	17.9	0.79	0.05
Ln*K* [-]	K_2CO_3	4.73	2.92	2.68
	K_2HPO_4	2.89	-0.24	-2.91
ΔLn*K* [-]	K_2CO_3	2.05	0.24	0.00
	K_2HPO_4	5.80	2.67	0.00

RH values are referred by Nozaki and Tanford (1970). All experiments were carried out at 25 ℃.

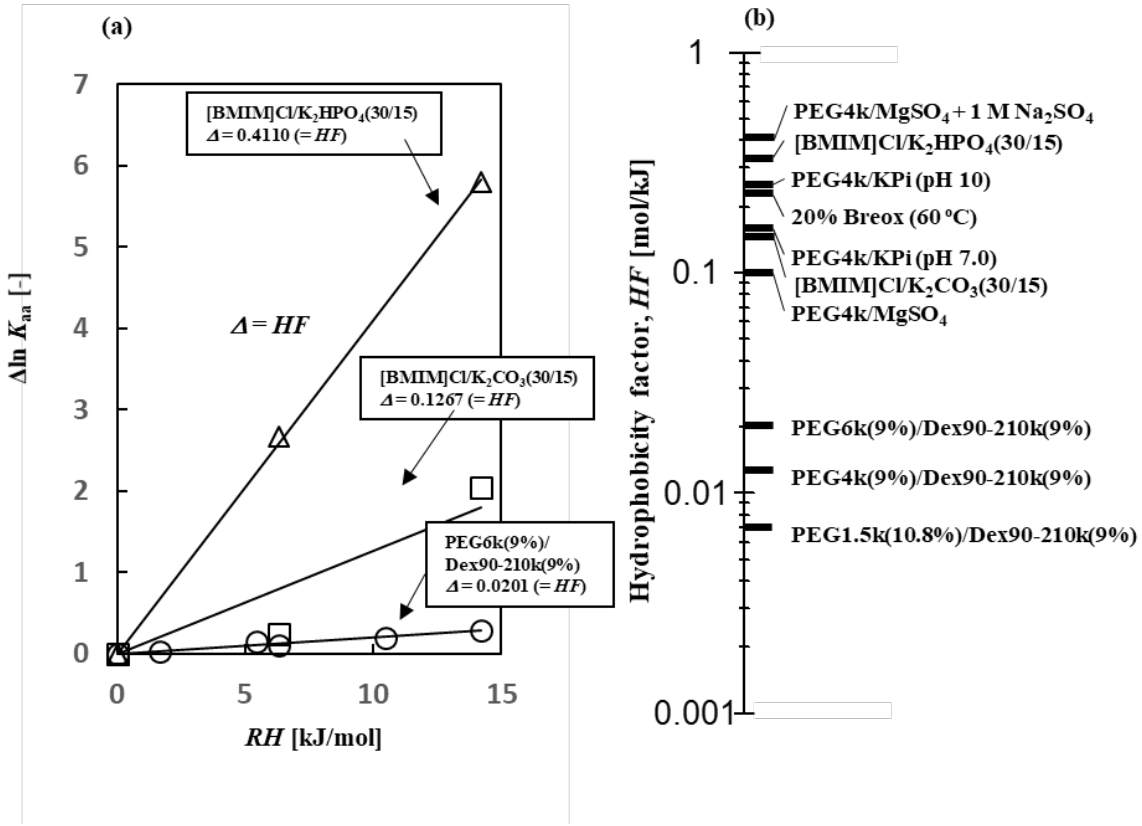

Figure 3-7 (a) Partitioning behaviors of amino acids in ATPS. The hydrophobicity of amino acid side residue (*RH*) is referred from Nozaki and Tanford [Nozaki, et al., 1970]. The *HF* values were calculated based on the slope (eq. (13)). (b) Comparison of *HF* values of ATPS. The *HF* values of conventional ATPS are referred from Kuboi and Umakoshi [Kuboi, R. et al., 2006].

The *HFS* value of the cellulase from *Trichoderma viride* (Yakult Pharmaceutical Industry (Tokyo, Japan)) was determined based on the partitioning behaviors in PEG/Dex system (**Figure 3-7**). The *HFS* value is −222.1 kJ/mol, indicating that cellulase has hydrophilic surface as well as bovine serum albumin (ca. -215 kJ/mol [Kuboi, R. et al., 2006]). Considering the *HF* values of IL-ATPS (0.13-0.41 mol/kJ), it is assumed that most of cellulase could be distributed into bottom phase.

Here, assuming a cellulose saccharification process, two targets in the system are an enzyme and cellulose as a substrate. Most of the enzymes are distributed to the lower phase because of a negative *HFS* (**Figure 3-8**). The other target cellulose, which exists as an individual in the system, increases the interfacial tension. It is conceivable that the amount of interfacial accumulation also increases. It is known that the amount of interfacial partitioned cells Interfacial Partitioning Factor (*IPF*) increases with *HF*. [Umakoshi et al., 1996]

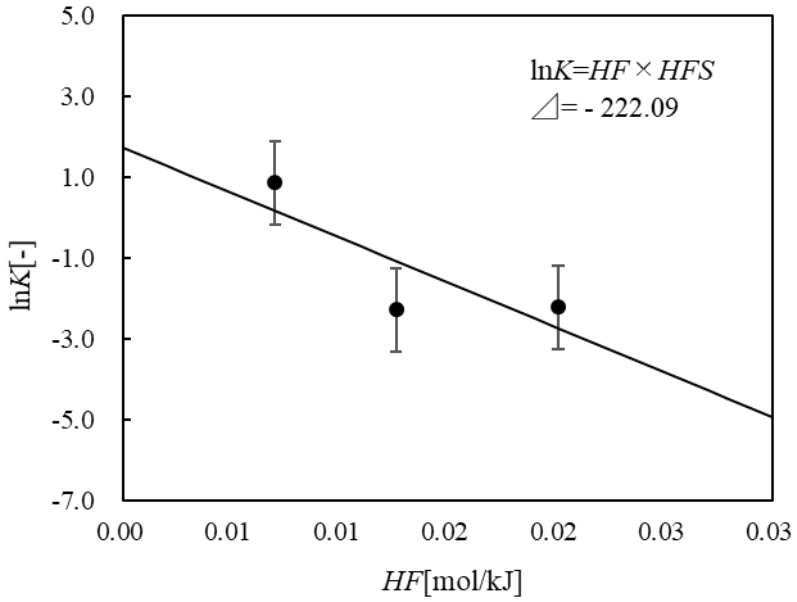

Figure 3-8 Partitioning behaviors of cellulase in PEG/Dex ATPS. The amount of cellulase in top and bottom phases were determined by fluorescamine method. Experiments were carried out at 25℃.

4. Strategy to design the bioconversion process using IL-ATPS.

In Chapter 2, the batch reaction system was evaluated quantitatively that the control of IL concentration in enzymatic hydrolysis greatly affects saccharification efficiency. In a single-phase system, when the IL concentration is 5 wt% or less, the reaction rate can be regarded as a first-order reaction, and it can be quantified by adopting the Langmuir adsorption model and the Michaelis-Menten type model. On the other hand, when the IL concentration was 5wt% or more, the denaturation of cellulase was remarkable and the substrate affinity of the enzyme decreased. Based on the kinetic analysis, the effects of [Amim] [Cl] and [Bmim] [Cl] on cellulose dissolution were compared, and the superiority of the former saccharification due to the amorphous ability was clarified. The logical flow in Chapter 2 is summarized in **Figure 3-9**.

In Chapter 3, the phase separation behavior and characteristics of an ionic liquid aqueous two-phase system were evaluated. IL-ATPS was prepared by mixing an ionic liquid ([Amim] [Cl] or [Bmim] [Cl]) and an aqueous salt solution (K_2CO_3 or K_2HPO_4), and their physical properties were evaluated based on the phase diagram. The phase separation behavior (Binodal curve, Tie-line length (*TLL*), and Slope of the Tie Lines (*STL*)) was determined under the conditions of changing the type, composition, and temperature of the ionic liquid and salt. The hydrophobicity index (*HF*) of IL-ATPS was determined based on the analysis results of partition coefficients K_{aa} of amino acids (Gly, Val, Trp) with different hydrophobicity in typical IL-ATPS. In addition, the *HF* value of IL-ATPS obtained in this chapter is similar to that of the conventional ATPS composed of PEG / $MgSO_4$, indicating that *HF* is maximized in the [BMIM] [Cl] / K_2HPO_4 system. In addition, it has UCST-type behavior in which the phase separation range expands with decreasing temperature, shows the widest phase separation under the temperature condition of 5 °C, and it was clarified that 95% or more of IL in the system can be separated into the upper phase. The logical flow in Chapter 3 is summarized as a flowchart (**Figure 3-9**). Even in the salt phase where the enzyme is distributed, the saccharification reaction of the enzyme does not proceed because IL is present at a high concentration. In other words, a one-pot process that uses enzymes and IL-ATPS simultaneously is difficult. Therefore, Chapter 4 proposes a process consisting of saccharification process, IL recovery, and enzymatic saccharification reaction for the

IL concentration dependence obtained in Chapter 2 and the phase separation behavior of IL-ATPS obtained in Chapter 3.

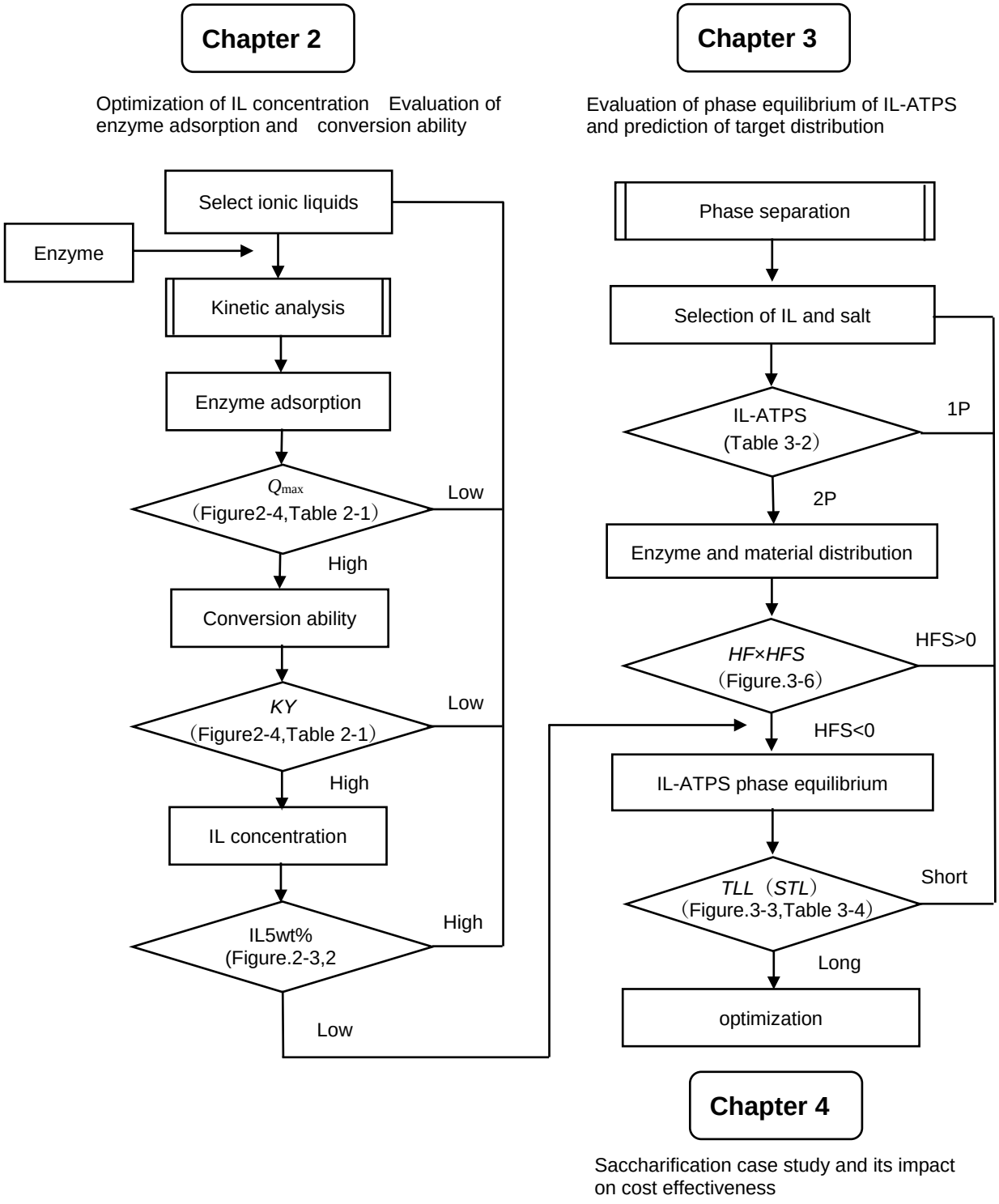

Figure 3-9 Design scheme for the application of saccharification process.

5. Summary

IL-ATPSs were prepared using [Amim][Cl] or [Bmim][Cl] and K_2CO_3 or K_2HPO_4, and their physical properties were evaluated on the basis of phase diagrams. The phase separation behavior changed due to the hydrophobicity of the alkyl chain of the IL cationic species, and the hydration entropy differed according to the position of the salt in the Hofmeister series. The IL-ATPSs prepared in this study exhibited temperature dependence. They were of the UCST type, in which the phase separation range expanded with decreased temperature. [Bmim][Cl]/K_2HPO_4 at 5 °C exhibited the widest phase separation, with about 97% of the total IL in the system being separated into the top phase. Furthermore, [Bmim][Cl]/K_2HPO_4 exhibited a high hydrophobicity towards water-soluble amino acids. A qualitative and quantitative determination method for the separation of a salt-rich bottom phase and an IL-rich top phase using information obtained from the phase map and the calculated values of the *HF* was demonstrated as 0.13-0.41 mol/kJ, suggesting that the hydrophobicity gap between top and bottom phases are large, as well as the conventional ATPS composed of PEG/$MgSO_4$. It is suggested that the obtained data regarding the fundamental characteristics of the IL-ATPSs can be applied to the rational design of the bioconversion/bioseparation process, as reported in previous case studies.

Chapter 4

Enzymatic Hydrolysis of Cellulose Recovered from Ionic Liquid-Salt Aqueous Two-phases system

1.Introduction

Effective utilization of biomass source has been considered to simultaneously solve problems of a stable and sustainable supply of energy resources substituted for oil, and of an emission control of carbon dioxide that causes global warming [Hill et al., 2006]. On the other hand, there is a concern that the utilization of biomass as industrial raw material is competitive to food problem. To solve such a competitive problem, several methods have been proposed that utilize cellulose contained in the waste portion of food crops and in wood. As feedstock for biomass refinery, lignocellulose, which comprises cellulose (33-45%), hemicellulose (20-30%), and lignin (15-30%), is perceived. Also, waste papers can be a candidate for biomass source, but the processing of cellulose has still included many challenges [Olivier-Bourbigou et al., 2010]. The saccharification of cellulose by enzymes is an environment-friendly energy production method because the reaction can proceed in mild condition [Habibi et al., 2010]. However, it is difficult to dissolve cellulose in water or organic solvents, because cellulose is a polymer material with a strong crystal structure derived from intermolecular hydrogen bonds. Until now, various kinds of enzymatic saccharification processes are reported: for instance, utilizing ionic liquid (IL) as pretreatment agent [Alvira et al., 2010]. To utilize plants e.g. woody and vegetation as biomass, pretreatment is necessary to dissolve cellulose. The crystalline cellulose is hardly hydrolyzed by cellulase, while the regenerated cellulose, which has less or no crystallinity, is easily hydrolyzed [Lee et al., 2009].

At present, the mainstream of cellulose pretreatment is an acid treatment method. In this process, there is an advantage in large-scale process while it requires a larger amount of energy because the reaction is performed under high temperature and pressure, and results in abundant waste liquids. After the first report of Fort et al. that ILs such as 1-butyl-3-methylimidazolium chloride ([Bmim][Cl]) can dissolve woods (i.e., lignocellulosic biomass) [Fort et al., 2007], researches focusing on their dissolution and saccharification have been accelerated [Zavrel et al., 2009, Lee et al., 2009]. Once

lignocellulosic biomass dissolved in IL, the anti-solvent such as ethanol, acetone, and water are used to recover component. In this step, lignin and hemicellulose are still dissolved in IL while cellulose is regenerated with less crystallinity [Moniruzzaman et al., 2018, Silverstein et al., 2007, Li et al., 2010, Shill et al., 2011]. The regenerated cellulose, which is provided by pretreatment with IL, is suitable for enzymatic hydrolysis because the amorphized cellulose (regenerated cellulose) is easily decomposed as compared to crystalline cellulose fiber [Lee et al., 2009]. Thus, it is expected that the hydrolysis reaction by cellulase is synergistically performed when regenerated cellulose is applied as substrate (feed) [Tanimura et al., 2018].

In addition, the coexistence of ILs and specific salts spontaneously form phase-separation systems ((IL-aqueous two-phase systems (IL-ATPSs)), wherein most of ILs are condensed in the upper phase [Tanimura et al., 2018]. IL-ATPSs have been applied for extraction and reaction system [Pratiwi et al., 2015, Matsumoto et al., 2014]. ILs should be recycled due to its high cost, however, there are only few studies on the cellulose saccharification process considering the reuse of expensive ILs. When the cellulose recovery was performed in IL-ATPS, the regenerated cellulose was accumulated between top and bottom phase [Shill et al., 2011]: Shill et al. reported about enzymatic saccharification of Miscanthus biomass, which was pretreated by IL-ATPS. They used K_2HPO_4 or K_3PO_4 as salt, and [Bmim][Cl] or [Emim][OAc] as IL. Because Miscanthus biomass is a type of lignocellulosic biomass, it is suggested that IL-ATPS could be used for dissolution of crystalline cellulose. Notably, both K_2HPO_4 (alkaline) and IL have a potential to dissolve cellulose, while cellulase (from *Trichoderma reesei*) is optimized in acidic pH. Also, a higher concentration of IL denature cellulose [Turner et al., 2003]. To better understand of the efficiency of IL-ATPS for pretreatment of cellulose, it is important to discuss the effect of pH on the bottom phase.

Based on our previous works, in the IL-ATPSs, the IL-enriched upper phase and the salt-enriched alkaline phase were separated [Tanimura et al., 2019]. Since the cellulase activity is enhanced at weak acid conditions, further optimizations are required to utilize IL-ATPS on the enzymatic saccharification process. In this study, the IL-ATPSs were prepared by ILs such as 1-allyl-3-methylimidazolium chloride ([Amim][Cl]) and [Bmim][Cl], and by salts such as K_2HPO_4, K_2CO_3, and mixed salt (NaH_2PO_4 and

Na_2HPO_4) which optimize the pH condition of IL-ATPS. After treatment of cellulose in IL-ATPSs, the regenerated cellulose was applied on the hydrolysis using cellulase from *Trichoderma viride*. Finally, we focused on the process design to enzymatically hydrolyze the pretreated regenerated cellulose.

2.Materials and methods

2.1 Materials

[Bmim][Cl] and [Amim][Cl] were purchased from Sigma Aldrich Japan (Tokyo, Japan). Crystalline cellulose powder, disodium hydrogen phosphate (Na_2HPO_4), and sodium dihydrogen phosphate (NaH_2PO_4) were purchased from Nacalai Tesque (Kyoto, Japan). Cellulase from *Trichoderma viride* (≥5,000 units/g solid) was purchased from Yakult Pharmaceutical Industry (Tokyo, Japan). Dipotassium hydrogen phosphate (K_2HPO_4) were purchased from Kanto Kagaku (Tokyo, Japan). Other chemicals were obtained from Wako Pure Chemical Corporation (Osaka, Japan), and used without further purification.

2.2 Preparation of IL-ATPS

[Amim][Cl] or [Bmim][Cl] powder was weighed in a screw tube and melted by heating at 100 °C for 5 min using a hot stirrer. An aqueous solution was prepared in which mixed salts consisting of K_2HPO_4, K_2CO_3, NaH_2PO_4 and Na_2HPO_4 were dissolved, and these were added to a weighed screw tube. After thoroughly stirring the sample, it was allowed to stand for 5 min to confirm the formation of a two-phase system. The weight fractions of salt, IL and pure water were changed to confirm the formation of two-phase system. The prepared samples were used to measure the pH of the upper and bottom phases.

2.3 Cellulose pretreatment in IL-ATPS

The cellulose was completely dissolved by heating and stirring in [Bmim][Cl] or [Amim][Cl] at 100 °C for 15 min. By heating with ILs, the dissolution of cellulose can be promoted [Swatloski, et al., 2002]. Herein, the crystalline cellulose was preliminary dissolved in ILs by heating at 100 ℃ for 5 min, then the dissolved cellulose (in IL) was

applied for IL-ATPS preparation. The salt was preliminaly dissolved in pure water. These solutions were added to IL in which cellulose was dissolved, and were sufficiently stirred using a magnetic stirrer. After standing for 1 h, an ATPS was formed, and regenerated cellulose was confirmed near the interface. After that, the regenerated cellulose solid was removed using tweezers, taking care not to take out the solution near the interface.

2.4 pH measurements of IL-ATPS.

To know the pH of mixed salt systems, the mixing ratio of NaH_2PO_4 and Na_2HPO_4 was changed to prepare salt solutions with concentration of 30 wt%, and the pH of each sample was measured (**Figure 4-1 and Table 4-1, Table 4-2**). For IL-ATPS, the upper and lower phases were physically separated using a biuret. From the results obtained, the mixing ratio of salts for adjusting the bottom phase to the optimum pH of cellulase was determined.

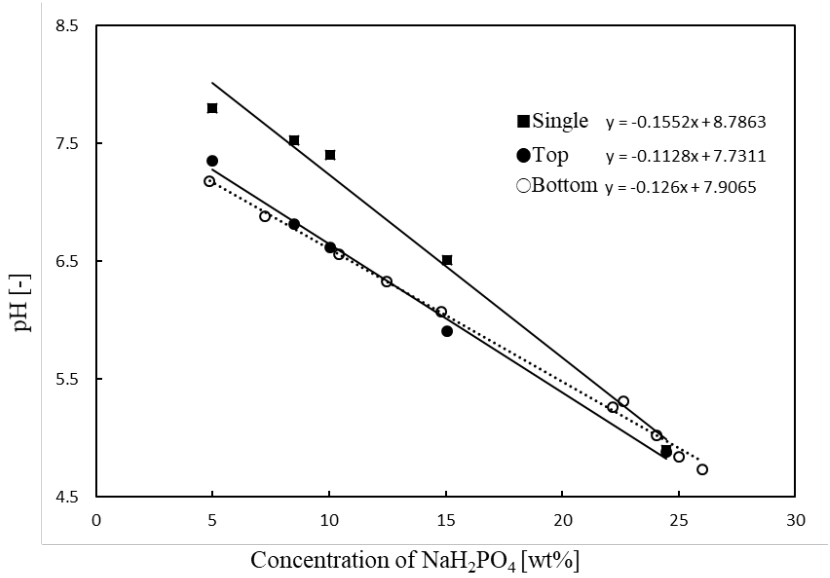

Figure 4-1 Relationship between NaH_2PO_4 concentration and pH. Total salt concentrations (= $[Na_2HPO_4]$ + $[NaH_2PO_4]$ were adjusted to 30 wt%. Single phase (closed square) indicates the pH of systems containing salt only. Top (closed circle) and Bottom (open circle) indicate the pH of upper and lower phases of IL/ATPS (include 20 wt% [Bmim][Cl], 30 wt % salt), respectively.

Table 4-1 Salt mixing ratio and pH variation in single phase systems.

Weight [g]				pH [-]
Sample	NaH_2PO_4	Na_2HPO_4	H_2O	
1	2.592	0.399	6.979	4.73
2	2.493	0.502	6.979	4.84
3	2.395	0.591	6.979	5.02
4	2.216	0.794	6.979	5.26
5	2.260	0.745	6.979	5.31
6	1.475	1.512	6.979	6.07
7	1.238	1.715	6.979	6.33
8	1.053	2.073	6.979	6.56
9	0.723	2.287	6.979	6.88
10	0.483	2.467	6.979	7.18

All samples have a salt concentration of 30 wt%.

Table 4-2 Salt mixing ratio and pH in IL-ATPS.

Sample	Weight [g]			pH [-]	
	NaH_2PO_4	Na_2HPO_4	ILaq	Top	Bottom
A	0.505	2.503	7.096	7.80	7.35
B	0.857	2.143	7.060	7.53	6.82
C	1.004	2.002	6.977	7.40	6.62
D	1.504	1.499	6.989	6.51	5.91
E	2.499	0.499	7.210	4.90	4.88

All samples have a salt concentration of 30 wt%.

2.5 Hydrolysis of regenerated cellulose by enzymes

The regenerated cellulose recovererd from IL-ATPS was subjected to enzymatic hydrolysis in 25 mM acetate buffer. Since aqueous solutions of K_2CO_3 and K_2HPO_4 show alkalinity, the pH of the regenerated cellulose dispersions were adjusted to 4.8 if necessary. The pH conditions before and after reaction were measured in all samples. The enzymatic saccharification was performed in a 100 mL Erlenmeyer flask under following conditions: enzyme concentration, 100 mg/L; reaction temperature, 45 °C (the optimum temperature for cellulase); shaking condition, 60 strokes/min. The glucose concentration was measured by taking out of 200 μL of the reaction solution at prescribed time. Glucose concentration was measured using Glucose CII Test Wako kit® (Osaka, Japan) [Miwa et al., 1972].

3. Results and discussion

3.1 Process design for saccharification reaction using IL-ATPS.

The imidazolium-based IL, which can be used as a cellulose solvent, forms a two-phase system by mixing with salts such as K_2CO_3 and K_2HPO_4 [Tanimura et al., 2019]. Advantages of the use of IL-ATPS are as follows: (i) reuse of IL after pretreatment of cellulose, and (ii) prevention of enzyme inactivation due to strong interaction between ILs. On the other hand, the existence of high concentration IL could inhibit the enzymatic activity of cellulase [Tanimura et al., 2018]. In cellulose hydrolysis by enzymes, it is necessary to control the reaction temperature and pH in process. In particular, the presence of salt drastically alters the pH condition.

Herein, three types of saccharification processes (A-C) were tested. In Process A, the regenerated cellulose obtained in IL-ATPS and in single-phase system were directly applied on saccharification (**Figure 4-2**). In Process B, the regenerated cellulose obtained in the IL-ATPS was washed to decrease the effect of salt, and used as a substrate for saccharification reaction with pH adjustments (**Figure 4-3**). Assuming the large-scale industrial plant, the operation processes such as cleaning and pH adjustment will be noticeable at the initial cost and maintenance of the facility. Particularly in the process using enzymes, the saccharification reaction

must be performed at optimum conditions (temperature, pH, and so on). Thus in Process C, the regenerated cellulose was dispersed in the pH-controlled reaction media, then the saccharification reaction was initiated (**Figure 4-3**). The differences in pretreatment process will influence on the efficiency of saccharification, thus the results will contribute to optimization of the process using IL-ATPS.

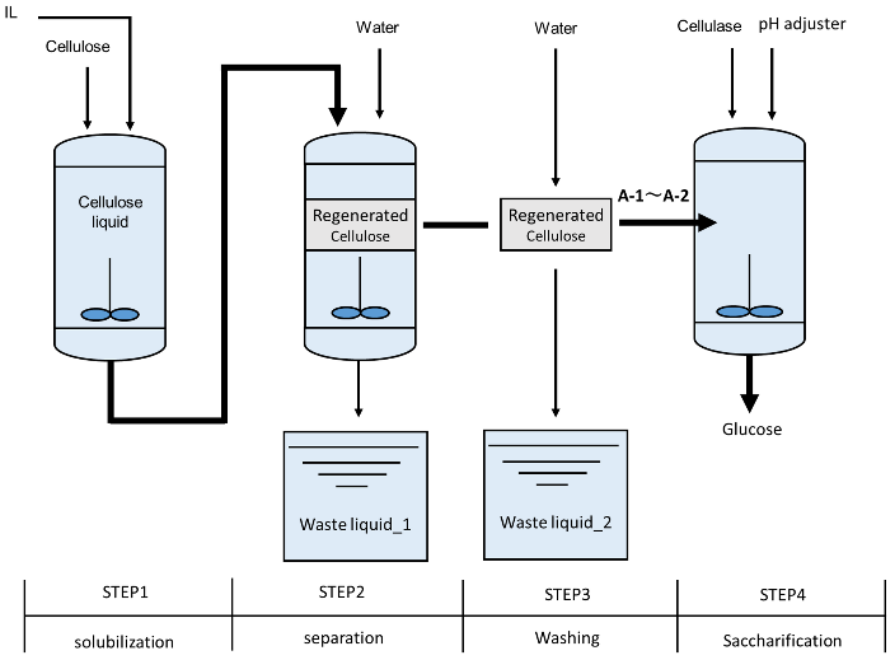

Figure 4-2 Schematic illustration Process A: enzymatic saccharification of the cellulose pretreated with IL monophasic solution. STEP 1: cellulose is completely dissolved by heating and stirring with IL at 100 ℃ for 15 min. STEP 2: regenerated cellulose is recovered from the solution by adding pure water. STEP 3: regenerated cellulose is washed with pure water to remove remained IL. STEP 4: pH is adjusted to the optimum pH 4.8, then saccharification is initiated by adding cellulase at 45 ℃.

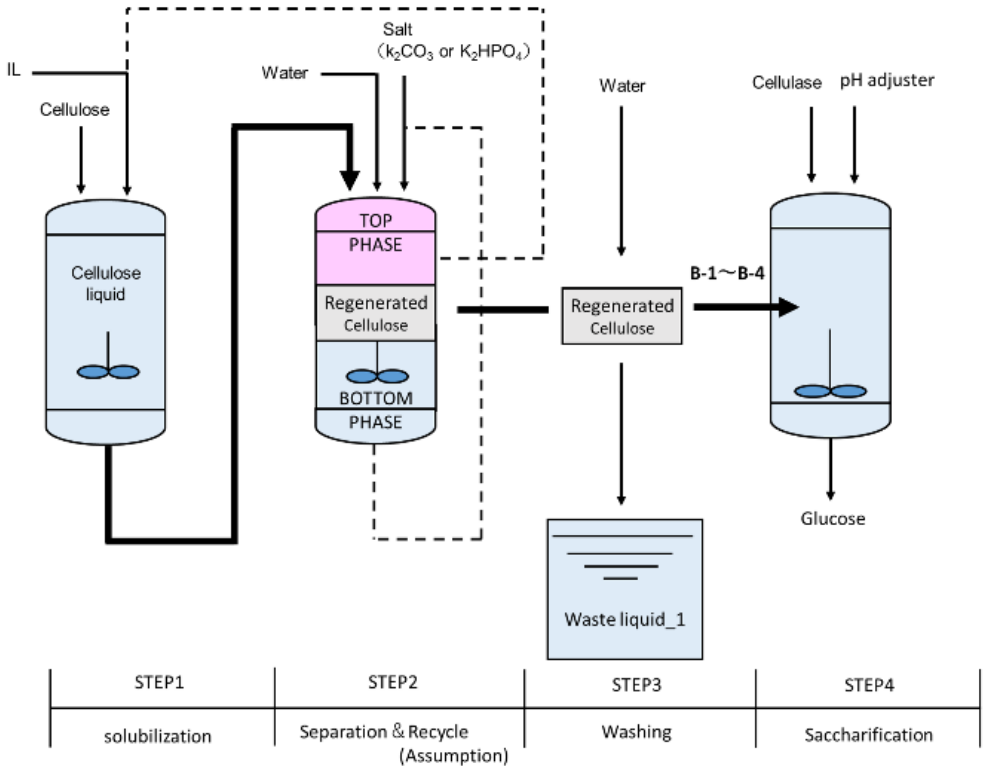

Figure 4-3 Schematic illustration Process B: enzymatic saccharification of cellulose pretreated with IL-ATPS. STEP 1: cellulose is completely dissolved by heating and stirring with IL at 100 ℃ for 15 min. STEP 2: regenerated cellulose is recovered from the solution by adding pure water and salt (K_2CO_3, K_2HPO_4). STEP 3: regenerated cellulose is washed with pure water to remove remained IL and salt. STEP 4: pH is adjusted to the optimum pH 4.8, then saccharification is initiated by adding cellulase at 45 ℃. Broken lines indicate the recycling process.

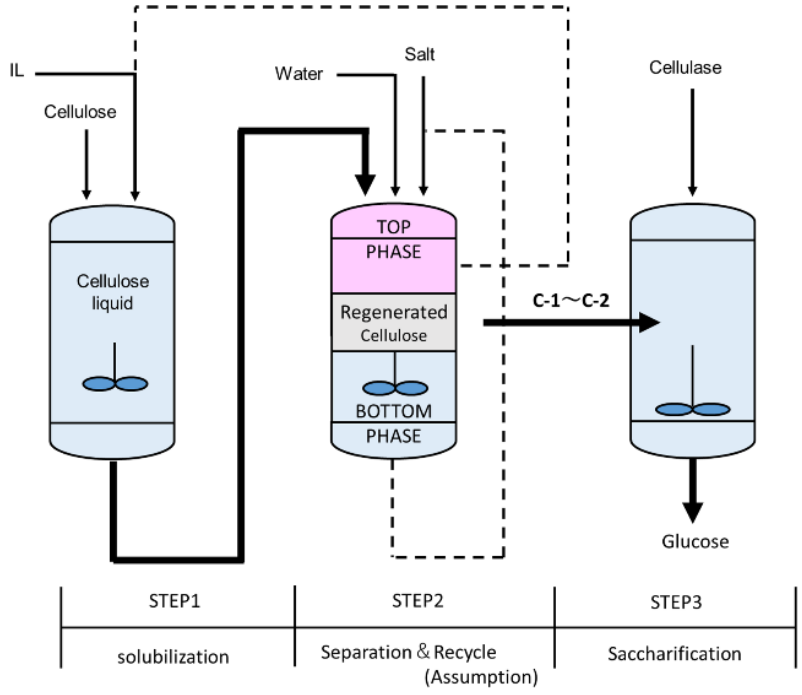

Figure 4-4 Schematic illustration Process C: enzymatic saccharification of cellulose pretreated with optimized IL-ATPS. STEP 1: cellulose is completely dissolved by heating and stirring with IL at 100 ℃ for 15 min. STEP 2: regenerated cellulose is recovered from the solution by adding pure water and mixed salt (NaH_2PO_4/Na_2HPO_4 = 5/1 (wt/wt)). STEP 3: regenerated cellulose is recovered from solution, then saccharification is initiated by adding cellulase at 45 ℃. Broken lines indicate the recycling process.

3.2 Recovery of regenerated cellulose.

As concept of this study, the recovered liquids should be recycled, thus the recovery of liquids was tested after the removal of regenerated cellulose. In results, 66-77 wt% of liquids were remained, which would include IL, salt, water, and dissolved cellulose (**Table 4-3**). Importantly, the recovered liquids formed two phases, suggesting that the recovered liquids include high concentrations of IL and salt. Shill et al also reported that the recovery of IL from lignocellulose-pretreated IL-ATPS was ca. 60-70% [Shill et al., 2011].

The collected regenerated cellulose was dispersed in acetate buffer. Some of samples showed basic pH: the solution pH slightly increased in the case of K_2HPO_4 salt, and drastically increased in the case of K_2CO_3 salt. This indicates that at least, aliquot amount of salt was associated with regenerated cellulose. Therefore, the salt which provides an optimal pH condition (pH 4.8) for enzyme is preferred. In the proposed process, both of upper and bottom phases should be recycled to form IL-ATPS. To improve the recovery yield of liquids, a centrifugation would be available, wherein regenerated cellulose is collected as precipitate. Hopefully, ca. 95 wt% of IL could be accumulated in the upper phase of IL-ATPS according to our previous study [Tanimura et al., 2019].

Table 4-3 Recovery of regenerated cellulose

IL-ATPS	Initial mass [g] (1)	Recovered liquids [g] (2)	Regenerated cellulose [g] (1) – (2) [c]	pH of regenerated cellulose dispersion [-] [d]
[Bmim][Cl]/K_2CO_3 [a]	10.05	6.67	3.38	6.69
[Bmim][Cl]/K_2HPO_4 [a]	10.05	6.21	3.84	5.98
[Bmim][Cl]/mixed salt [b]	10.05	7.23	2.82	4.74
[Amim][Cl]/K_2CO_3 [a]	10.05	6.31	3.74	10.2
[Amim][Cl]/K_2HPO_4 [a]	10.05	6.01	4.04	4.92
[Amim][Cl]/mixed salt [b]	10.05	7.52	2.53	4.83

[a] IL-ATPS was composed of IL: 3.0 g, salt: 1.5 g, water: 5.5 g, and cellulose: 0.05 g.

[b] IL-ATPS was composed of IL: 2.0 g, salt: 3.0 g, water: 5.0 g, and cellulose: 0.05 g. Salt included NaH_2PO_4: 2.5 g, Na_2HPO_4: 0.5 g.

[c] calculated by (1) – (2)

[d] regenerated cellulose was dispersed in acetate buffer

3.3 Effect of IL-ATPS on enzymatic hydrolysis

The dissolved cellulose pretreated with [Amim][Cl] or [Bmim][Cl] was added to K_2HPO_4 or K_2CO_3 aqueous solution, which successfully resulted in IL-ATPS. After removal of solution, regenerated cellulose was washed twice with 20 mL of pure water, then the saccharification reaction with cellulase was performed. The concentration of glucose produced after 48 h showed different values. The order of glucose production was [Amim][Cl]/K_2HPO_4 > [Bmim][Cl]/K_2HPO_4 > [Bmim][Cl]/K_2CO_3 > [Amim][Cl]/K_2CO_3 (**Figure 4-5**). This result could be explained by the difference of pH during the reaction. All of samples were initially prepared at pH 4.8, but the final pH after reaction was different (**Table 4-4**). Obviously, the samples pretreated with IL/K_2CO_3 systems showed higher (alkaline) pH after reaction, as compared to K_2HPO_4. The shift of pH drastically decreased the yield of glucose, suggesting that salt tends to remain in regenerated cellulose (**Table 4-4**). It was found that the choice of salt had a great influence on saccharification efficiency: it is better to use the salt which maintain the solution pH neutral or acidic conditions. The phase separation behavior of IL-ATPS is generally followed by the Hofmeister series [Bridges et al., 2007, Pei et al., 2007, Nockemann et al., 2008, Zafarani-Moattar et al., 2007, Pei et al, 2009], wherein no significant differences are reported between K_2CO_3 and K_2HPO_4. Although there is a possibility that the regenerated cellulose includes IL molecules [Feng et al., 2008], the washing process could remove most IL and reduce inhibitory effect of IL in enzymatic saccharification. Because the alkalinity of K_2HPO_4 is weaker than K_2CO_3, the sample pH of systems B-1 and B-2 were stable during the reaction.

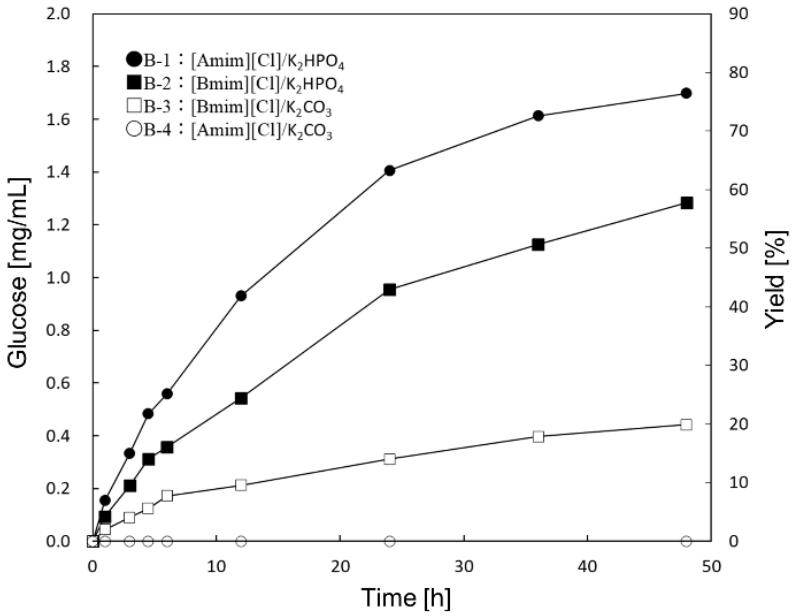

Figure 4-5 Time courses of glucose concentration produced in the hydrolysis at 45℃. Samples B-1 to B-4 are shown as follows. Sample B-1: [Amim][Cl]/K_2HPO_4 (closed circle), Sample B-2: [Bmim][Cl]/K_2HPO_4 (closed square), Sample B-3: [Bmim][Cl]/K_2CO_3 (open square), Sample B-4: [Amim][Cl]/K_2CO_3 (open circle). For all samples, the compositions (IL/salt/water) were = (30/15/50). The amount of initially charged cellulose was 50 mg, and the cellulase concentration was 100 mg/L.

Table 4-4 Composition and pH of sample B-1 to B-4.

[a] Mass-based composition (IL/salt/water) was 30/15/50.

[b] The final pH means the pH of the reaction solution prepared after saccharification. [c] Glucose yield was calculated at the reaction time of 48 h.

Sample	B-1[a]	B-2 [a]	B-3 [a]	B-4 [a]
IL	[Amim][Cl]	[Bmim][Cl]	[Bmim][Cl]	[Amim][Cl]
Salt	K_2HPO_4	K_2HPO_4	K_2CO_3	K_2CO_3
Final pH[b]	4.92	5.98	6.69	10.2

Glucose yield [%][c]	73.8	57.7	19.9	0

3.4 Comparison of regenerated cellulose obtained by IL-ATPS and IL mono-phasic solution

IL-ATPS was prepared with a composition of IL/salt/water = (30/15/55) [wt%], and a phase diagram was experimentally created at 25 °C (**Figure 4-6A, B**). As negative controls, the regenerated cellulose was prepared by the mono-phasic IL solutions which did not include any salts (IL/water = (30/70), A-1 and A-2). As shown in **Figure 4-2**, the regenerated cellulose was also obtained. Thus, the comparisons of samples A and B would clarify the effect of salt on the saccharification efficiency of regenerated cellulose. As a result, the regenerated cellulose pretreated with IL-ATPS showed ca. 10% improvement in the yield (**Figure 4-6C, D**). It is suggested that the upper phase in IL-ATPS include ~40 wt% of ILs, which could promote amorphosization of crystalline cellulose. It is considered that the cellulose dissolution ability of IL depends on the alkyl chain length [Erdmenger et al., 2007], and the amorphization ability of [Amim][Cl] is superior than [Bmim][Cl] [Kilpeläinen, I. et al., 2007, Xing, L. et al., 2014]. In summary, the dissolution of crystalline cellulose and recovery of regenerated cellulose was most promoted by the pretreatment with [Amim][Cl]/K_2HPO_4 ATPS. The solubility of cellulose is linked to the hydrogen bond accepting ability of anions [Xu et al., 2010], because the dissolution of cellulose could be mainly caused by the interaction of carbohydrate and IL anions [Remsing, R. C. et al., 2008]. Within the ILs composed with $[Bmim]^+$ ($[C_4min]^+$), the dissolution abilities of Avicel® cellulose depend on the anion species: in the order of OAc^- > Cl^- > $HCOO^-$ > DCA^- > NTf2 [Wang et al., 2012]. Comparing the IL cations, the dissolution ability of $[Amim]^+$ is higher than $[Bmim]^+$ [Swatloski et al., 2002]. In addition, the alkyl chain length of IL cations influences on the dissolution ability: a shorter chain could be preferred to promote cellulose dissolution [Wang et al., 2012, Vitz et al., 2009].

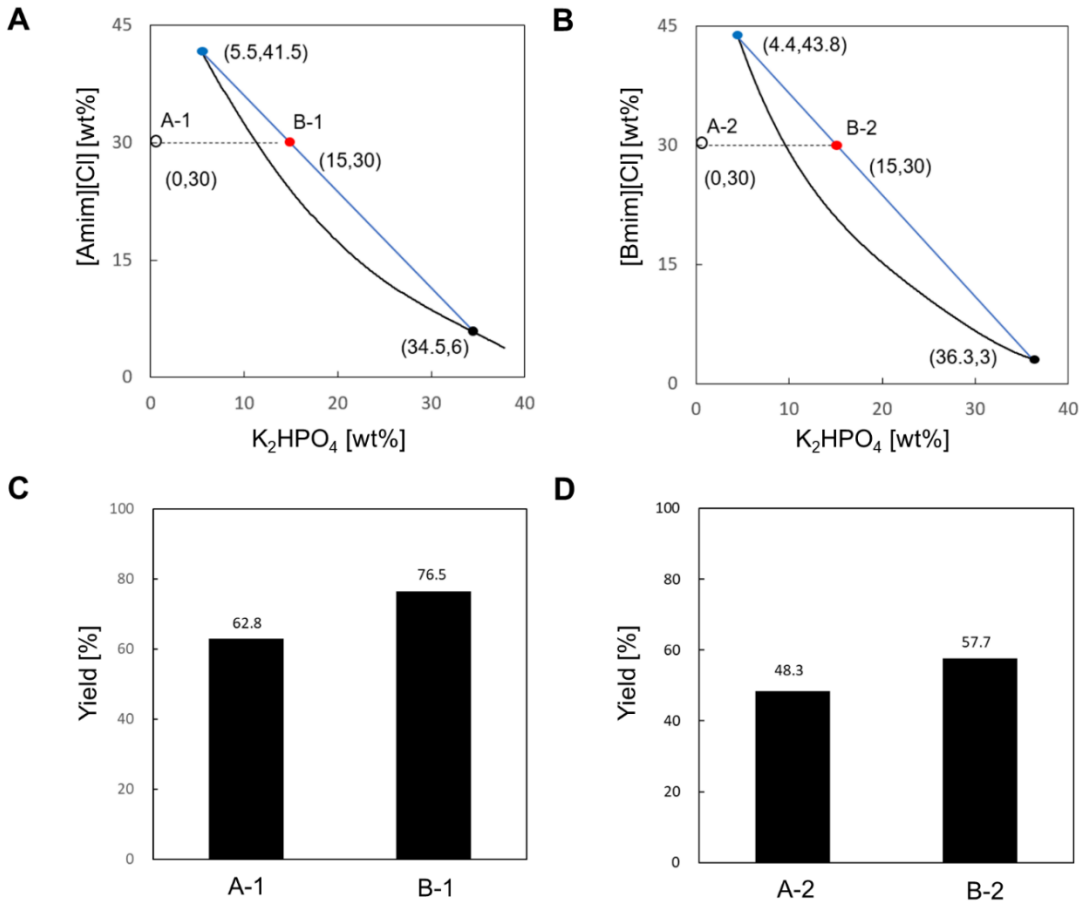

Figure 4-6 Phase diagrams of [Amim][Cl]/K_2HPO_4 ATPS (A) and [Bmim][Cl]/K_2HPO_4 ATPS (B). The binodal curves are shown in black solid lines. The mass-based compositions (IL/salt/water) of B-1 and B-2 were (30/15/55), and tie lines are shown as blue. The composition of the top and bottom phases are described as blue and black circles, respectively. The mono-phase systems including 30 wt% of IL (A-1 and A-2) are shown as open circles. Experimental temperature was 25 ℃. The glucose yield at 48 h, performed by the regenerated cellulose from IL-ATPS or IL mono-phasic systems (C, D). Compositions were as follows: A-1, [Amim][Cl]/water = 30/70; B-1, [Amim][Cl]/K_2HPO_4/water = 30/15/45; A-2, [Bmim][Cl]/water = 30/70; B-2, [Bmim][Cl]/K_2HPO_4/water = 30/15/45. The total IL concentration was adjusted to 30 wt% both in two-phase system and in mono-phasic system.

3.5 Optimized IL-ATPS prepared by mixed salts of NaH_2PO_4 and Na_2HPO_4

The enzymatic hydrolysis of regenerated cellulose pretreated with IL-ATPS needs a substrate washing process, because the residual salt made the pH of reaction mixture to alkaline conditions. Ideally, the design of IL-ATPS that shows an optimum pH for enzymatic hydrolysis is required. To simplify the process, the IL-ATPS composed with the mixed salts of NaH_2PO_4 and Na_2HPO_4 was prepared, and the saccharification efficiency was investigated. For pH adjustment, the optimum ratio of NaH_2PO_4 and Na_2HPO_4 was experimentally determined (**Table 4-1**). The influence of the formation of a two-phase system on pH was investigated, suggesting that the IL-ATPSs with the composition of IL/total salt/water = (20/30/50) became two-phases, and the ratio of NaH_2PO_4/Na_2HPO_4 = 5/1 resulted in the optimum pH (4.8-4.9) for cellulase activity (**Table 4-2**).

The regenerated cellulose obtained by pretreatment with IL/mixed salt ATPS systems were applied to enzymatic saccharification, wherein the washing of regenerated cellulose is not needed before reaction (**Figure 4-4**). The yield at 48 h was 70% for both [Amim][Cl] or [Bmim][Cl]/mixed salt ATPS systems, and throughout the reaction, and the glucose production at the initial reaction period was greater with [Amim][Cl]/mixed salt ATPS as compared to [Bmim][Cl]/mixed salt ATPS (**Figure 4-7**). No significant pH changes were observed after the reaction (**Table 4-5**), and notably, the total IL used in these systems were 20 wt%. The final glucose production at 48 h were almost similar in IL/mixed salt ATPS (IL/salt/water = (20/30/50)) and in IL/K_2HPO_4 ATPS (IL/salt/water = (30/15/45)). It is thus suggested that the use of mixed salts (NaH_2PO_4/Na_2HPO_4 = 5/1 (wt/wt)) systems has a benefit in eliminating the washing step of regenerated cellulose, and in the reduction of the IL amount in pretreatment process.

The enzymatic saccharification process of cellulose can be constructed by three steps: (i) dissolution of crystalline cellulose, (ii) regeneration of amorphous cellulose in aqueous medium, (iii) enzymatic hydrolysis. Especially in step (iii), the coexistence of IL brings both advantage and disadvantage. The intermolecular hydrogen bonds between cellulose, decomposed cellulose (oligosaccharide), and cellobiose (glucose dimer) are broken by their interaction with IL cations and

anions (33-34). This suggests that the coexistence of IL prevents a recombination (recoupling) of generated products. In contrast, the presence of ILs, especially high concentration of Cl^-, leads the unfolding of enzyme, resulting in the decrease of the hydrolysis rate of cellulase from *Trichoderma reesei* [Turner et al., 2003]. In our previous study, the coexistence of 5 wt% ILs ([Amim][Cl], [Bmim][Cl]) promoted the saccharification of cellulose, while the hydrolysis activities decreased with >10 wt% ILs [Tanimura et al., 2018]. Also, the existence of product (glucose) or intermediate (cellobiose) leads inhibitory effect on the enzymatic saccharification of softwood substrates: Zhizhuang et al. reported that the final of glucose was ca. 80% [Xiao et al., 2004]. It is assumed that water-soluble oligosaccharide are remained after reaction. Higher conversion values is of course preferred, but some of oligosaccharides are also valuable products because they are expensive as compared to glucose.

Table 4-5 Compositions and pH conditions of Samples C-1 and C-2.

Sample	C-1[a]	C-2 [a]
IL	[Bmim][Cl]	[Amim][Cl]
Salt (wt/wt)	NaH_2PO_4/ NaH_2PO_4 =5/1	NaH_2PO_4/ NaH_2PO_4 =5/1
Final pH[b]	4.75	4.83

[a] Mass-based composition (IL/salt/water) was 30/15/50.

[b] The final pH mean the pH of the reaction solution prepared after saccharification.

3.6 Process flow of saccharification reaction using IL-ATPS

According to the results obtained in this study, the yield after 48 h when using the mixed salt was about 70 %, which was achieved with the use of 20 wt% IL in the initial ATPS preparation. Because the pH of IL/mixed salt ATPS was weekly acidic (almost optimal for cellulase), the dissolution of cellulose could promoted by condensed IL in the upper phase. Therefore, when considering plant design, we examined flow plans for materials, chemicals, etc. Two patterns were considered as a system to compare. One is a system in which IL for pretreatment of cellulose solution is mixed with K_2HPO_4 solution (**Figure 4-7**), and the other is a system using a mixed salt (**Figure 4-8**). The equipment that can be simplified when using mixed salts is a pH adjuster. Tanks for storing pure water, conveyors for cleaning and transporting regenerated cellulose, pumps for transporting various fluids, and valves are necessary for flow control. An item number is provided on the flow sheet so as to confirm the simplified contents. In addition, the device names and roles were summarized to correspond to the flow sheet numbers (**Table 4-6** and **Table 4-7**).

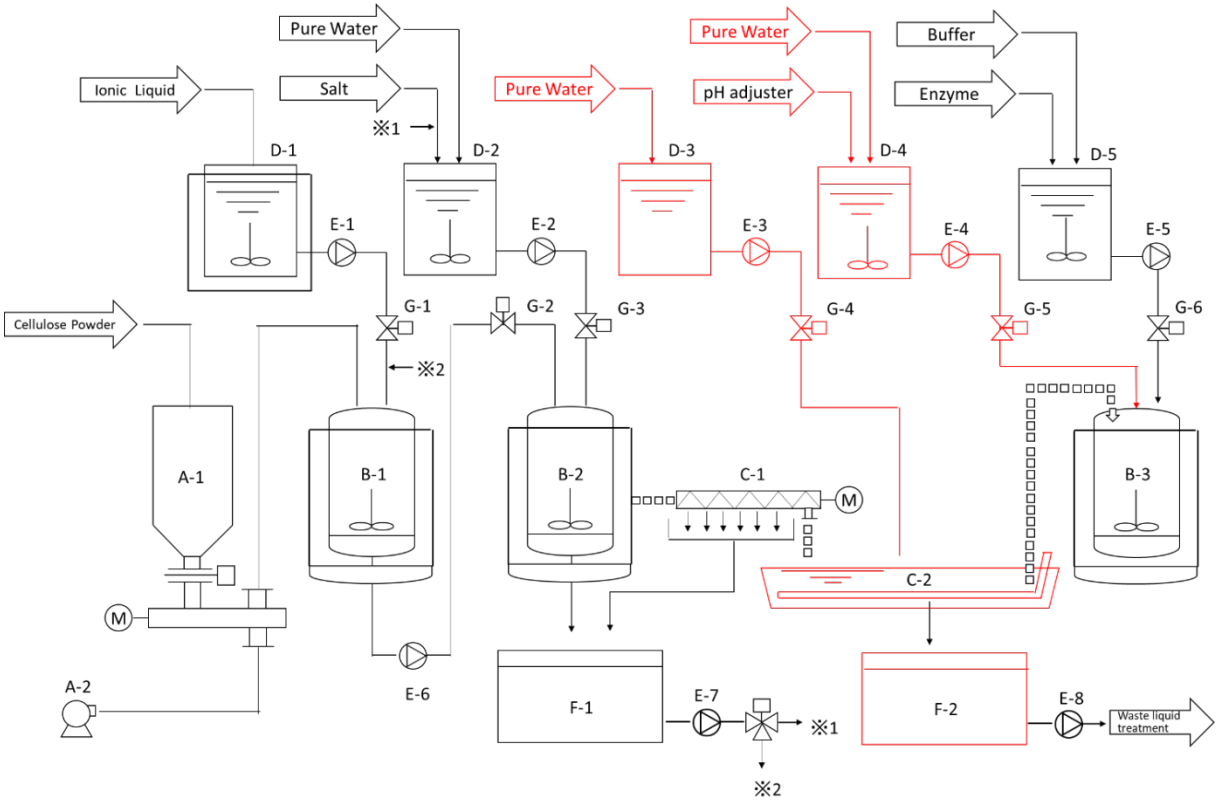

Figure 4-7 Process flow for enzymatic saccharification of cellulose using IL-ATPS.

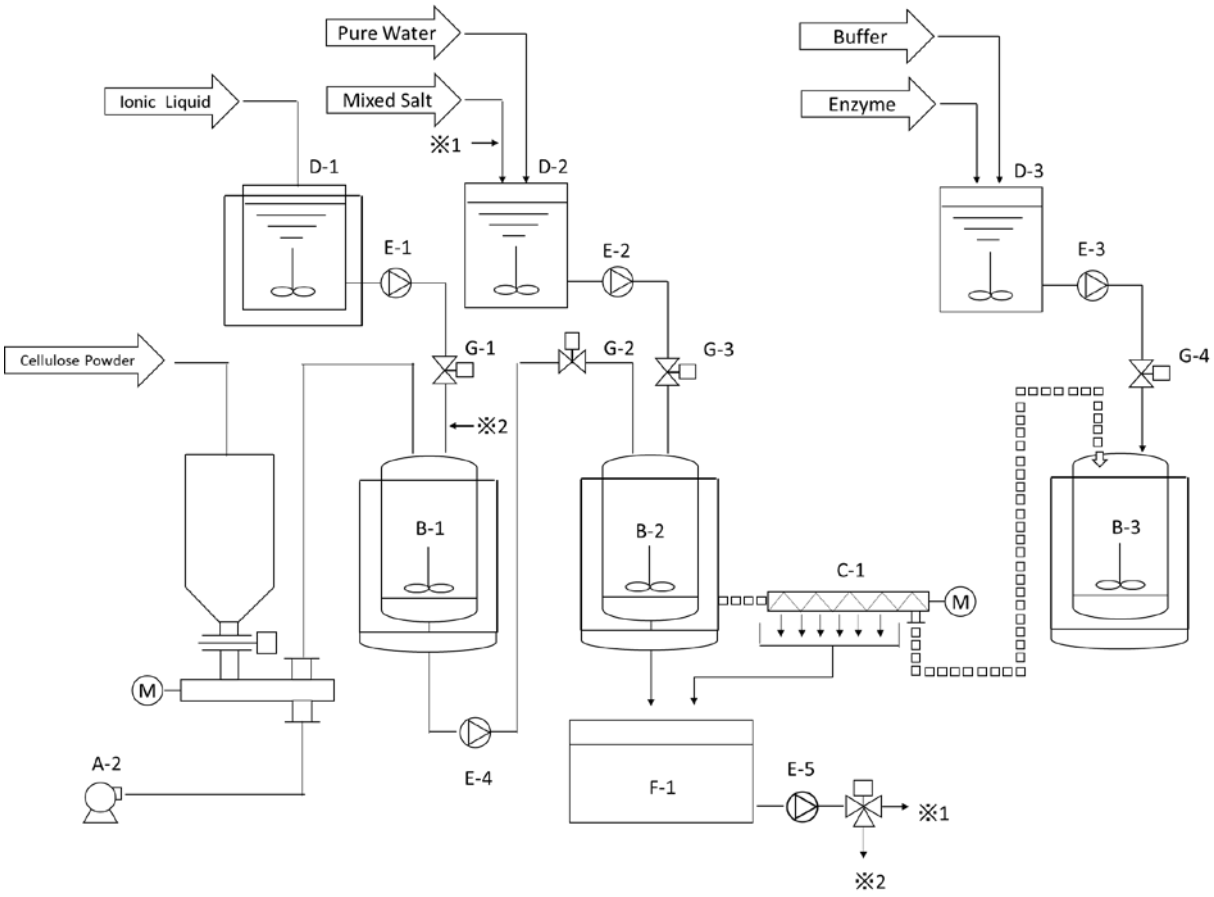

Figure 4-8 Process flow using optimized IL-ATPS after cellulose pretreatment.

By employing the IL-ATPS composed of mixed salt, it is possible to significantly reduce utility costs such as the amount of pure water used, the amount of pH adjuster used, and the amount of power consumed in washing.

Table 4-6 Apparatus and their purpose for assumed process flow in IL-ATPS prepared with K_2CO_3 and K_2HPO_4.

No	Apparatus name	Purpose / state
A : The supply of cellulose		
A-1	Cellulose storage tank Constant cutting device	Storage and supply of cellulose
A-2	Blowing unit	Supply of powdered cellulose by blower
B : Tanks for Cellulose Pretreatment and Saccharification		
B-1	Mixing tank	Mixing of cellulose and IL at around 100 ° C
B-2	Phase separation tank	Separation of IL-ATPS and regenerated cellulose
B-3	Reaction tank	Enzymatic hydrolysis of regenerated cellulose
C : Conveyor for transport of regenerated cellulose solids		
C-1	Screw conveyor	Transport and squeeze regenerated cellulose
C-2	Submerged scraper conveyer	Transport and cleaning of regenerated cellulose
D : Storage tanks for cellulose pretreatment and saccharification		
D-1	IL storage tank	Storage of IL solution (IL dissolution temperature conditions)
D-2	Salt water storage tank	Saltwater storage
D-3	Pure water storage tank	Pure water storage
D-4	pH adjuster storage tank	pH adjuster storage
D-5	Enzyme solution storage tank	Enzyme solution storage
E : Pumps for cellulose pretreatment and saccharification		
E-1	IL Supply pump	Transport of IL solution (IL dissolution temperature conditions)
E-2	Salt water pump	Salt water supply
E-3	Pure water feed pump	Pure water supply
E-4	ph adjuster supply pump	Supply of pH adjuster
E-5	Enzyme solution supply pump	Supply of enzyme solution
E-6	Cellulose Liquid Supply pump	Transport of cellulose solution at around 100 ° C
E-7	IL-ATPS reuse pump	Recycling of the upper and lower phases of ILATPS
E-8	Drainage water pum	Transportation of washing drainage
F : Tanks for IL and Salt Recovery and waste liquid		
F-1	IL-ATPS recovery storage tank	IL and Salt recovery
F-2	Waste tank	Retain the recovered liquid after washing with regenerated cellulose
G : Valve for Flow control and switching		
G-1	IL flow control valve	Adjustment of IL flow rate
G-2	Cellulose solution control valve	Flow rate control of the cellulose solution
G-3	Salt water flow control valve	Flow rate adjustment of salt water
G-4	Pure water flow control valve	Flow adjustment of pure water
G-5	pH adjuster flow control valve	Flow rate adjustment of the pH adjusting agent
G-6	Enzyme solution flow control valve	Flow rate adjustment of the enzyme solution
G-7	Phase switching valve for recycling	Switching in reuse of TOP phase (IL rich) and Bottom phase (salt rich)

Table 4-7 Apparatus and their purpose for assumed process flow in IL-ATPS prepared with a mixed salt.

No	Apparatus name	Purpose / state
A : The supply of cellulose		
A-1	Cellulose storage tank Constant cutting device	Storage and supply of cellulose
A-2	Blowing unit	Supply of powdered cellulose by blower
B : Tanks for Cellulose Pretreatment and Saccharification		
B-1	Mixing tank	Mixing of cellulose and IL at around 100°C
B-2	Phase separation tank	Separation of IL-ATPS and regenerated cellulose
B-3	Reaction tank	Enzymatic hydrolysis of regenerated cellulose
C : Conveyor for transport of regenerated cellulose solids		
C-1	Screw conveyor	Transport and squeeze regenerated cellulose
D : Storage tanks for cellulose pretreatment and saccharification		
D-1	IL storage tank	Storage of IL solution (IL dissolution temperature conditions)
D-2	Salt water storage tank	Saltwater storage
D-3	Enzyme solution storage tank	Enzyme solution storage
E : Pumps for cellulose pretreatment and saccharification		
E-1	IL Supply pump	Transport of IL solution (IL dissolution temperature conditions)
E-2	Salt water pump	Salt water supply
E-3	Enzyme solution supply pump	Supply of enzyme solution
E-4	Cellulose Liquid Supply pump	Transport of cellulose solution at around 100 °C
E-5	IL-ATPS reuse pump	Recycling of the upper and lower phases of ILATPS
F : Tanks for IL and Salt Recovery and waste liquid		
F-1	IL-ATPS recovery storage tank	IL and Salt recovery
G : Valve for Flow control and switching		
G-1	IL flow control valve	Adjustment of IL flow rate
G-2	Cellulose solution control valve	Flow rate control of the cellulose solution
G-3	Salt water flow control valve	Flow rate adjustment of salt water
G-4	Enzyme solution flow control valve	Flow rate adjustment of the enzyme solution
G-5	Phase switching valve for recycling	Switching in reuse of TOP phase (IL rich) and Bottom phase (salt rich)

3.7 Cost-effectiveness of glycation process using IL-ATPS

Although high concentrations of IL can improve dissolution of crystalline cellulose, the IL itself hampers enzymatic reactions because it induces enzyme denaturation [Tanimura et al., 2018]. Since regenerated cellulose has more amorphous parts than untreated cellulose, the saccharification efficiency by cellulase is significantly improved with regenerated cellulose [Xing et al., 2014]. That is, the production of regenerated cellulose is an important step in the enzymatic hydrolysis of cellulose. Furthermore, IL-ATPS holds 90 wt% or more of IL in the upper phase [Tanimura et al., 2019]. Therefore, IL consumption can be minimized by repeated use. As shown in literature, [Emim][OAc] is one of most powerful ILs for cellulose dissolution. Comparing the IL cations, the dissolution ability of $[Amim]^+$ is higher than $[Bmim]^+$ [Swatloski et al., 2002]. In addition, the alkyl chain length of IL cations influences on the dissolution ability: a shorter chain could be preferred to promote cellulose dissolution [Wang et al., 2012, Vitz, 2009]. According to the above, the saccharification efficiency of IL should in the following order: [Emim][OAc] > [Amim][Cl] > [Bmim][Cl]. On the other hand, the prices are in the following order: [Amim][Cl] = [Emim][OAc] > [Bmim][Cl]. It is considerable that availability and performance of IL might be in a trade-off relation. Because [Bmim][Cl] is one of the most studied IL in cellulose saccharifaction, a process utilizing [Bmim][Cl] is worth to be studied.

As for the cost of equipment, there are factors to be considered in detail, such as the tank material, motor capacity, and water usage. However, here we do not make a quantitative reference regarding the specific amount. By comparison with conventional method, the IL-ATPS system does not require stirring motor, tank, and transport by omission of washing process and pH adjustment process installation of devices (**Figure 4-7**). As a result, it is possible to significantly reduce utility costs such as the amount of pure water used, the amount of pH adjuster used, and the amount of power consumed in washing (**Figure 4-8**).

In conclusion, the IL-ATPSs were utilized to generate dissolved cellulose, and then the saccharification efficiency of the regenerated cellulose using cellulase were investigated. In comparison to IL mono-phasic system (IL/water = (70/30)),

the IL-ATPS (IL/salt/water = (30/15/45) promoted glucose production, suggesting that the IL-enriched upper phase could promote dissolution of crystalline cellulose, while the resulted regenerated cellulose potentially include the remained salts which increase the solution pH to alkaline. Thus, the washing of regenerated cellulose and the pH adjustment of reaction mixture (for enzymatic saccharification) are necessary. As optimized system, we suggest the [Amim][Cl]/mixed salt ATPS: composition, IL/total salt/water = (20/3/50); ratio of NaH_2PO_4/Na_2HPO_4 = 5/1 (wt/wt). This system showed an optimum pH condition for cellulase, and the saccharification efficiency was as well as the regenerated cellulose pretreated by [Amim][Cl]/K_2HPO_4 ATPS (including 30 wt% of IL). By employing IL/ATPS to obtain regenerated cellulose, the final yield of glucose was ca. 70%. Theoretically, the removed IL and salt solution could be reused for further pretreatment of crystalline cellulose. Although more detailed studies are required, the optimized IL/ATPS pretreatment method could improve the enzymatic saccharification processes particularly in large scale. A certain amount of cellulose is also present, such as waste papers. Such biomass source could be dissolved by pretreatment with IL in the heating condition, therefore, waste papers could be a target for the feedstock of IL-ATPS. Organosolv pretreatment method, which uses water and organic solvent (e.g., 1-butanol), can be applied for delignification [Zhang et al., 2016, Nakasaka et al., 2017]. Combining such methods and IL-ATPS, a novel saccharification process can be constructed.

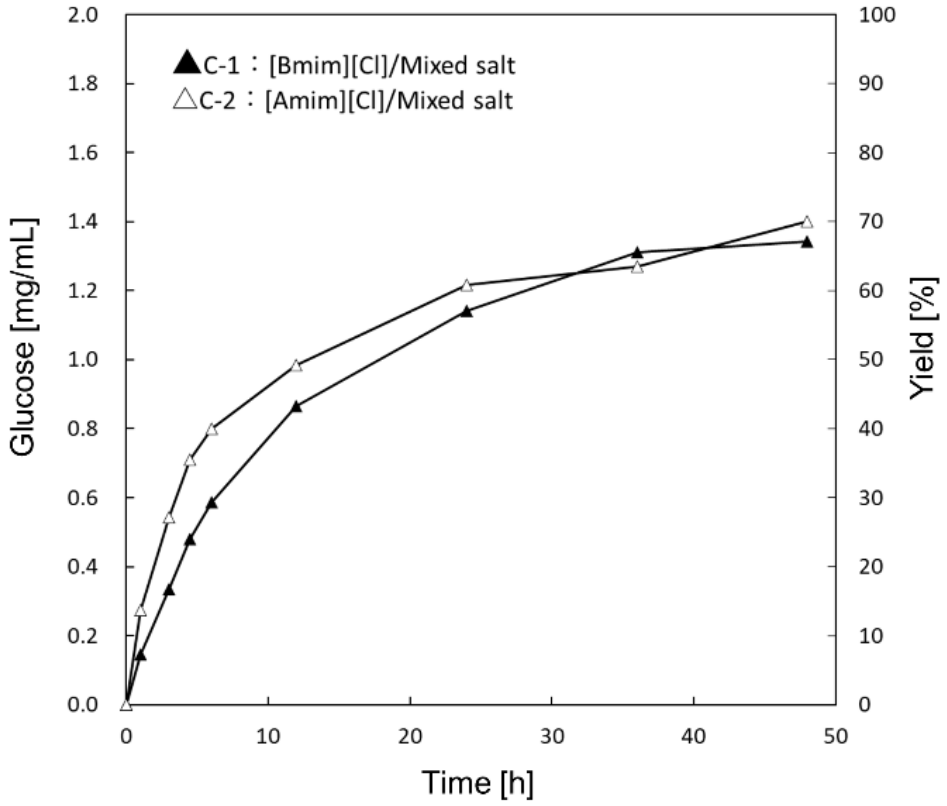

Figure 4-9 Time courses of glucose concentration in enzymatic saccharification at 45 ℃. Regenerated cellulose was obtained by pretreatment with Sample C-1, [Bmim][Cl]/mixed salt ATPS (closed triangle), and with Sample C-2, [Amim][Cl]/mixed salt ATPS (open triangle). The compositions (IL/total salt/water) were (20/30/50). Initially charged cellulose, 50 mg; cellulase concentration, 100 mg/L.

4. Summary

Regenerated cellulose can be prepared by treatment with an ionic liquid (IL) and an anti-solvent such as water, which significantly enhances the enzymatic hydrolysis in comparison to crystalline cellulose. The IL-aqueous two-phase system (IL-ATPS) is consisted of IL-condensed upper phase and salt-condensed bottom phase, which could be suitable to produce regenerated cellulose with smaller amount of IL. Using IL-ATPS with different pH, the enzymatic saccharification efficiency of crystalline cellulose was determined. The use of 1-allyl-3-methylimidazolium chloride resulted in relatively higher yield of glucose production as compared to 1-butyl-3-methylimidazolium chloride. The IL-ATPS showing optimal pH for cellulase was prepared with mixed salt (NaH_2PO_4/Na_2HPO_4 = 5/1 (wt/wt)), which provide a regenerated cellulose with the pH range of 4.8-4.9 in enzymatic reaction mixture. Using such regenerated cellulose as feed of saccharification, the final yield of glucose was about 70%.

Chapter 5
General Conclusion

In Chapter 2, Cellulose hydrolysis was promoted and inhibited by ILs ([Amim][Cl], [Bmim][Cl]). Depending on the IL concentration. In the presence of IL with higher concentration ([IL] >10wt%), a denature of cellulase was significant, which reduced the substrate affinity. When IL concentration lower than 5wt%, the Langmuir adsorption model can be applied to understand the actual concentration of substrate (dissolved cellulose) available for hydrolysis reaction. Based on the kinetic parameter analysis, the effect of [Amim][Cl] for cellulose dissolution was more effective as compared to [Bmim][Cl]. It is important to maintain lower IL concentration for enzymatic activity, while higher IL concentration are considered to be superior to generate dissolved substrate. Thus, the control of IL concentration could be dominantly affected on the efficiency in enzymatic saccharification, in batch reactor process.

In Chapter 3, IL-ATPSs were prepared using [Amim][Cl] or [Bmim][Cl] and K_2CO_3 or K_2HPO_4, and their physical properties were evaluated on the basis of phase diagrams. The phase separation behavior changed due to the hydrophobicity of the alkyl chain of the IL cationic species, and the hydration entropy differed according to the position of the salt in the Hofmeister series. The IL-ATPSs prepared in this study exhibited temperature dependence. They were of the UCST type, in which the phase separation range expanded with decreased temperature. [Bmim][Cl]/K_2HPO_4 at 5 °C exhibited the widest phase separation, with about 97% of the total IL in the system being separated into the top phase. Furthermore, [Bmim][Cl]/K_2HPO_4 exhibited a high hydrophobicity towards water-soluble amino acids. A qualitative and quantitative determination method for the separation of a salt-rich bottom phase and an IL-rich top phase using information obtained from the phase map and the calculated values of the *HF* was demonstrated as 0.13-0.41 mol/kJ, suggesting that the hydrophobicity gap between top and bottom phases are large, as well as the conventional ATPS composed of PEG/$MgSO_4$. It is suggested that the obtained data regarding the fundamental characteristics of the IL-ATPSs can be applied to the rational design of the bioconversion/bioseparation process, as reported in previous case studies.

In Chapter 4, the IL-ATPSs were utilized to generate dissolved cellulose, and then the saccharification efficiency of the regenerated cellulose using cellulase were investigated. In comparison to IL mono-phasic system (IL/water = (70/30)), the IL-ATPS (IL/salt/water = (30/15/45) promoted glucose production, suggesting that the IL-enriched upper phase could promote dissolution of crystalline cellulose, while the resulted regenerated cellulose potentially include the remained salts which increase the solution pH to alkaline. Thus, the washing of regenerated cellulose and the pH adjustment of reaction mixture (for enzymatic saccharification) are necessary. As optimized system, we suggest the [Amim][Cl]/mixed salt ATPS: composition, IL/total salt/water = (20/30/50); ratio of NaH_2PO_4/Na_2HPO_4 = 5/1 (wt/wt). This system showed an optimum pH condition for cellulase, and the saccharification efficiency was as well as the regenerated cellulose pretreated by [Amim][Cl]/K_2HPO_4 ATPS (including 30 wt% of IL). By employing IL/ATPS to obtain regenerated cellulose, the final yield of glucose was ca. 70%. Theoretically, the removed IL and salt solution could be reused for further pretreatment of crystalline cellulose. Although more detailed studies are required, the optimized IL/ATPS pretreatment method could improve the enzymatic saccharification processes particularly in large scale. A certain amount of cellulose is also present, such as waste papers. Such biomass source could be dissolved by pretreatment with IL in the heating condition, therefore, waste papers could be a target for the feedstock of IL-ATPS. Organosolv pretreatment method, which uses water and organic solvent (e.g.; 1-butanol), can be applied for delignification. Combining such methods and IL-ATPS, a novel saccharification process can be constructed.

Abbreviation

IL	Ionic Liquid
[Amim][Cl	1-allyl-3-methylimidazolium chloride
[Bmim][Cl]	1-butyl-3-methylimidazolium chloride
[Emim][OAc]	1-Ethyl-3-methylimidazolium acetate
TLL	Tie Line Length
STL	Slope of Tie Line
ATPS	Aqueous Two Phase System
IL-ATPS	Ionic-liquid Aqueous Two Phase System
UCST	Upper Critical Solution Temperature
LCST	Lower Critical Solution Temperature

Nomenclature

C	Concentration of glucose precursor available for reaction [mol/L]
C_{ini}	Initial concentration of glucose precursor available for reaction [mol/L]
Q_{max}	Maximal adsorption value [g/g]
Conv%	Conversion value of glucose precursor [%]
C_{enz}	Concentration of enzyme [g/L]
K	Affinity coefficient between enzyme and substrate
KY	Conversion ability [-]
k_c	Coefficient of primary kinetics [-/h]
V_{max}	Maximum velocity achieved by the system [M/h]
K_m	Michaelis constant [mol/L]
[S]	Concentration of the substrate [mol/L]
HF	Hydrophobic Factor [mol/kJ]
RH	Relative Hydrophobicity [kJ/mol]
HFS	Hydrophobic Factor of solutes [kJ/mol]
K_{aa}	Partition coefficient of amino acids [-]
W_1^{t}	Salt concentration in top phase [w/w]
W_1^{b}	Salt concentration in bottom phase [w/w]
W_2^{t}	Ionic liquid concentration in top phase [w/w]
W_2^{b}	Ionic liquid concentration in bottom phase [w/w]
W_t	Weight of top phase [mg]
W_b	Weight of bottom phase [mg]
V_t	Volume of top phase [ml]
V_b	Volume of bottom phase [ml]
ρ_t	Top phase density [mg/mL]
ρ_b	Top phase density [mg/mL]

References

Abbott, N. L.; Blankschtein, D.; Hatton, T.A. Protein partitioning in two-phase aqueous polymer systems. 5. Decoupling of the effects of protein concentration, salt type, and polymer molecular weight. *Macromol* **1993**, *26*, 825–828.

Abe, M.; Fukaya, Y.; Ohno, H. Extraction of polysaccharides from bran with phosphonate or phosphinate-derived ionic liquids under short mixing time and low temperature. *Green Chem* **2010,** *12*, 1274-1280.

Adams, C. J.; Earle, M. J.; Roberts, G.; Seddon, S. R. Stereoselective hydrogenation reactions in chloroaluminate (III) ionic liquids: a new method for the reduction of aromatic compounds. *Chem. Commun.* **1999**, 1043-1044.

Agbor, V. B.; Cicek, N.; Sparling, R.; Berlin, A.; Levin, D. B. Biomass pretreatment fundamentals toward application. *Biotechnol* 2011, *29*, 675–685.

Albertsson, P. Partition of cell particles and macromolecules in polymer two-phase systems. *Adv. Protein Chem.* **1970**, *24*, 309-341.

Albertsson, P.-A.; Johansson, G.; Tjerneld, F. Aqueous two-phase system.; Separation Processes in Biotechnology (ed. AsenjO, J. A.), Marcel Dekker, New York **1990**, 287-327.

Albertsson, P.-Å. Partition of Cell Particles and Macromolecules, 3rd ed.; Wiley, New York. **1986**

Alvira, P.; Tomás-Pejó, E.; Ballesteros, M.; Negro, M. J. Pretreatment technologies for an efficient bioethanol production process based on enzymatic hydrolysis: A review, *Bioresource Technol*. **2010**, *101*, 4851-4861.

Annat, G.; Forsyth, M.; MacFarlane, D. R. Ionic liquid mixtures variations in physical properties and their origins in molecular structure. *J. Phys. Chem. B* **2012**, *116*, 8251−8258.

Baskir, J.N.; Hatton, T.A.; Suter, U.W. Thermodynamics of the partitioning of biomaterials in two-phase aqueous polymer systems: Comparison of lattice model to experimental data. *J. Phys. Chem.* **1989**, *93*, 2111-2122.

Beldman, G.; Voragen, A. G.; Rombouts, F. M.; Searle-van Leeuwen, M. F.; Pilnik, W. Adsorption and kinetic behavior of purified endoglucanases and exoglycanases from Trichoderma viride. *Biotechnol. Bioeng.* **1987**, *30* (2), 251-257.

Bonhote, P.; Dias, A.-P.; Papageorgiou, N.; Kalyanasundaram, K.; Gratzel, M. Hydrophobic, highly conductive ambient-temperature molten salts. *Inorg. Chem.* **1996**, *35*, 1168-1178.

Bose, S.; Barnes, C. A.; Petrich, J. W. Enhanced stability and activity of cellulase in an ionic liquid and the effect of pretreatment on cellulose hydrolysis. *Biotechnol. Bioeng.* **2012**, *109*, 434-443.

Bosmann, A.; Datsevich, L.; Jess, A.; Lauter, A.; Schmitz, C.; Wasserscheid, P. Deep desulfurization of diesel fuel by extraction with ionic liquids. *Chem. Commun.* **2001**, 2494–2495.

Bridges, N.J.; Gutowski, K. E.; Rogers, R. D. Investigation of aqueous biphasic systems formed from solutions of chaotropic salts with kosmotropic salts (salt-salt-ABS). *Green Chem.* **2007**, *52*, 177-183.

Carmichael, A. J.; Seddon, K. R. Polarity study of some 1-alkyl-3-methylimidazolium ambient-temperature ionic liquids with the solvatochromic dye, Nile Red. *J. Phys. Org. Chem.* **2000**, *13*, 591-595.

Chung, Y. H.; R. Rin.; F. S. Todd. Published Patent Publication (A) Method for Hydrolyzing Polysaccharide Substances such as Cellulose Patent Document 1-2. **2007**

Cínthiadas, D.; Aguiar, P.; Aparecida, L.; Machado, B.; Giordano, A. Nelson, H.; Teixeira, L, L.; Sindra, V. Phase behavior at different temperatures of ionic liquid based aqueous two-phase systems containing {[Bmim]BF_4 + salt sulfate (Zn^{2+} or Ni^{2+}) + water}. *J. Chem. Thermodynamics* **2017**, *108*, 105-117.

Dadi, A. P.; Varanasi, S.; Schall, C. A. Enhancement of cellulose saccharification kinetics using an ionic liquid pretreatment step. *Biotechnol. Bioeng*. **2006**, *95* (5), 904-910.

David D.; Daphne, B. Overview of the effect of salts on biphasic ionic liquid / water solvent extraction systems: Anion exchange, mutual solubility, and hemimorphic properties. *J. Phys. Chem. B.* **2015**, *119*, 6747-6757.

De maria, P. D. Recent trends in (ligno) cellulose dissolution using neoteric solvents: switchable, distillable and bio-based ionic liquids. *J. Chem. Tecnol. Biotechnol.* **2014**, *89* (1) 11-18

Deng, Y.F.; Long, T.; Zhang, D.L.; Chen, J.; Gan, S.C. Phase diagram of [Amim] Cl salt aqueous biphasic systems and its application for [Amim] Cl recovery. *J. Chem. Eng.* **2009**, *9*, 2470-2473.

Deng, Y.F.; Zhang, D.L. Phase diagram data for several salt aqueous biphasic systems at 298.15K. *J. Chem. Eng. Data*. **2007**, *52*, 1332–1335.

Earle, M. J.; Seddon, K. R. Ionic liquids. Green solvents for the future. *Pure Appl. Chem.* **2000**, *72*, 1391-1398.

Erdmenger, T.; Haensch, C.; Hoogenboom, R.; Schubert, U. S. Homogeneous tritylation of cellulose in 1-butyl-3-methylimidazolium chloride, *Macromol. Biosci.;* **2007**, *7*, 440-445.

Feng, L.; Chen, Z. I. Research progress on dissolution and functional modification of cellulose in ionic liquids, *J. Mol. Liq.;* **2008**, *142*, 1-5.

Fischer, T.; Sethi, A.; Welton, T.; Woolf, J. Diels-Alder reactions in room-temperature ionic liquids. *Tetrahedron Lett.* **1999**, *40*, 793–796.

Forsyth, S. A.; Pringle, J. M.; MacFarlane, D. R. Ionic liquids - An overview. *Aust. J. Chem.* **2004**, *57*, 113–119.

Fort, D. A.; Remsing, R. C.; Swatloski, R. P.; Moyna, P.; Moyna, G.; Rogers, R. D. Can ionic liquids dissolve wood? Processing and analysis of lignocellulosic materials with 1-n-butyl-3-methylimidazolium chloride, *Green Chem.* **2007**, *9*, 63–69.

Fukaya, Y.; Hayashi, K.; Wada, M.; Ohno, H. Cellulose dissolution with polar ionic liquids under mild conditions: required factors for anions. *Green Chem.* **2008**, *10*, 44-46.

Fukaya, Y.; Sekikawa, K.; Murata, K.; Nakamura, N.; Ohno, H. Miscibility and phase behavior of water-dicarboxylic acid type ionic liquid mixed systems. *Chem. Commun*. **2007**, *29*, 3089−3091.

Fukumoto, K.; Ohno, H. LCST-Type Phase Changes of a Mixture of Water and Ionic Liquids Derived from Amino Acids. *Angew. Chem.; Int. Ed.* **2007**, *46*, 1852−1855.

Galinski, M.; Lewandowski, A.; Stepniak, I. Ionic liquids as electrolytes. *Electrochim. Acta*. **2006**, *51*, 5567–5580.

Ghasemi, M.; Tsianou, M.; Alexandridis, P. Assessment of solvents for cellulosedissolution. *Bioresour. Technol.* **2017**, *228*, 330-338.

Gifford, P. R.; Palmisano, J. B. A Substituted imidazolium chloroaluminate molten salt possessing an increased electrochemical window. *J. Electrochem. Soc.* **1987** *134*, 610.

Grethlein, H. E.; Converse, A. O. Common aspects of acid prehydrolysis and steam explosion for pretreating wood. **1991**, 77-82

Gustafsson, A.; Wennerstrom, H.; Tjerneld, F. The nature of phase separation in aqueous two-polymer systems. *Polymer* **1986**, *27*, 1768-1770.

Gutowski, K. E.; Broker, G. A.; Willauer, H. D.; Huddleston, J. G.; Swatloski, R. P.; Holbrey, J. D.; Rogers, R. D. Controlling the aqueous miscibility of ionic liquid: Aqueous biphasic systems of water-miscible ionic liquids and water-structuring salts for recycle, metathesis and separations. *J. Am. Chem. Soc.* **2003**, *125*, 6632-6633.

Habibi, Y.; Lucia, L. A.; Rojas, O. J. Cellulose nanocrystals: Chemistry, self-assembly and applications, *Chem. Rev.;* **2010**, *110*, 3479-3500.

Hagiwara, H.; Sugawara, Y.; Isobe, K.; Hoshi, T.; Suzuki, T. Immobilization of $Pd(OAc)_2$ in ionic liquid on silica: Application to Sustainable Mizoroki−Heck reaction. *Org. Lett.* **2004**, *6*, 2325–2328.

Hatti-Kaul, R. Aqueous Two-Phase Systems. Springer, Berlin, 2000.

Trindade, J.R.; Visak, Z.P.; Blesic, M.; Marrucho, I. M.; Coutinho, J. A. P.; Canongia Lopes, J.N.; Rebelo, L. P. N. Salting-out effects in aqueous ionic liquid solutions: Cloud-point temperature shifts. *J. Phys. Chem. B* **2007**, *111*, 4737−4741.

Hill, J.; Nelson, E.; Tilman, D.; Polasky, S.; Tiffany, D. Environmental, economic, and energetic costs and benefits of biodiesel and ethanol biofuels, *Proc. Nat. Acad. Sci. USA*, **2006**, *103*, 11206-11210.

Huddleston, J. D.; Visser, A. E.; Reichert, W. M.; Willauer, R. D.; Broker, G. A.; Rogers, R. D. Characterization and comparison of hydrophilic and hydrophobic room temperature ionic liquids incorporating the imidazolium cation. *Green Chem*. **2001**, *3*,156-164.

Hustedt, H.; Kroner, K. H.; Menge, U.; Kula, M.-R. Protein recovery using two phase system. *Trends Biotechnol.* **1985**, *3*, 139-144.

Hustedt, H.; Kroner, K.; IL, Kula, M.-R. Partitioning in aqueous Two-Phase Systems: Theory, Methods, Uses, and Applica- nology (eds. Walter, H, Brotions to Biotech oks, D.E.; Fisher, D.) Academic Press, **1985**, 529-587.

Llin, K.K.; Cherkasov, D.G. Phase equilibria and salting-out effects in a cesium nitrate-triethylamine-water system at 5−25°C. *Russ. J. Phys. Chem. A.* **2013**, *87*, 598−602.

Itoh, T. Ionic liquids as tool to improve enzymatic organic synthesis. *Chem. Rev.* **2017**, *117* (15), 10567-10607.

Jiang, B.; Li, Z.-G.; Dai, J.-Y.; Zhang, D.-J.; Xiu, Z.-L. Aqueous two-phase extraction of 2, 3-butanediol from fermentation broths using an ethanol/phosphate system. *Process Biochem*. **2009,** *44*, 112–117.

Johansson, G. Studies on aqueous dextran-poly (ethylene glycol) two-phase systems containing charged poly (ethylene glycol) I. Partition of albumins. *Biochim. Biophys. Acta* **1970**, *222*, 381-389.

Johansson, G. The effect of poly (ethyleneglycol) esters on the partition of proteins and fragmented membranes in aqueous biphasic systems. *Biochim. Biophys. Acta* **1976**, *451*, 517-529.

Karimi, K.; Taherzadeh, M. J. A critical review of analytical methods in pretreatment of lignocelluloses: composition, imaging, and crystallinity. *Bioresour. Technol*. **2016**, *200*, 1008–1018.

Karr, L.J.; van Alstine, J.M.; Snyder, R.S.; Shafer, S.G.; Harris, J.M. Cell separation by immunoaffinity partitioning with polyethylene glycol-modified protein a in aqueous polymer two-phase systems. *J. Chromatogr.* **1988**, *442*, 219-227.

Kilpeläinen, I.; Xie, H.; King, A.; Heikkinen, S.; Argyropoulos, D. S. Dissolution of wood in ionic liquids, *J. Agric. Food Chem*. **2007**, *55*, 9142–9148.

Knappert, D.; Grethlein, H. Converse, A. Partial acid hydrolysis of cellulosic materials as a pretreatment for enzymatic hydrolysis. *Biotechnol. Bioeng.* **1980,** *22*, 1449-1463.

Kohno, Y.; Arai, H.; Saita, S.; Ohno, H. Material design of ionic liquids to show temperature-sensitive LCST-type phase transition after mixing with water. *Aust. J. Chem.* **2011**, *64*, 1560−1567.

Kohno, Y.; Ohno, H. Ionic liquid / water mixtures: From hostility to conciliation. *Chem. Commun.* **2012**, *48*, 7119−7130.

Kohno, Y.; Ohno, H. Temperature-responsive ionic liquid / water interfaces: Relation between hydrophilicity of ions and dynamic phase change. *Phys. Chem. Chem. Phys.* **2012**, *14*, 5063−5070.

Kohno, Y.; Saita, S.; Men, Y.; Yuan, J.; Ohno, H. Thermoresponsive polyelectrolytes derived from ionic liquids. *Polym. Chem.* **2015**, *6*, 2163−2178.

Kroner, K. H.; Hustedt, H.; Kula, M.-R. Extractive enzyme recovery: Economic considerations. *Process. Biochem.* **1984**, *19*, 170-179.

Kuboi, R.; Tanaka, H.; Komasawa, I. Hydrophobicities and partition properties of proteins in aqueous two-phase extraction system. *Agr. Biol. Chem.* **1990**, *54*, 2003-2008.

Kuboi, R.; Umakoshi, H. Analysis and separation of amyloid beta-peptides using aqueous two-phase systems under stress conditions ~From aqueous two-phase system to liposome membrane system~. *Solvent Extr. Res. Dev. Jpn.* **2006**, *13*, 9-21.

Kuboi, R.; Wakayama, A.; Yano, K.; Komasawa, I. Separation of α-lactalbumin and β-lactoglobulin using surface net and local hydrophobicities in aqueous two-phase partitioning systems. *Kagaku Kogaku Ronbunshu (in Japanaese)* **1995**, *21*, 181-188.

Kuboi, R.; Yamahara, K. Purification process for β-galactosidase using aqueous two-phase partitioning and PEG fractional precipitation. *Kagaku Kogaku Ronbunshu (in Japanaese)* **1998**, *24*, 285-290.

Kuboi, R.; Yano, K.; Tanaka, H.; Komasawa, I. Evaluation of Surface Hydrophobicities During Refolding Process of Carbonic Anhydrase using Aqueous Two-Phase Partitioning Systems. *J. Chem. Eng. Jpn.* **1993**, *26*, 286-290.

Kuboi, R.; Yoshimoto, M.; Walde, P.; Luisi, P.L. Refolding of carbonic anhydrase assisted by 1-palmitoyl-2-oleoyl-sn-glycero-3-phosphocholine liposomes. *Biotechnol. Prog.* **1997**, *13*, 828-836.

Kula, M.-R.; Kroner, K. H.; Hustedt, H. Purification of enzymes by Liquid-liquid Extraction. *Biochem. Eng.* **1982**, *24*, 73-118.

Kumari, D.; Singh, R. Pretreatment of lignocellulosic wastes for biofuel production: A critical review. *Renewable Sus. Energy Rev.* **2018**, *90*, 877-891

Lee, S. H.; Doherty, T. V.; Linhardt, R. J.; Dordick, J. S. Ionic liquid-mediated selective extraction of lignin from wood leading to enhanced enzymatic cellulose hydrolysis. *Biotechnol. Bioeng.;* **2009**, *102*, 1368-1376.

Li, C.; Knierim, B.; Manisseri, C.; Simmons, B. A.; Singh, S. Comparison of dilute acid and ionic liquid pretreatment of switchgrass: Biomass recalcitrance, delignification and enzymatic saccharification, *Bioresource Technol.* **2010**, *101*, 4900-4906.

Li, C.; Yoshimoto, M.; Tsukuda, N.; Fukunaga, K.; Nakao, K. A kinetic study on enzymatic hydrolysis of a variety of pulps for its enhancement with continuous ultrasonic irradiation. *Biochem. Eng. J*. **2004**, *19* (2), 155-164.

Li, Y.; Wang, J.; Liu, X.; Zhang, S. Towards a molecular understanding of cellulose dissolution in ionic liquids: anion/cation effect, synergistic mechanism and physicochemical aspects, *Chem. Sci*.; **2018**, *9*, 4027-4043.

Liu, C.-L.; Kamei, D.T.; King, J.A.; Wang, D.I.C.; Blankschtein, D. Separation of proteins and viruses using two-phase aqueous micellar systems. *J. Chromatogr. B* **1998**.*711*, 127-138.

Lopes, J. M.; Bermejo, M. D.; Martín, Á.; Cocero, M. J. Ionic liquid as reaction media for the production of cellulose-derived polymers from cellulosic biomass, *ChemEngineering* **2017**, *1* (2), 10.

Louwrier, A. Model phase separations of proteins using aqueous/ethanol components. *Biotechnol Tech.* **1998**, *12*, 363–365.

Mansfield, S. D.; Mooney, C.; Saddler, J. N. Substrate and enzyme characteristics that limit cellulose hydrolysis. *Biotechnol. Prog.* **1999**, *15* (5), 804-816.

Matsumoto, H.; Yanagida, M.; Tanimoto, K.; Nomura, M.; Kitagawa, Y.; Miyazaki, Y. Highly conductive room temperature molten salts based on small trimethylalkylammonium cations and bis (trifluoromethylsulfonyl) imide. *Chem. Lett.* **2000**, *29*, 922–923.

Matsumoto, M.; Sugimoto, T.; Ishiguro, Y.; Yamaguchi, H.; Kondo, K. Effect of organic solvents and ionic liquids on resolution of 2-epoxyhexane by whole cells of *Rhodotorula glutinis* in a two-liquid phase system. *J. Chem. Technol. Biotechnol*. **2014**, *89*, 522-527.

Merchuk, J. C.; Andrews, B. A.; Asenjo, J. A. Aqueous two-phase systems for protein separation. Studies on phase inversion. *J. Chromatogr B.* **1998**, *711*, 285–93.

Miorner, H.; Albertsson, P.A.; Kronvall, G. Isoelectric points and surface hydrophobicityof gram-positive cocci as determined by cross-partition and hydrophobic affinity partition in aqueous two-phase systems. *Infect. Immun.* **1982**, *36*, 227-234.

Miorner, H.; Johansson, G.; Kronvall, G. Lipoteichoic acid is the major cell wall component responsible for surface hydrophobicity of group *A streptococci*. *Infect. lmmun*. **1983**, *39*, 336-343.

Miwa, I.; Okuda, J.; Maeua, K.; Okuda, G. Mutarotase effect on colorimetric determination of blood glucose with β-D-glucose oxidase. *Clinica Chim. Acta* **1972**, *37* (C), 538-540.

Moniruzzaman, M.; Goto, M. Ionic liquid pretreatment of lignocellulosic biomass for enhanced enzymatic delignification, pp. 1-17, in: *Advances in Biochemical Engineering/Biotechnology.* Springer, Berlin, Heidelberg. **2018**.

Moniruzzaman, M.; Ono, T. Separation and characterization of cellulose fibers from cypress wood treated with ionic liquid prior to laccase treatment. *Bioresour. Technol.* **2013**, *127*, 132-137.

Mora-Pale, M.; Mwli, L.; Doherty, T. V.; Linhaardt, R. J.; Dordick, J. S. Room temperature ionic liquids as an emerging solvent for the pretreatment of lignocellulogic biomass. *Biotechnol. Bioeng.* **2011**, *108*, 1229-1245.

Nakasaka, Y.; Yoshikawa, T.; Kawamata, Y.; Tago, T.; Sato, S.; Takanohashi, T.; Koyama, Y.; Masuda, T.; Fractionation of degraded lignin by using a water/1-butanol mixture with a solid-acid catalyst: A potential source of phenolic compounds, *ChemCatChem*, **2017**, *9*, 2875-2880.

Ngo, H. L.; Lecompte, K.; Hargens, L.; McEwen, A. B. Thermal properties of imidazolium ionic liquids. *Thermochim. Acta*. **2000**, *357*, 97-102.

Nockemann, P.; Thijs, B.; Parac-Vogt, T.N.; van Hecke, K.; van Meervelt, L.; Tinant, B.; Hartenbach, I.; Schleid, T.; Ngan, V. T.; Nguyen, M. T.; Binnemans, K. Carboxyl-functionalized task-specific ionic liquids for solubilizing metal oxides. *Inorg. Chem.* **2008**, *47*, 9987−9999.

Noda, A.; Watanabe, M. Highly conductive polymer electrolytes prepared by in situ polymerization of vinyl monomers in room temperature molten salts. *Electrochim. Acta.* **2000**, *45*, 1265-1270.

Novoselov, N. P.; Sashina, E. S.; Petrenko, V. E.; Zaborsky, M. Study of dissolution of cellulose in ionic liquids by computer modeling, Fibre Chem. **2007**, *39*, 153-158.

Nozaki, Y.; Tanford, C. The solubility of amino acids, diglycine, and triglycine in aqueous guanidine hydrochloride solutions. *J. Biol. Chem.* **1970**, *245*, 1648-1652.

Ohno, H. *Electrochemical aspects of ionic liquids*: 2nd Ed. John Wiley & Sons, Inc. 2011.

Ohno, H.; Fukaya, Y. Task specific ionic liquids for cellulose. *Technolog. Chem. Lett.* **2009**, *38*, (1), 2-7.

Olivier-Bourbigou, H.; Magna, L.; Morvan, D**.** Ionic liquids and catalysis: Recent progress from knowledge to applications, *Appl. Catal. A*, **2010**. *373*, 1-56.

Ooi, C.W.; Tey, B.T.; Hii, S.L.; Kamal, S. M. M.; Lan, J. C.W.; Ariff, A.; Ling, T. C. Purification of lipase derived from Burkholderia pseudomallei with alcohol/salt-based aqueous two-phase systems. *Process Biochem.* **2009**, *44*, 1083–1087.

Pei, Y.; Wang, J.; Wu, K.; Xuan, X.; Lu, X. Ionic liquid-based aqueous two-phase extraction of selected proteins. *Sep. Purif. Technol.* **2009**, *64*(3), 288.

Pei, Y.C.; Wang, J.J.; Liu, L.; Wu, K.; Zhao, Y. Liquid–liquid equilibria of aqueous biphasic systems containing selected imidazolium ionic liquids and salts. *J. Chem. Eng.* **2007**, *52*, 2026-2031.

Pinkert, A.; Marsh, K. N.; Pang, S.; Staiger, M. P. Ionic liquids and their interaction with cellulose. *Chem. Rev.* **2009**, *109*, (12), 6712-6728.

Pratiwi, A. I.; Yokouchi, T.; Matsumoto, M.; Kondo, K. Extraction of succinic acid by aqueous two-phase system using alcohols/salts and ionic liquids/salts. *Sep. Purif. Technol*. **2015**, *155*, 127-132.

Remsing, R. C.; Hernandez, G.; Swatloski, R. P.; Massefski, W. W.; Rogers, R. D.; Moyna, G. Solvation of carbohydrates in *N,N'*-dialkylimidazolium ionic liquids: A multinuclear NMR spectroscopy study, *J. Phys. Chem. B*, **2008**, *112*, 11071-11078.

Rogers, R.D.; Seddon, K.R. Ionic Liquids - Solvents of the future? *Science* **2003**, *302*, 792-793

Saita, S.; Mieno, Y.; Kohno, Y.; Ohno, H. Ammonium based zwitterions showing both LCST- and UCST-type phase transitions after mixing with water in a very narrow temperature range. *Chem. Commun.* **2014**, *50*, 15450−15452.

Seddon, K. R. Ionic liquids for clean technology. *Chem. Technol. Biotechnol.* **1997**, *68*, 351–356.

Sen, S.; Martin, J. D.; Argyropoulos, D. S. Review of cellulose non-derivatizing Solvent interactions with emphasis on activity in inorganic molten salt hydrates. *ACS Sutinable Chem. Eng.* **2013**, *1*, (8), 858-870.

Shahla, S.; Catarina, M.S.; Neves, S.; Freire, M.G.; Coutinho, J.A.P. Role of the hofmeister series in the formation of ionic-liquid-based aqueous biphasic systems. *J. Phys. Chem. B* **2012**, *116*, 7252-7258.

Shill, K.; Padmanabhan, S.; Xin, Q.; Clark, D. S.; Blanch, H. W. Ionic liquid pretreatment of cellulosic biomass: Enzymatic hydrolysis and ionic liquid recycle, *Biotechnol. Bioeng.* **2011**, *108*, 511-520.

Silverstein, R. A.; Chen, Y.; Sharma-Shivappa, R. R.; Boyette, M. D.; Osborne, J. A comparison of chemical pretreatment methods for improving saccharification of cotton stalks, *Bioresource Technol.* **2007**, *98*, 3000-3011.

Sjoberg, A.; Karlstrom, G.; Tjerneld, F. Effects on the cloud point of aqueous poly (ethylene glycol) solutions upon addition of low molecular weight saccharides. *Macromolecules* **1989**, *22*, 4512-4516.

Snedden, P.; Cooper, A. I.; Scott, K.; Winterton, N. Synthesis of macroporous polymer beads by suspension polymerization using supercritical carbon dioxide as a pressure-adjustable porogen. *Macromolecules* **2003**, *36*, 4549–4556.

Stein, S.; Böhlen, P.; Stone, J.; Dairman, W.; Udenfriend, S. Amino acid analysis with fluorescamine at the picomole level. *Arch. Biochem. Biophys.* **1973**, *155*, 203−212.

Swatloski, R. P.; Spear, S. K.; Holbrey, J. D.; Rogers, R. D. Dissolution of cellose with ionic liquids. *J. Am. Chem. Soc*. **2002**, *124*, (18), 4974-4975.

Tanford, C. Contribution of hydrophobic interactions to the stability of the globular conformation of proteins. *J. Am. Chem. Soc.* **1962**, *84*, 4240-4247.

Teramoto, Y.; Lee, S.-H.; Endo, T. Pretreatment of woody and herbaceous biomass for enzymatic saccharification using sulfuric acid-free ethanol cooking. *Bioresour. Technol.* **2008,** *99*, (18), 8856-8863.

Tjerneld, F.; Johansson, H.-O. Compartmentalization of enzymes and distribution of products in aqueous two-phase systems. *Int. Rev. Cytology* **2000**, *192*,137-151.

Tjerneld, F.; Persson, I.; Albertsson, P.-A.; Hahn-Hagerdal, B. Biotechnol. Enzymatic hydrolysis of cellulose in aqueous two-phase systems. I. Partition of celluloses from Trichoderma reesei. *Bioeng.* **1985**, *27*, 1036-1043.

Tjerneld, F.; Persson, I.; Albertsson, P.-A.; Hanh-Hagerdal, B. Enzymatic hydrolysis of cellulose in aqueous two-phase systems. II. Semicontinuous conversion of a model substrate, solka floc BW 200, *Biotechnol. Bioeng.* **1985**, *27*, 1044-1050.

Tsioptsias. C.; Stefopoulos. A.; Kokkinomalis. I.; Papadopoulou, L.; Panayiotou. C. Development of micro- and nano-porous composite materials by processing cellulose with ionic liquids and supercritical CO_2. *Green Chem.* **2008**, *10*, 965–971.

Turner, M. B.; Spear, S. K.; Huddleston, J. G.; Holbrey, J. D.; Rogers, R. D. Ionic liquid salt-induced inactivation and unfolding of cellulase from Trichoderma reesei. *Green Chem.* **2003**, *5*, 443-447.

Umakoshi, H.; Kuboi, R.; Komasawa, I. Characterization of partitioning behaviors of microorganisms and their homogenates in aqueous two-phase systems. *Solvent Extr. Res. Dev.; Jpn.* **1996**, *3*, 74-85.

Umakoshi, H.; Nishida, A. Modulation of yeast hexokinase on bio-inspired membranes. *Biochem. Eng. J.* **2012**, *69*, 138-143.

Umakoshi, H.; Yano, K.; Kuboi, R.; Komasawa, I. Extractive cultivation of recombinant Escherichia coli using aqueous two-phase systems for production and separation of intracellular heat shock proteins. *Biotechnol. Prog.* **1996**, *12*, 51-56.

Vancouver, T.; Austin, A.-S.; Brown, T.; Mcintosh, S. Use of ionic liquids in converting lignocellulosic material to biofuels. *Renewable Energy* **2012**, *45*, 1-6.

Veide, A.; Lindback, T.; Enfors, S. O. Continuous extraction of B-D. galactosidase from Escherichia coli in an aqueous two-phase system effects of biomass concentration on partitioning and mass transfer. *Enzyme Microb. Technol.* **1984**, *6*, 325-330.

Visak, Z.P.; Canongia Lopes, J.N.; Rebelo, L. P. N. Ionic liquids in polyethylene glycol aqueous solutions: Salting-in and salting-out effects. *Monatsh. Chem.* **2007**, *138*, 1153−1157.

Vitz, J.; Erdmenger, T.; Haensch, C.; Schubert, U. S. Extended dissolution studies of cellulose in imidazolium based ionic liquids, *Green Chem* **2009**, *11*, 417-424.

Wahlström, R.M.; Suurnäkki, A. Enzymatic hydrolysis of lignocellulosic polysaccharides in the presence of ionic liquids. *Green Chem.* **2015**, *17* (2), 694-714.

Walter, H.; Brooks, D.E.; Fisher, D. *Partitioning in Aqueous Two-Phase Systems: Theory, Methods, Uses and Applications to Biotechnology.* **1985**, *327.*

Wang, H.; Gurau, G.; Rogers, R. D. Ionic liquid processing of cellulose, *Chem. Soc. Rev.;* **2012**, *41*, 1519-1537.

Wasserscheid, P.; Keim, W. Ionic liquids - New 'solutions' for transition metal catalysis. *Angew. Chem. Int. Ed.* **2000**, *39*, 3773-3789.

Welton, T. Room-temperature ionic liquids. Solvents for synthesis and catalysis. *Chem. Rev.* **1999**, *99*, 2071-2083.

Wilkes, J. S.; Zaworotko, M.J. Air and water stable 1-ethyl-3-methylimidazolium based ionic liquids. *J. Chem. Commum*. **1992**, 965.

Wilkes, J.S. A short history of ionic liquids - From molten salts to neoteric solvents. *Green Chem.* **2002**, *4*, 73-80.

Xiao, Z.; Zhang, X.; Gregg, D. J.; Saddler, J. N. Effects of sugar inhibition on cellulases and β-glucosidase during enzymatic hydrolysis of softwood substrates, *Appl. Biochem. Biotechnol.;* **2004**, *115*, 1115–1126.

Xing, L.; Wu, Z.; Gong, G. Dissolution of cotton cellulose with ionic liquids 1-butyl-3-methylimidazolium chloride and 1-allyl-3-methylimidazolium chloride to prepare reducing sugar. *J. Energy Eng.* **2014**, *140* (2), 04013013.

Xu, A.; Wang, J.; Wang, H. Effects of anionic structure and lithium salts addition on the dissolution of cellulose in 1-butyl-3-methylimidazolium-based ionic liquid solvent systems, *Green Chem.;* **2010**, *12,* 268-275.

Yamada, Y.; Kuboi, R.; Komasawa, I. Effective bioconversion with continuous product recovery using AOT/lecithin mixed reverse micellar systems and centrifugal partition chromatography as a novel bioreactor. *Biotechnol. Prog.* **1995**, *11*, 682-688.

Yano, K.; Hasegawa, T.; Ryoichi, R.; Komasawa, I.; Tsuchido, T. Characterization of surface properties of heat shock proteins for the separation using aqueous two-phase systems. *J. Chem. Eng. Jpn.* **1994**, *27*, 808-814.

Yoshida, T.; Honaka, H.; Matsumura, Y. Hydrothermal Treatment of Cellulose as a Pretreatment for Ethanol Fermentation: Cellulose hydrolysis Experiments. *J. Jpn. InstEnergy* **2005**, *84*, 544-548.

Yoshimoto, M.; Tanimura, K.; Tokunaga, K.; Kamimura, A. Hydrolysis of insoluble cellulose to glucose catalyzed by cellulase-containing liposomes in an aqueous solution of 1-butyl-3-methylimidazolium chloride. *Biotechnol. Prog.* **2013**, *29*, 1190-1196.

Yoshimoto, N.; Hashimoto, T.; Felix, M.M.; Umakoshi, H.; Kuboi, R. Artificial chaperone-assisted refolding of bovine carbonic anhydrase using molecular assemblies of stimuli-responsive polymers. *Biomacromol*. **2003**, *4*, 1530-1538.

Yousefifar, A.; Baroutian, S.; Farid, M. M.; Gapes, D. J.; Young. B. R. Hydrothermal processing of cellulose: A comparison between oxidative and non-oxidative processes. *Bioresour. Technol.* **2017**, 229-237.

Yüksel, A; Hydrothermal treatment of cellulose in hotpressurized water for the production of clavulanic acid. *Uludağ University Journal of The Faculty of Engineering*, Vol. 21, No. 2, 2016.

Zafarani-Moattar, M. T.; Hamzehzadeh, S. Liquid-liquid equilibria of aqueous two-phase systems containing 1-butyl-3-methylimidazolium bromide and potassium phosphate or dipotassium hydrogen phosphate at 298.15 K. *J. Chem. Eng. Data* **2007**, *52*, 1686-1692.

Zahid, N. I.; Abou-Zied, O. K.; Hashim, R. Evidence of basic medium in the polar nanochannels of the inverse bicontinuous cubic phase of a guerbet glycolipid: a steady-state and time-resolved fluorescence study. *J. Phys. Chem. C* **2013**, *117*, 26636–26643.

Zavrel, M.; Bross, D.; Funke, M.; Buchs, J.; Spiess, A.C. High-throughput screening for ionic liquids dissolving (ligno-)cellulose, *Bioresour. Technol.;* **2009**, *100*, 2580-2587.

Zhang, Y.; Cremer, P. S. Interactions between macromolecules and ions: The Hofmeister series. *Curr. Opin. Chem. Biol.* **2006**, *10*, 658–663.

Zhang, Y.; Xu, J.-L.; Qi, W.; Yuan, Z.-H.; Zhuang, Z.-S.; Liu, Y.; He, M.-C. A fractal-like kinetic equation to investigte temperature effect on cellulose hydrolysis by free and immobilized cellulase. *Appl. Biochem. Biotechnol.* **2012**, *168* (1), 144-153.

Zhang, Z.; Harrison, M. D.; Rackemann, D. W.; Doherty, W. O. S.; O'Hara, I. M.; Organosolv. Pretreatment of plant biomass for enhanced enzymatic saccharification, *Green Chem* **2016**, *18*, 360-381.

Zhao, H. B.; Baker, G. A.; Cowins, J. V. Fast enzymatic saccharification of switchgrass after pretreatment with ionic liquids. *Biotechnol. Prog* **2010**, *26*, 127-133.

Zhao, H.; Jones, C. L.; Baker, G. A.; Xia, S.; Olubajo, O.; Person, V. N. Regenerating cellulose from ionic liquids for an accelerated enzymatic hydrolysis. *J. Biotechnol* **2009**, *139*, 47-54.

List of Publications

[Papers]

1. Kazuhiko Tanimura, Yoshiko Ooe, Keishi Suga, Hiroshi Umakoshi, Effective Concentration of Ionic Liquids for Enhanced Saccharification of Cellulose, *ChemEngineering*, **2018**, *2*, 47 (8 pages)

2. Kazuhiko Tanimura, Misaki Amau, Ryosuke Kume, Keishi Suga, Yukihiro Okamoto, Hiroshi Umakoshi, Characterization of Ionic Liquid Aqueous Two-Phase Systems: Phase Separation Behaviors and the Hydrophobicity Index between the Two Phases, *J. Phys. Chem. B*, **2018**, *123* ,27, 5866-5874

3. Kazuhiko Tanimura, Keishi Suga, Yukihiro Okamoto, Hiroshi Umakoshi, Enzymatic Hydrolysis of Cellulose Recovered from Ionic Liquid-Salt Aqueous Two-Phase System. *J. Biosci. Bioeng.;* **2019**, in press

[Rerated Papers]

1. Makoto Yoshimoto, Kazuhiko Tanimura, Kazuki Tokunaga, Akio Kamimura, Hydrolysis of Insoluble Cellulose to Glucose Catalyzed by Cellulase-Containing Liposomes in an Aqueous Solution of 1-Butyl-3-methylimidazolium Chloride. *Biotechnol. Prog.* **2013**, *29*, 1190-1196

[International Conference]

1. Kazuhiko Tanimura, Ryosuke Kume, Winnie H Shi, Keishi Suga, Yukihiro Okamoto, Makoto Yoshimoto, Hiroshi Umakoshi, Ionic Liquid-Aqueous Two-Phase System for Enzymatic Saccharification Process [Invited Lecture], 11th Int'l Conf. on Separation Science and Technology (ICSST17), Heaundae Grand Hotel, Busan, Korea, Nov 9th-11th (2017).

2. Kazuhiko Tanimura, Yoshiko Ooe, Keishi Suga, Yukihiro Okamoto, Makoto Yoshimoto, Hiroshi Umakoshi Effects of Ionic Liquids and Liposomes on Enzymatic Cellulose Hydrolysis Process, 2017 AIChE Annual Meeting, Minneapolis Convention Center, Minneapolis, MN, USA, Oct 30th-Nov 3rd (2017).

3. Kazuhiko Tanimura, Keishi Suga, Makoto Yoshimoto, Yukihiro Okamoto, Hiroshi Umakoshi, Optimization of Ionic Liquid-Salt Aqueous Two-Phase System for Enzymatic Saccharificaation of Cellulose, 2018 AIChE Annual Meeting, David L. Lawrence Convention Center, Pittsburgh, PA, USA, Oct 28th-Nov 2nd (2018).

Acknowledgements

The author is deeply grateful to Prof. Dr. Hiroshi Umakoshi (Division of Chemical Engineering, Graduate School of Engineering Science, Osaka University), for his insightful comments, suggestions, and warm encouragement throughout this work. The author is thankful to Prof. Dr. Takayuki Hirai, Prof. Dr. Nobuyuki Matsubayashi, (Division of Chemical Engineering, Graduate School of Engineering Science, Osaka University) and Ass. Prof. Dr. Makoto Yoshimoto (Division of Chemical Engineering, Graduation School of Sciences and Technology for Innovation, Yamaguchi University) for a number of valuable comments and suggestions during the completion of this thesis. The author also would like to express the greatest appreciation to Assist. Prof. Dr. Keishi Suga (Division of Chemical Engineering, Graduate School of Engineering Science, Osaka University), and for his valuable comments, and helpful advises. The author would like to express my gratitude to Prof. Emeritus Dr. Masahito Taya, Prof. Emeritus Dr. Koichiro Jitsukawa, Prof. Dr. Yasunori Okano, Prof. Dr. Masayoshi Nakano, Prof. Dr. Norikazu Nishiyama, Prof. Dr. Tomoo Mizugaki, Prof. Dr. Shinji Sakai, and Assoc. Prof. Dr. Yukihiro Okamoto (Division of Chemical Engineering, Graduate School of Engineering Science, Osaka University) for their valuable comments. The author would like to offer one’s special thanks to Ms. Keiko Fukumoto for her kind support during this work.

The authors would like to thank to Hitachi Zosen Corporation for giving the author the opportunities to study as a doctor course student of Osaka University. The author would like to send his special thanks to Mr. Hideo Sato, Mr. Tetsuya Kumada, and Mr. Takeshi Katayama for their kind supervision at Hitachi Zosen and for helpful discussions and ongoing support to complete his thesis. The author would also like to thank Dr. Junichi Tajima for his help on various issues, including comments on the author's work and suggestions during this work as a technical and scientific advisor.

The author is particularly grateful for the assistance given by Y. Ooe, R. Kume and M. Amau. Special thanks are given to following colleagues for their experimental collaboration: Dr. N. Watanabe, Dr. S. Taguchi, Dr. M. Hirose, Mr. A. Tauchi, Mr. D. Wada, Ms. J. Han, Mr. R. Ito, Mr. T. Wakita, Mr. R. Kawakami, Mr. R. Kawakami, Mr. R. Nishino, Mr. K. Yoshida, Mr. Y. Iimure, Mr. K. Kitagawa, Mr. Y. Murata, Mr. M. Faried, Mr. N. Ikushima, Mr. K. Kojima, Mr. Y. Seno, Mr. Y. Hasunuma, Mr. D. Matsui, Ms. S. Matsushita, Mr. R. Murazawa, Mr. M. S. Chern, Ms. C. Lishi, Ms. C. Tran, Mr. A. Ajaikumar, Mr. R. Wakerlin, Ms. Y.-C. Lai, Mr. H. J. Kim, Ms. D. Etwaru, Ms. B. S. Kan and all the member in Bio-Inspired Chemical Engineering Laboratory.

The author would like to express deepest appreciation to his parents Masahiko Tanimura and Ritsuko Tanimura and his sisters Akiko Tanimura for their continuous encouragements and great support throughout this work.

The author gratefully acknowledges the financial support of this work by the by Hitachi Zosen Corporation.